Electronic Thesis and Dissertation Repository

11-14-2022 11:15 AM

Exploration of the pathophysiological mechanisms underlying hemodialysis associated cardiac ischemic injury

Lisa Yun Jeong Hur, *The University of Western Ontario*

Supervisor: McIntyre, Christopher W., *The University of Western Ontario*
A thesis submitted in partial fulfillment of the requirements for the Doctor of Philosophy degree in Medical Biophysics
© Lisa Yun Jeong Hur 2022

Follow this and additional works at: https://ir.lib.uwo.ca/etd

🔵 Part of the Cardiovascular Diseases Commons, Circulatory and Respiratory Physiology Commons, and the Nephrology Commons

Recommended Citation
Hur, Lisa Yun Jeong, "Exploration of the pathophysiological mechanisms underlying hemodialysis associated cardiac ischemic injury" (2022). *Electronic Thesis and Dissertation Repository*. 8987.
https://ir.lib.uwo.ca/etd/8987

This Dissertation/Thesis is brought to you for free and open access by Scholarship@Western. It has been accepted for inclusion in Electronic Thesis and Dissertation Repository by an authorized administrator of Scholarship@Western. For more information, please contact wlswadmin@uwo.ca.

Abstract

Hemodialysis (HD) provides life-saving treatment in individuals with kidney failure. However, HD is associated with poor quality of life and extremely high mortality rates mainly caused by cardiovascular disease due to heart failure and sudden cardiac death. Standard pharmacological treatment developed within the non-kidney disease community are largely ineffective in HD patients because of the difference in pathophysiology of cardiovascular mortality. HD treatment causes hypotension and recurrent ischemic injury to multiple vascular beds including the heart, leading to heart failure. These injuries can be abrogated by improving the patient's tolerability of the treatment. To apply interventions that may improve hemodynamic tolerability of HD, it is crucial to understand the mechanisms of HD-induced injury at every layer of the vasculature: the endothelial, microvasculature and macrovasculature. The purpose of this thesis was to study the endothelial and vascular dysfunction affecting tissue perfusion as a result of HD and under conditions of intradialytic exercise and alteration of dialysate sodium concentration.

In one study, computed tomography (CT) imaging and echocardiography was used to identify the presence of coronary artery disease (CAD), quantify myocardial perfusion, and determine myocardial segments with stunning. HD induced myocardial ischemia and stunning in all participants independent of CAD. However, individuals with CAD demonstrated reduction in segmental myocardial perfusion which corresponded to an increased number of myocardial segments experiencing stunning compared to HD participants without CAD. The findings from this study suggest that the addition of CAD is associated with reduced tolerance to HD, even if the CAD is not clinically evident.

The second study in this thesis investigated the role of dialysate sodium as a contributor to HD-induced endothelial injury, predisposing HD patients to microvascular dysfunction and ischemia. The choice of dialysate sodium concentration is a difficult but crucial decision for the care of HD patients. High sodium dialysate is prescribed to prevent intradialytic hypotension but it is associated with high ultrafiltration, excess sodium deposition in the tissue, and injury to the endothelial glycocalyx. In this study, sodium concentration was manipulated in a rat HD model to study its effect on the endothelium as measured by plasma syndecan-1, and intravital video microscopy to quantify microvascular perfusion. The findings of this study suggest high sodium dialysate induced endothelial injury leading to functional changes in perfusion. Hence, a low dialysate sodium prescription could be beneficial if the patient demonstrates hemodynamic stability during HD.

In a third study, the mechanism and effects of intradialytic exercise was investigated using CT perfusion imaging for quantification of myocardial perfusion and echocardiography to assess myocardial stunning. In contrast to the hypothesis made by other investigators, intradialytic exercise did not increase perfusion in the muscle. However, HD participants demonstrated a decrease in myocardial stunning with exercise. These results suggest that intradialytic exercise is not driven by perfusion-related mechanisms but rather by means of cardioprotection to improve ischemic tolerability of the tissue in the HD setting of challenged perfusion.

Keywords

End stage renal disease, hemodialysis, endothelial dysfunction, myocardial stunning, myocardial perfusion, coronary artery disease

Lay Summary

Kidney failure is common, and it is the inability for the kidneys to clean the blood in our body from waste and toxins. The build-up of waste products can be very dangerous, and it must be removed regularly by a machine (hemodialysis, HD) that acts as an artificial kidney. HD is a life-saving therapy but people who need it die much more often than people with healthy kidneys. The most common cause of death in patients on HD is heart failure. This is because HD requires removal of blood from your body into a circuit that is outside of your body, causing the blood flow in the small blood vessels in the heart tissues to fall. Low blood flow means not enough oxygen will be delivered to the tissue causing it to fail. The purpose of this thesis was to study the changes in the blood vessels effecting blood flow in the tissue due to HD and under conditions of exercise and alteration in sodium levels of the dialysis fluid.

In one study, blood flow in the heart tissue and the contractile function of the heart during HD was studied in patient with large vessel disease using computed tomography (CT) imaging and a heart ultrasound. HD affected blood flow in all patients, whether or not they had large vessel disease. Compared to HD patients without large vessel disease, individuals with large vessel disease had even lower blood flow to certain tissue regions of the heart during HD that corresponded to the loss in contractility of the heart. Therefore, large vessel disease added to the injury that HD patients experienced during HD treatment.

In a second study, a rat HD model was used to study the role of sodium in the small vessels and its circulation. The purpose of this study was to determine the optimal sodium level for the dialysate fluid which helps the patient's tolerate HD treatment better. The results showed that high levels sodium in the blood caused damage to the walls of the blood vessels that reduced the

effectiveness of the vessel from circulating blood in the tissue. This study concluded that dialysis fluid with low sodium would cause less damage to the blood vessel wall and reduce the risk of low blood flow during HD.

In a third study, exercise during HD treatment was evaluated in human participants to study its effect on blood flow and overall heart function. In this study, we showed that exercise did not change blood flow in the heart tissue, but it improved heart contractility. It was concluded that exercise is able to protect the heart from low blood flow and starvation of oxygen that is experienced during HD.

Acknowledgments

I would like to first and foremost thank my supervisor Dr. Christopher McIntyre. You have provided endless guidance and mentorship throughout my graduate career and have shown so much support in the things I aspire to do in the future. Your honesty and words of encouragement have motivated me to produce the best version I could, let it be seminar presentations, conference abstracts, and scholarship applications.

I give my thanks to the advisory committee members: Drs. Maria Drangova, Geoffrey Pickering, and Allan Skanes. The projects I proposed to you in our first meeting varied significantly from what is now presented in this thesis and despite these changes, you have all committed your time and interest to help me understand the clinical value of the work I aimed to do and have directed me to the resources necessary to succeed. Special thanks to Dr. Maria Drangova— it seems only yesterday I was scripting the acknowledgement section of my master's thesis thanking you for the support you gave as a supervisor—you have continued to provide academic and life mentorship throughout the past six years, to which I am grateful for.

The work that has been accomplished in this thesis would not have been possible without the devoted members of the kidney clinical research unit (KCRU). Jarrin Penny, Justin Dorie, Tanya Tamasi have polished my bedside manners and have ensured the safe execution of all clinical studies in our lab. I have had the pleasure of working alongside Drs. Barry Janssen and Yanmin Zhang, who have shown me the importance of preclinical studies and the translation of this work to the bedside. I thank my fellow lab mates, Dr. Alireza Akbari, Janice Gomes, and Dr. Fabio Salerno, for your valuable scientific discussions. Of course, to the administrative staff of KCRU: Diane Heaslip, Virginia Schumann, and Laura Chambers, thank you for all your help organizing meetings, conference finances, and funding applications.

To the friends that I have made during my time in London as a graduate student, thank you for all the fun times rock climbing, drinking wine on the sidelines of the soccer field, birthday parties for our dog children, and endless nights at Schulich Palooza. Miriam Hewlett, Christina Francia, Pascal Michelberger, Rachel Eddy, you guys truly are "humid, prepossessing Homo Sapiens with full sized aortic pumps". To the old and new friends that I have made along the way,

"Mischief Managed."

Moony, Wormtail, Padfoot & Prongs

This thesis is dedicated to my late grandfathers

Contents

List of Figures

List of Tables

List of Abbreviations

AKI	Acute Kidney Injury
ANOVA	Analysis of Variance
ASiR	Adaptive Statistical Iterative Reconstruction
ASL	Arterial Spin Labelling
AV	Arteriovenous
AVF	Arteriovenous Fistula
AVG	Arteriovenous Graft
BP	Blood Pressure
BUN	Blood Urea Nitrogen
CA	Coronary Angiography
CAC	Coronary Artery Calcification
CAD	Coronary Artery Disease
CCTA	Coronary CT Angiography
CKD	Chronic Kidney Disease
CPM	Counts Per Minute
CRP	C-Reactive Protein
CT	Computed Tomography
cTnT	Cardiac Troponin T
CV	Cardiovascular
CVC	Central Venous Catheter
CVD	Cardiovascular Disease
DBP	Diastolic Blood Pressure
DCE	Dynamic Contrast Enhanced
ECDV	Extravascular Contrast Distribution Volume
ECG	Electrocardiogram
EDL	Extensor Digitorum Longus
eGFR	Estimated Glomerular Filtration Rate
ELISA	Enzyme-linked Immunosorbent Assay
ESRD	End Stage Renal Disease

GFR	Glomerular Filtration Rate
HCT	Hematocrit
HD	Hemodialysis
IACUC	Institutional Animal Care and Use Committee
IDE	Intradialytic Exercise
IVM	Intravital Microscopy
KDIGO	Kidney Disease Improving Global Outcomes
LAD	Left Anterior Descending
LCx	Left Circumflex
LS	Longitudinal Strain
LV	Left Ventricular
LVH	Left Ventricular Hypertrophy
MP	Myocardial Perfusion
MPR	Myocardial Perfusion Reserve
MRI	Magnetic Resonance Imaging
Na^+	Sodium
NO	Nitric Oxide
PET	Positron Emission Tomography
PTH	Parathyroid Hormone
RBV	Relative Blood Volume
RCA	Right Coronary Artery
RIFLE	Risk, Injury, Failure, Loss, and End Stage Kidney Disease
RPM	Rotations Per Minute
RRT	Renal Replacement Therapy
RWMAs	Regional Wall Motion Abnormalities
SBP	Systolic Blood Pressure
Syn-1	Syndecan-1
UFR	Ultrafiltration Rate

List of Appendices

Chapter 1

1   Introduction

Parts of this chapter has been published in Current Opinions in Nephrology and Hypertension: this is a non-final version of an article published in final form in Current Opinions in Nephrology and Hypertension 29 (6), 555-563. November 2020., Authored by Lisa Hur and Christopher W. McIntyre, titled "Current and novel imaging techniques to evaluate myocardial dysfunction during hemodialysis."

1.1   Overview of Thesis

The purpose of this thesis was to study the endothelial and microcirculatory dysfunction effecting tissue perfusion as a consequence of hemodialysis (HD) and under conditions of intradialytic exercise and alteration of dialysate sodium. The studies presented in this thesis applied techniques such as echocardiography, dynamic contrast enhanced computed tomography (CT), coronary CT angiography, intravital microscopy, and enzyme-linked immunosorbent assay (ELISA) to study the endothelial, microvascular, macrovascular, and functional changes in both human HD participants and pre-clinical rodents during HD.

Section 1.2.1-1.2.2 of this chapter provides a brief summary of the anatomy, function and pathophysiology surrounding the kidney and it related-disease forms. Section 1.2.3-1.2.4 summarized the available treatment methods for end stage renal disease and its associated complications. The remaining sections (Sections 1.3-1.5) address the techniques that have been used to assess HD-induced injury and detail the techniques that were utilized in this thesis.

The completed scientific investigations are described in the following three chapters. Chapter 2 investigates the association between the vascular bed of the heart (myocardial perfusion) and the health of the coronary arteries (macrovasculature) supplying the blood in response to HD.

It was hypothesized that the impairment of the coronary arteries would exasperate the ischemic injury associated with HD as measured by dynamic myocardial CT perfusion and significantly reduce cardiac function as assessed with echocardiography. In line with this hypothesis, myocardial segments with hemodynamically significant stenoses were less perfused and participants with this impairment experienced higher levels of myocardial stunning with HD.

In Chapter 3 of this thesis, intravital microscopy was utilized in a preclinical platform to examine the endothelial and microvascular response to levels of dialysate sodium during HD. It was hypothesized that levels of acute sodium loading during HD results in direct endothelial cell injury marked by increased plasma syndencan-1, and a decrease in microvascular perfusion.

With the interest of minimizing the adverse effects of HD, an intradialytic imaging study was performed (Chapter 4) to examine intradialytic exercise as a way of mitigating the HD-induced ischemic injury. The effects of intradialytic exercise were assessed by quantification of plasma syndecan-1, global myocardial perfusion, and segmental myocardial stunning.

The last chapter of this thesis (Chapter 5) summarizes the scientific contributions of these works and details opportunities for future investigations.

1.2 The Kidneys

1.2.1 Kidney Anatomy and Function

The kidneys are part of the renal system, and its principle function is the production of urine which is composed of water, metabolic by-products, and ions[1]. From this, we know that it plays a major role in the regulation of water and electrolyte balance, the excretion of waste products, the absorption and secretion of bicarbonate and hydrogen ions, as well as the secretion of essential hormones involved in the regulation of physiological functions[2,3].

The kidneys are located in the dorsal abdomen and each kidney has an adrenal gland on its upper surface responsible for the production of hormones. Each kidney is composed of three layers: the renal capsule of collagen fibers (innermost layer), the perirenal fat capsule (a layer of adipose tissue), and the renal fascia outermost later of collagen fibers[1–3]. These three layers together provides each kidney structural stability [1–3]. Within the cross section of the kidney (Figure 1-1), the outermost region is referred to as the renal cortex and inner layer, the renal medulla [1–3]. The renal medulla can be separated into two distinct regions: the renal pyramids and the renal columns that separate the renal pyramids [1–3]. Nearing the center of the kidey, each renal pyramid opens into the minor calyces (singular: minor calyx) which mergers together at the core of the kidney to form the major calyx that leads into the renal pelvis [1–3].
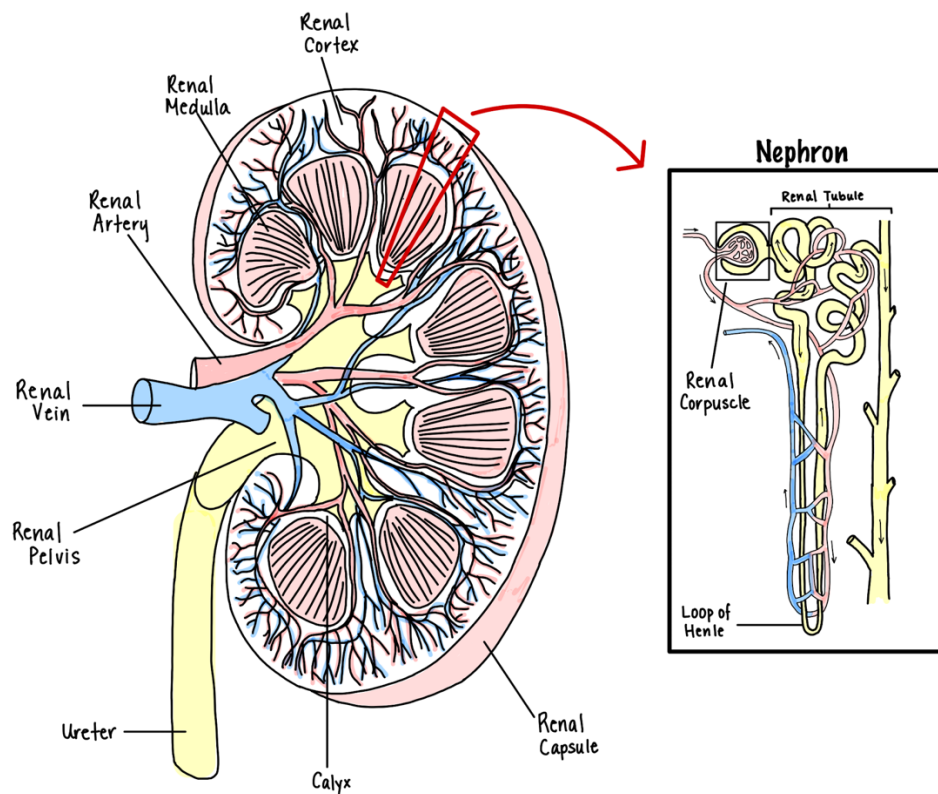
Figure 1-1 Anatomy of the kidney and nephron

The nephron is known to be the basic functional unit of the kidney, populating at one million per kidney. The nephron consists of two distinct parts: the renal corpuscle and the renal tubule. The renal corpuscle is composed of the glomerulus (a bundle of capillaries) and the Bowman's capsule (site of storage for the glomerular filtrate). First, the blood flows into the kidney through the renal artery that branch into smaller vessels, entering a glomerulus where filtration takes places through an afferent arteriole[1]. The amount of glomerular filtrate produced is dependent on the percentage of the body's cardiac output being delivered to the kidneys, roughly twenty to twenty-five percent. Everyday approximately 180 liters (or 125 mL per minute) of filtrate is produced by the glomerulus[4–6]. The rate at which the glomerulus filters the blood is referred to as the glomerular filtration rate (GFR, $mL/min/1.73m^2$), and it is determined by the filtration pressure gradient between the glomerulus and the Bowman's capsule and can be modified by the contraction and relaxation of the smooth muscles surrounding the afferent and efferent arterioles[4–6]. The volume of filtrate produced during this process are stored in the Bowman's capsule before making its way into the renal tubule while the filtered blood returns to the systemic circulation through the efferent arterioles[7]. Within the renal tubule, the glomerular filtrate will undergo further modifications via tubular reabsorption and secretion within the compartments of the renal tubule for the production of urine.

1.2.2 Renal Pathophysiology

1.2.2.1 Acute Kidney Injury

Acute kidney injury (AKI) is the sudden loss of kidney function defined by a decrease in urine output (less than 0.5ml/kg/hr within 6 - 12 hours) and/or a rapid increase in serum creatinine (greater than 1.5-fold from baseline over 10 days; greater than 26.4μmol/L in 48 hours)[8]. In the early 20th century, the term acute renal failure was used to characterize the compounding effects

of abrupt decrease in urine output and the accumulation of uraemic toxins[8]. This terminology was re-examined and replaced by the standardized terminology AKI, that is associated with the RIFLE (Risk, Injury, Failure, Loss and End-stage kidney disease) classification system to grade the severity of the injury[8]. The RIFLE classification system is dependent on serum creatinine and urine output and was adopted into the KDIGO (Kidney Disease Improving Global Outcomes) guidelines to ensure international coherence of research.

Approximately 10 - 15% of hospitalization involve complications of AKI, making up more than 50% of the intensive care unit[9]. The diagnosis and treatment of AKI is complicated due to the presentation of multiple underlying causes including sepsis, ischemia, and nephrotoxicity. The etiology of AKI can be divided into three major categories: pre-renal, intra-renal, and post-renal[10]. Pre-renal causes of AKI result from impairment in renal perfusion, ultimately decreasing the GFR without further damage to the renal parenchyma; possible abnormalities include hypovolemia, impaired cardiac function, systemic vasodilation, and increased vascular resistance[11]. Intrinsic AKI results from damage to parts of the kidney itself, for example, damage to the tubular, glomerular, interstitial and the intra-renal vasculature. Lastly, post-renal AKI results from an acute obstruction in the extrarenal and intrarenal space that impedes urinary flow[8,9].

Urine and blood samples have been used to detect biomarkers of AKI including tissue inhibitor of metalloproteinase-2, neutrophil gelatinase associated lipocalin, and cystatin C[10]. Upon clinical presentation and diagnosis, AKI injuries are managed pharmacologically or through the initiation of renal replacement therapy in the form of dialysis depending on the severity of the injury.

1.2.2.2 Chronic Kidney Disease

Chronic kidney disease (CKD) is an umbrella term encompassing any renal disease resulting in the progressive loss of kidney function over time and is characterized by a reduction in estimated GFR (eGFR) of less than 60 mL/min/1.73m^2 [12,13]. In the recent years, the prevalence of CKD has been rising worldwide; amounting to more than ten percent of the worldwide population or over 850 million people[14–16]. CKD is most common in females (11.8%)[16], in individuals over 70 years of age (27.9%)[16], and in ethnic minority groups[17]. CKD can be categorized into five stages of severity depending on the eGFR and is summarized in Table 1-1.

Table 1-1 Stages of chronic kidney disease

Stage of CKD	eGFR (mL/min/1.73m^2)	Classification of Renal Impairment
1	≥ 90	Normal
2	60 – 89	Mild
3a/b	30 - 59	Moderate
4	15 -29	Severe
5	< 15	Kidney Failure

The primary causes of CKD are diabetes (diabetic nephropathy)[18–21] and hypertension (hypertensive nephrosclerosis)[21–23], and these factors contribute to increased risk for cardiovascular (CV) morbidity and mortality in this population. According to the United States Renal Data System's 2020 report, over thirty-five percent of individuals diagnosed with CKD are diabetic[17]. Diabetes mellitus is characterized by hyperglycemia resulting from defective insulin action and secretion. Chronic hyperglycemia increases the deposition of extracellular matrix protein which induces the expansion of the mesangium. At this time, the glomerular basement membrane that assists with the filtration of waste and fluid from the blood thickens alongside the development of glomerulosclerosis. These changes that occur in the glomeruli as a result of

hyperglycemia cause disturbances in the glomerular filtration rate, reducing kidney function as a consequence of diabetes. Clinical trials investigating preventative measures of diabetic induced kidney injury demonstrated that the practice of intensive blood glucose control early in the course of the disease may delay or even prevent the progression of renal damage[24].

Worldwide, hypertension is the strongest risk factor for cardiovascular disease (CVD) and its association with CKD is well recognized[25]. The role of hypertension in renal disease is complicated because it can be both a cause and a consequence, creating a vicious cycle that ultimately exacerbates high blood pressure (BP) in CKD population. Mechanism of systemic hypertension in this population include volume overload, salt retention, changes in BP regulating hormones, overactive sympathetic nervous system, and endothelial dysfunction[22,23]. To manage hypertension in CKD appropriately, acquisition of BP measurements and quantification of proteinuria are key. Based on these measurements, hypertension can be managed through pharmacological (antihypertensive medication) and non-pharmacological (such as reducing dietary sodium intake and weight loss) treatment methods[23].

Generally, CKD remains silent, and its symptoms are not evident until substantial decline in kidney function. Prior to irreversible kidney failure, CKD can be diagnosed through routine blood work and urinalysis. In advanced kidney disease, common symptoms include chest pain, itchiness, loss of energy, irregular urination, muscle cramps, loss of appetite and shortness of breath. With time, the kidney will gradually lose its ability to function and reach stage 5 of CKD (kidney failure), requiring renal replacement therapy (RRT) to remove waste and fluid.

1.2.2.3 End Stage Renal Disease

In 2010, approximately 2.6 million individuals worldwide were newly registered as having treated end stage renal disease (ESRD) amounting to 4.9 – 9.7 million people with prevalent ESRD that required treatment; an estimated 2.3 million or more people died prior to treatment initiation due to the lack of access[26]. ESRD is the final stage of CKD where the kidney will no longer function to rid toxins and waste from the body and is clinically defined by a GFR of less than 15mL/min/1.73m^2. The two main causes of ESRD are diabetes and hypertension leading to glomerulonephritis (inflammation of the glomerulus)[22,23]. One of the common characteristics of rapidly progressing kidney injury from early stages of CKD to ESRD is the worsening of uremia[27]. Uremia is the elevation in concentration of urea in the blood that is associated with electrolyte, fluid, and hormonal imbalance experienced with a decline in kidney function[28]. In patients with ESRD prior to RRT, urea levels in the blood are typically ten times greater than in healthy individuals. In the past, urea was considered an inert molecule with no evidence of toxic effects. However, in recent years, urea has been shown to interact and interfere with many biochemical pathways (including the generation of cyanate and ammonia) and modulate organ function [29–31]. Uremia can be asymptomatic or symptomatic, nevertheless in conjunction with decline in kidney function it may be an indication for the initiation of RRT to reverse uremic symptoms and prolong life. With ESRD, the health of the kidney cannot be reversed.

1.2.3 Renal Replacement Therapy in ESRD

There are many clinical approaches to RRT, all of which have the common objective to replace the function of a failed kidney and remove waste and toxin from the blood[32,33]. The point at which to start RRT is a topic of debate. Observational studies have shown that early initiation or preemptive interventions does not improve survival[34–36]. Generally, more than half of the ESRD

patient population begin RRT when eGFR reaches a threshold of 10mL/min/1.73m^2. If RRT is initiated too late, the patients are at risk for complications of uremia, reduced quality of life, and increased mortality rate. The decision to start RRT is not simply made on a single objective measurement but is rather based on a combination of symptoms, biochemistry, fluid overload, eGFR and most importantly, the patient's preference. Modes of RRT include kidney transplant, peritoneal dialysis, and hemodialysis (HD). In principle, the patients must only consider one question to decide which form of RRT to receive: will transplantation improve my quality of life compared to peritoneal dialysis or HD? To most patients and their kidney care team, the answer is glaringly apparent because certain treatment methods are not available or unaffordable. The upcoming sections 1.2.3.1 -1.2.3.3 aims to detail the different modes of RRT and the associated risks and benefits.

1.2.3.1   Kidney Transplantation

When successful, kidney transplant remains the most favorable treatment option for ESRD as it is associated with fewer complications and reduced mortality rates, while significantly improving the quality of life[33]. Kidney transplantation as a potential method of treatment is widely dependent on the availability of organs for transplantation, existing comorbid conditions of the patient and their commitment to lifelong need for immunosuppressant drugs. Often, the general public's understanding of transplantation is an immediate cure. However, it involves regular follow-up and continuous effort from the patient and the family to adhere to the medication protocols[37]. With successful transplantation, the life-expectancy of a transplanted patient is still much shorter than age- and sex-matched individuals with normal kidney function[38]. An additional risk factor that transplanted patients face is the maintenance of the graft; the graft is lost prior to death in more than half of the population with kidney transplant. When a graft is deemed lost or

failed after a transplant, the recipient undergoes a re-transplantation procedure, or proceeds to dialysis treatment. Long term survival of a graft depends on a multitude of factors including the donor and recipient's age, the type of immunosuppressant medication, the frequency of acute rejection episodes, living versus deceased donor, and the delayed functionality of the graft[39–43]. However, studies indicate superior outcomes with kidney transplantation compared with peritoneal dialysis and HD treatment methods.

1.2.3.2   Peritoneal Dialysis

Peritoneal dialysis is one of the alternative modes of RRT and it is a process at which solutes, fluids, and waste products are removed within the patient's peritoneal cavity[44–48]. A suitable healthy peritoneum is required to pursue this form of dialysis; contraindications include adhesions, fibrosis, or malignancy in the peritoneum. For the performance of peritoneal dialysis, a catheter is surgically inserted into the abdomen enabling the transfer of fluid in and out of the abdominal cavity. The dialysis fluid, composed of varying levels of electrolyte and salt concentration, precisely formulated to manage the solute composition in the plasma is connected to the catheter to allow inflow of the dialysate into the peritoneal cavity. The exchange of solutes, toxins, and fluids takes place across the peritoneal barrier between the dialysate fluid and the blood within the peritoneal capillaries. The peritoneum itself is densely lined with the capillary-rich wall and the efficiency at the which the solutes are cleared is dependent on multiple factors including the permeability of the peritoneal barrier, the blood flow and vascularity within the capillary walls, the surface area of the peritoneum, and osmotic or oncotic gradient generated through the instilled dialysate content. Once, the waste products are filtered, it is drained out of the body into an empty bag for disposal.

Peritoneal dialysis can be delivered in two forms: continuous ambulatory peritoneal dialysis and automated peritoneal dialysis. With continuous ambulatory peritoneal dialysis, patients manually perform exchanges three to five times per day ranging at 1.5 to 3L per exchange[49]. The automated peritoneal dialysis takes place at night while the patient sleeps. With this form of peritoneal dialysis, the patient is hooked up to a machine that runs through the night and a series of overnight exchanges are carried out automatically for 7 to 10 hours[49]. Peritoneal dialysis is the favorable form of dialysis treatment allowing independence and flexibility for the patient. It is often the method of choice for infants and children, in patients with difficult vascular access for HD and in those who are active and working.

1.2.3.3   Hemodialysis

In the United States, over 500 000 ESRD patients were on HD as their primary mode of RRT in 2019, of which approximate 492 000 individuals receive treatment in-center[17]. Patients on HD require short daily treatments, typically thrice weekly for 3 to 5 hours per session or long nocturnal treatment every other night for 8 to 10 hours per session[50,51]. Regardless of the type of HD treatment, all patients require a well-functioning, durable vascular access for the performance of the treatment. The three major types of vascular access are: primary arteriovenous (AV) fistulas, synthetic arteriovenous fistulas (AV graft), and a central venous catheter (Figure 1-2) [52,53]. Due to its longevity and fewer probable complications, the AV fistula is the preferred vascular access for HD.
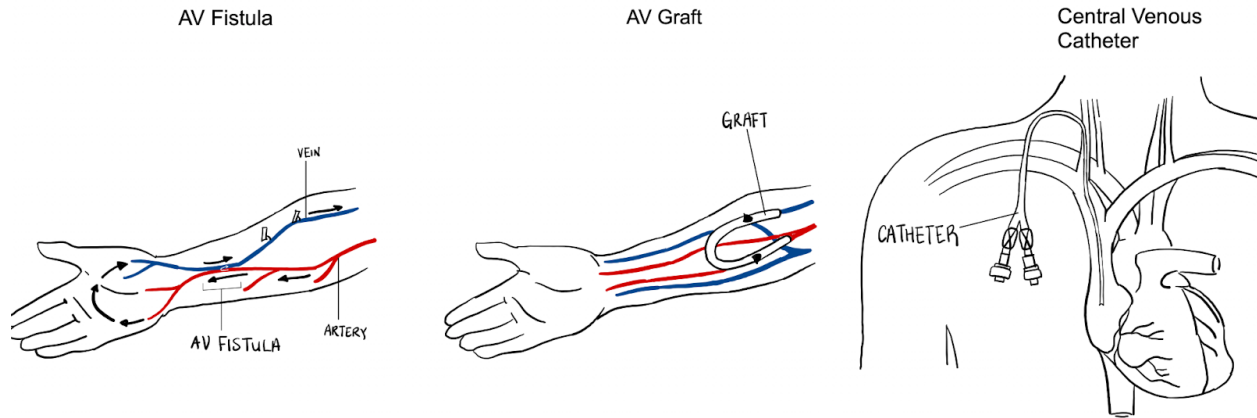
Figure 1-2 Types of hemodialysis vascular access. Recreated from *Challenges and novel therapies for vascular access in haemodialysis* by Lawson, Niklason and Roy-Chaudhury, 2020.

At the start of HD treatment, the two dialysis lines are connected to the vascular access of the patient; the arterial line allows the flow of blood from the body to the dialysis machine and the venous line allows the filtered blood to return from the dialysis machine to the body (Figure 1-3) [54]. To prevent coagulation of blood within the extracorporeal circuit, heparin is infused into the dialysis line. The exchange of water molecules, electrolytes and toxins occur once the blood reaches the dialyzer, through a semi-permeable membrane. On the opposing sides of the membrane, there is countercurrent flow of blood and dialysate fluid allowing the equilibrium of solute concentration to be reached as solutes of specific size and charge pass through the semi-permeable membrane. HD employs two processes for solute and fluid clearance: diffusive and convective [33]. Diffusive clearance involves the movement of solutes down a concentration gradient, from region of high concentration to low concentration and is most effective in the movement of small solutes. Water molecules "follow" the solutes and its exchange is facilitated by the osmotic gradient. Convective clearance, also known as ultrafiltration, is the most effective way of removing fluid, utilizing the difference in transmembrane pressure to forcibly push water through the membrane down a pressure gradient. Along this bulk transfer of plasma water, a great proportion

of middle-sized water-soluble molecules (500-5000 Dalton) are dragged across the membrane for removal. Dialysate that has been used is pumped out of the dialysis machine for disposal and the filtered blood is returned to the patient through the venous line.

Adequacy of HD treatment refers to the delivery of the treatment dose that is sufficient enough to promote the patient's well-being[55]. It is conventionally assessed by the clearance of small solutes, mainly urea. Urea clearance is commonly represented in terms of urea reduction ratio index, quantified using acquired levels of blood urea nitrogen before and after the treatment[56] and through the quantification of Kt/V index where, K is the dialyzer blood water urea clearance (L/hr), t is the dialysis time (hr), and V is the volume (L) of water in the body[57]. The Kt/V index is the most widely used and a minimum single pool dose of 1.2 per dialysis is recommended.
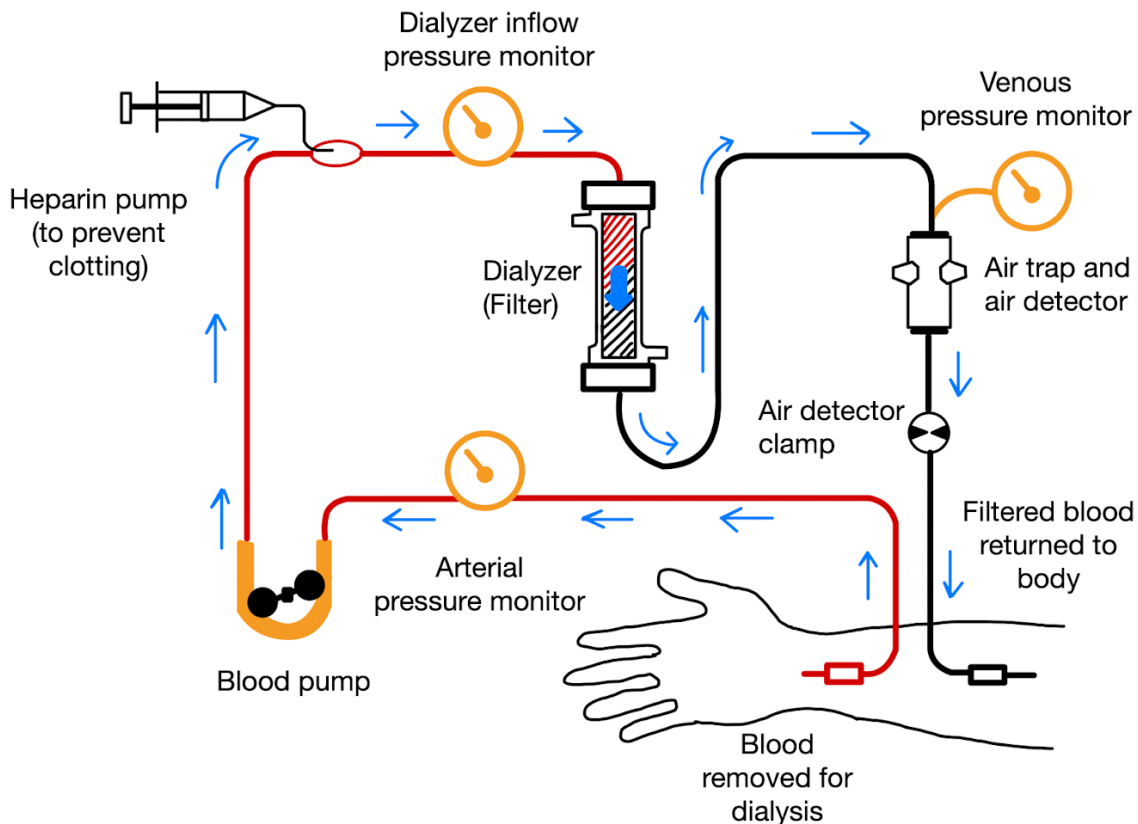
Figure 1-3 Hemodialysis circuit diagram. Recreated from *Hemodialysis* by NIH: National
Institute of Diabetes and Digestive and Kidney Disease, 2018.

1.2.4 Complications of HD

Common acute CV complications that occur with HD treatment are hypotension,
hypertension, and arrythmias[58]. A reduction in BP or hemodynamic instability during HD is a
direct response to the ultrafiltration and the rapid removal of fluid in attempts to achieve dry
weight[59–67]. There are a few approaches to managing hypotension during dialysis. For example,
intradialytic hypotension can be managed by reducing and maintaining a steady, constant
ultrafiltration rate as well as increasing the dialysate sodium concentration to prevent decline in
plasma osmolality and protect extracellular volume[68–71]. Recent studies have also demonstrated

14

controlling the temperature of the dialysate to cool or isothermic (below 36.5°C) levels can contribute to hemodynamic stability and improve patient tolerability to dialysis treatment[72–76].

While ultrafiltration during HD reduces BP in most patients, up to 15% of HD patients demonstrate paradoxical increases in BP during dialysis, and this is referred to as intradialytic hypertension[77–79]. Furthermore, hypertension outside of dialysis is prevalent in 70-90% of patients and is associated with adverse events. Management of intradialytic hypertension includes reduction in dry weight, antihypertensive pharmacological therapy, increasing the frequency of dialysis sessions, and reducing dialysate sodium concentration.

Ventricular and atrial arrhythmias are common causes of sudden cardiac death in the HD population[80–89]. Studies have utilized implantable loop recorders for continuous monitoring of irregular heart rhythms and have demonstrated high prevalence of bradycardias and atrial fibrillations[90,91]. It was revealed that rates of clinically significant arrhythmias were highest at the first dialysis session of the week in patients receiving HD thrice weekly and the frequency of episodes increased during the last twelve hours of the interdialytic interval. These findings could be due to the fluctuation in fluid and electrolyte levels during dialysis and other studies have suggested dialysate potassium concentration to be a contributing factor. However, the mechanism of HD induced arrhythmia remain unclear and further investigation is needed.

1.2.4.1   Effects of HD induced Circulatory Stress

1.2.4.1.1   Endothelial Dysfunction

The proper functioning of the microcirculation and its endothelial cell layer is important for CV function.[92] Endothelial dysfunction is known to occur in CKD patients undergoing HD,

possibly contributing significantly to CV dysfunction such as defective BP control, impaired

vasodilation, ischemic tissue injury, and increased inflammation[93–95].

The mechanisms by which endothelial dysfunction contributes to CV dysfunction include

impaired release of endothelial nitric oxide (NO) secondary to reduced endothelial NO synthase

activity[93,94]. NO is a vasodilator, an anti-inflammatory, and an inhibitor of platelet aggregation[96,97].

Impaired vasodilation results in impaired circulatory autoregulation which has implications for

altered perfusion in vascular beds such as the heart and brain, especially in situations of circulatory

stress such as during dialysis. Loss of the anti-inflammatory and anti-platelet effects of NO due to

endothelial dysfunction may exacerbate the pro-inflammatory state of CKD patients and contribute

to atherosclerosis[98–100] in this population.

It is thought that the dysregulation of the renin-angiotensin-aldosterone system in CKD

induces endothelial dysfunction primarily due to the dysregulation of angiotensin II[101,102]. This

assertion is supported by prior studies observing that increased levels of angiotensin II increased

the levels of reactive oxygen species and promotes vascular inflammation[94,103]. It has also been

shown that increased levels of reactive oxygen species results in oxidative excess and leads to

diminished NO. In fact, in patients with CKD, markers of oxidative excess correlates with markers

of endothelial dysfunction.

As discussed previously, one of the most common causes of CKD and ESRD is

nephropathy secondary to diabetes. In diabetes, insulin signaling is altered, downregulating the

expression of endothelial NO synthase activity, resulting in decreased NO release, with the CV

consequences as described above[104,105]. Advanced glycation end products are also produced in

states of hyperglycemia such as diabetes, which also impair endothelial function[106–108]. With

reduced GFR in CKD, clearance of advanced glycation end products is impaired, creating a vicious cycle of endothelial dysfunction.

Importantly, endothelial dysfunction may be induced by the life-saving HD treatment that patients with renal disease rely on. Coupled with the fact that endothelial dysfunction may not only be related to cardiovascular disease such as impaired myocardial perfusion and contractility, but may in fact precede it, it is crucial that endothelial dysfunction be sensitively assessed in the CKD and hemodialysis population. As discussed further in this thesis and as demonstrated in the work, one method to measure endothelial dysfunction is via plasma syndecan-1 levels.

Endothelial dysfunction has been assessed by quantification of injury to the endothelial surface layer. The endothelial glycocalyx is a protective barrier overlying the monolayer of endothelial cells that line the blood vessels, and its degradation is an early indicator of endothelial damage[109,110]. The glycocalyx is comprised of cell-bound proteoglycans (e.g., syndecan protein family) which are bound to glycosaminoglycan side chains (e.g., heparan sulfate), and this layer protects the endothelium from damage by direct interaction with ions and proteins that are present in the plasma[109]. Degradation of the endothelial glycocalyx can result from sepsis, prolonged hyperglycemia, and ischemic-reperfusion injury, which ultimately causes 'shedding' of its constituents into the circulation. Syndecan-1 is a protein in the heparan sulfate proteoglycan, and elevation of this glycocalyx constituent in serum correlate with damage to the glycocalyx[111]. Clinical studies have shown glycocalyx damage in kidney disease that is associated with endothelial dysfunction and the level of glycocalyx damage, marked by increased glycocalyx constituent 'shedding', is proportional to kidney dysfunction (i.e., markers of glycocalyx shedding increased incrementally with CKD stages)[111,112]. This marked damage to the glycocalyx is the precursor to injury or dysfunction of the endothelium.

Exactly how glycocalyx damage results in endothelial dysfunction is still an active area of research. One possible mechanism is that the molecular structure of glycocalyx molecules such as syndecan-1 results in their oscillation when exposed to fluid (blood) flow, generating a lifting force that keeps red blood cells away from the endothelial cell and allows them to glide with minimal friction along the vascular endothelium[113,114]. The electrostatic charge of the glycocalyx also helps with this. Damage to the glycocalyx results in the loss of this lifting force, increasing friction to blood flow, with implications for microvascular resistance and perfusion[113,114]. A second possible mechanism is the mechanical coupling between the glycocalyx and the endothelial cell's actin cytoskeleton[113,114]. Shear forces on the glycocalyx creates tension on the actin cytoskeleton triggering a signaling cascade resulting in production of NO. This mechanical relationship is modulated by osmotic stress and hydrostatic stress as these stresses can result in remodeling of the actin cytoskeleton[113,114]. This has implications for the endothelial cell's ability to produce NO, with the resulting cardiovascular consequences as discussed above.

1.2.4.1.2   Large Vessel Disease in Uremia

In non-CKD patients, atherosclerosis is characterized by plaque development in the intimal layer of the arteries. Lipoproteins composed of proteins, phospholipids and lipids are deposited in the underlying smooth muscle of the intima layer, initiating proliferation of fibrous tissues[115]. With the formation of the atherosclerotic plaque (Figure 1-4), the conduit function of the artery is disturbed by the restriction of blood flow and induces ischemia to tissues downstream of the narrowed region, leading to myocardial damage. Risk factors of atherosclerosis in non-CKD population include high cholesterol, hypertension, smoking, diabetes mellitus, obesity, and age.
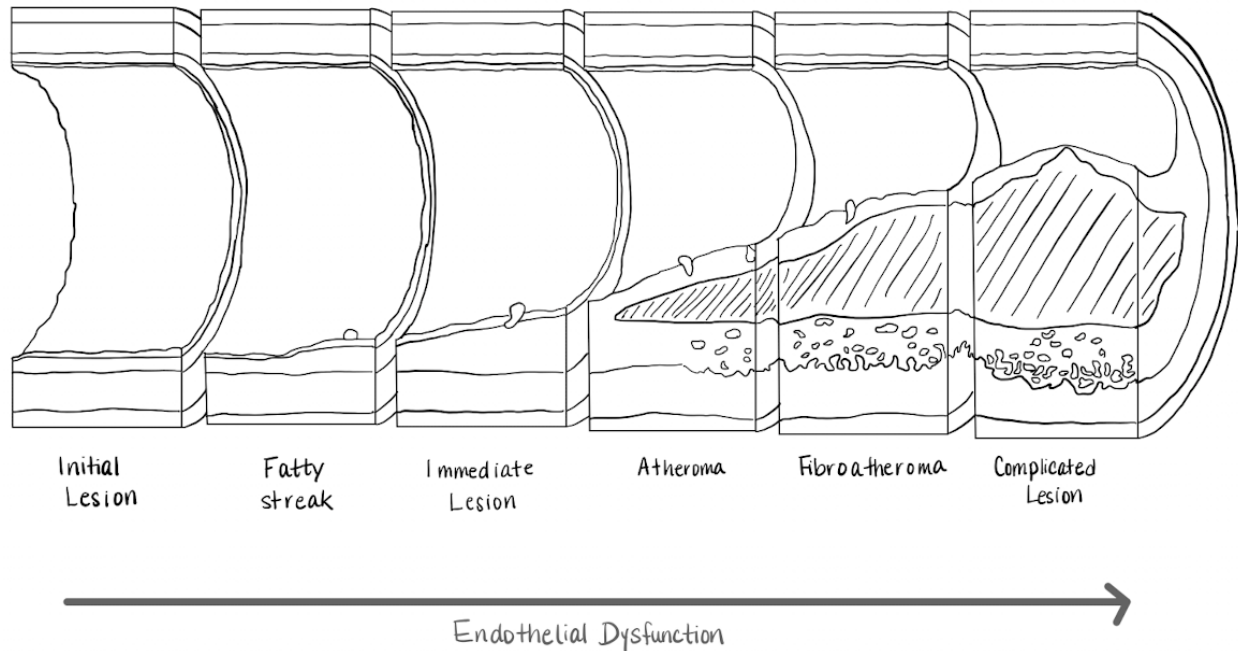
Figure 1-4 Progression of atherosclerosis. Recreated from *Late complications of atherosclerosis* by Wikimedia Commons, 2020.

Coronary artery disease (CAD) is highly prevalent in ESRD and the underlying pathogenesis of atherosclerosis in this cohort of patients is from the local inflammatory response to endothelial dysfunction. In autopsy studies, coronary plaques in ESRD have been documented in its advanced stages with heavy calcification in the medial layer, deposited as phosphate, with an increased media thickness which differed from the mostly fibroatheromatous plaques of non-renal patients[116] (Figure 1-5). The degree of calcification was also shown to increase with longer exposure to dialysis treatment[117,118]. Investigations to date questioned the mechanism of accelerated atherosclerosis and it was hypothesized that the rate of plaque growth in CKD increased with decrease in renal function, which possibly was responsible for the high CV event rate in this group. However, the acceleration and nature of atherosclerotic plaque in ESRD remains

a topic of debate[119–123]. Diagnosis of CAD in CKD is discussed further in section 1.3.4.1 of this chapter.

	Normal Coronary Artery	**CKD related CAD**		**Non-CKD CAD**
Intima	No calcification No Plaque Contains normal endothelial cells	No atherosclerotic plaque	Heavily calcified atherosclerotic plaque	Calcified atherosclerotic plaque
Media	No calcification Organized smooth muscle	Calcification	Calcification	Generally, no calcification

Figure 1-5 Morphology of coronary artery in chronic kidney disease. Recreated from *Diagnosis and management of atherosclerotic cardiovascular disease in chronic kidney disease: a review* by Mathew et al., 2017.

Risk factors for atherosclerosis in CKD include mineral bone metabolism, vascular calcification, uremic toxins, inflammation, oxidative stress, and endothelial dysfunction; all of which are commonly experienced in patients undergoing HD[120,124]. In this thesis, we aim to further evaluate the compounding effects of CAD and HD-induced circulatory stress on cardiac function.

1.2.4.1.3 Structural and Functional Cardiac Injury

Although dialysis is a life-saving treatment for patients with CKD, their CV comorbidities make them susceptible to HD-induced cardiac injury. In this patient population, there is a high prevalence of CAD[125], as well as increased peripheral artery stiffness[126]. Increased peripheral artery stiffness results in increased peripheral vascular resistance and ultimately left ventricular hypertrophy (LVH) a common finding in CKD patients[127]. Microcirculatory changes in patients

with CKD have also been reported. Together, larger vessel and microcirculatory changes result in reduced coronary flow[128–130], while LVH result in increased myocardial demand. The reduced ability to increase coronary blood flow to match the increased myocardial demand creates a flow-demand mismatch, reducing the ischemic threshold and creating susceptibility to demand ischemia.

Because of this, the circulatory stress imparted by dialysis treatment is enough to induce acute reversible segmental myocardial hypoperfusion and contractile dysfunction[131–133]. Repeated dialysis treatments cause recurrent ischemic injury, although initially reversible, eventually accumulates into long-term loss of segmental and global cardiac contractility. The amount of injury may be related to the amount of relative hypotension experienced by the patient during HD as well as the rate of ultrafiltration during dialysis. Defective BP control due to impaired baroreflex sensitivity, decreased vascular compliance, and microvascular/endothelial dysfunction in CKD patients may also contribute to the amount of injury[126].

However, the relative contributions of the macro-cardiac circulation (i.e., CAD) versus the micro-cardiac circulation (i.e., endothelial dysfunction) remains unclear. This exact question is investigated in this thesis.

If relative hypotension is one of the main factors determining the amount of HD-induced cardiac injury, it then follows that therapies targeted at improving the hemodynamic response during dialysis may be protective against HD-induced cardiac injury. As discussed previously, therapies that have been studied include dialysate cooling[73–76], remote ischemic preconditioning[134,135], and intradialytic exercise[136–152]. Intradialytic exercise as a cardioprotective therapy is further investigated in this thesis.

1.3 Imaging Modalities to Assess HD-induced Myocardial and Microcirculatory Injury

The acute changes to a patient's heart function during HD treatment are still not fully elucidated. Imaging offers a non-invasive means to explore these changes and to shed light on how to effectively address the associated clinical concerns. Currently available imaging modalities can identify morphological and functional changes to the heart during dialysis and may be sensitive enough to detect the heart's response to cardioprotective interventions. Here, we describe and compare currently available and emerging modalities for intradialytic myocardial assessment and discuss the latest insights gleaned from recent imaging studies exploring HD-induced myocardial dysfunction. In particular, we focus upon new developments in cardiac CT which can allow the totality of cardiac structure and function to be imaged, at rest and under the stress of HD.

1.3.1 Positron Emission Tomography

A number of research studies have investigated the functional changes within the myocardium associated with dialysis treatment using position emission tomography (PET). Radioactive tracers such as ^{13}N-Ammonia or ^{15}O-labeled water are administered intravenously to quantitatively measure myocardial perfusion[133,153]. A metric called myocardial perfusion reserve (MPR) can then be calculated from perfusion measurements at rest and during a stress test, and is defined as the global myocardial perfusion at stress normalized to the myocardial perfusion at rest[154,155]. MPR reflects the capacity at which the vascular bed responds to a maximal increase in perfusion and is considered a surrogate measure of endothelial dysfunction. To ensure a maximal increase in perfusion during stress, a pharmaceutical agent is typically administered to induce systemic vasodilation. Adenosine, dobutamine, and dipyridamole are commonly used vasodilators during this test.

Research teams have conducted intradialytic PET studies investigating the change in myocardial perfusion during a single dialysis session. A case study reported a significant decrease in myocardial perfusion at peak dialysis stress (220 minutes of HD) relative to both baseline and early dialysis (30 minutes of HD). Similarly, McIntyre *et al.* reported an acute decrease in global myocardial perfusion during HD[133]. They also showed that PET measurements can be complementary to ultrasound measurements, as myocardial segments developing RWMAs had significantly greater reductions in perfusion.

Despite its use in current clinical practice, a major limitation of PET imaging is its accessibility. PET tracers with the best performance have short half-lives and require additional on-site access to cyclotron facilities to produce the isotopes for immediate utilization. Another drawback of PET imaging is its poor spatial and temporal resolution which limits the morphological or anatomical information it provides. Due to the low spatial resolution of PET, CT images may also be acquired concomitantly for anatomical reference using a PET/CT hybrid scanner. This provides additional structural information but no additional information about contractile function.

1.3.2 Magnetic Resonance Imaging

1.3.2.1   Four Dimensional MRI to Assess Contractile Function

Magnetic resonance imaging (MRI) is a powerful and versatile modality capable of obtaining detailed local and global mechanical function of the myocardium. Zerhouni *et al.* was first to describe the use of tissue tagging to track the motion of the myocardium in four-dimensions[156]. Tissue tagging is achieved by using magnetization saturation to null the signal from specific spatial locations in the tissue. These signal voids can then be used as dark fiducial markers to track movement, allowing the calculation of mechanical parameters that describe the regional

wall motion of the myocardium in HD population[157]. These parameters include strain, strain rate, twist and torsion.

Strain is defined as the ratio of the change in length of the myocardial fibers to their initial dimension and can be measured in 3D[158,159]. Measurement of radial, circumferential, and longitudinal strain enables the calculation of the 3D deformation of myocardial wall. The rate at which strain changes over time can also be determined. Both 3D deformation and strain rate are considered measures of left ventricular (LV) function and are sensitive indicators of ventricular wall remodelling. On the other hand, twist and torsion are parameters that indicate the amount of opposing rotation between the base and apex of the heart and are considered to be sensitive to changes that occur in both systolic and diastolic dysfunction.

There are many inherent limitations of 4D MRI. As tissue tagging involves a continuous sequence of (radiofrequency) pulses to create the signal voids, increased energy deposition in the tissue and non-uniform tag intensity can occur[158]. Also, because the tags are created using magnetization saturation, they will fade with time due to T_1 relaxation. This can lead to inaccuracies in the measurement of myocardial wall motion especially in diastole.

1.3.2.2 Exogenous and Endogenous Contrast MRI for Assessment of Perfusion

In exogenous contrast-enhanced MRI, a gadolinium-based contrast agent is administered to the patient prior to the scan. A dynamic image is acquired, and a tracer kinetic model is applied to the measured local blood volume to estimate perfusion[160]. This validated technique offers high spatial and temporal resolution images of the heart. However, in patients with impaired kidney function, there is a risk that injecting gadolinium could precipitate nephrogenic systemic fibrosis[161]. Newer formulations of gadolinium contrast have reduced these risks but use in patients

receiving maintenance dialysis is still discouraged. Therefore, in a cohort of CKD population, taking advantage of an endogenous tracer of blood flow is a favorable option.

Arterial spin labelling (ASL) is a non-invasive imaging technique that magnetically labels the protons of water in the blood and uses it as a free diffusible endogenous tracer[155,160]. Protons are labelled by an inversion pulse, which inverts its magnetic spin. After a delay to allow the labelled blood to flow into and perfuse the tissue of interest, the tissue is imaged. As perfusion occurs, the labelled protons in the blood exchange with protons in the tissue, resulting in a reduction of signal. A perfusion weighted image can then be generated by taking the difference between a labelled and a non-labelled image.

A short-term trial studying the effects of hemodiafiltration, and HD on CV response utilized intradialytic ASL-MRI to detect a decrease in myocardial perfusion during dialysis treatment to baseline[157]. These results are broadly comparable to studies done using PET, suggesting that MRI, a more accessible technique, may be able to provide similar information to PET.

1.3.2.3 MRI to Assess Tissue Viability

There are many specialized MRI sequences that can be used for assessing specific changes to the myocardium. For example, T_1-weighted images can be used to detect fat, fibrosis, and calcification, while T_2-weighted images can identify areas of infarct, edema, and inflammation[162–164]. Both types of images can be used concurrently to study the progression of a chronic CV disease over time, as well as the identification of viable myocardium post ischemic injury[165–168].

Cardiac MR imaging remains challenging because of the long acquisition time, which needs to be minimized to reduce the effects of inherent cardiac and breathing motion. In almost all

cases, steady breathing or breath-hold techniques are necessary for producing high quality images. Improper breath-holds result in motion artefact and inaccurate measurement of perfusion. Although patients with CV disease could benefit from MR imaging, many struggle to comply with breathing directions and coaching; especially when multiple repeated acquisition is necessary for signal averaging to improve the signal-to-noise ratio (e.g. ASL). In HD research studies, combining high field magnets with HD equipment is very challenging and further limits the application of these techniques to HD-based CV challenges.

1.3.3 Echocardiography

Echocardiography is an imaging tool that uses high frequency ultrasound waves to produce two-dimensional images of the heart in real-time. Ultrasound is a popular imaging modality because it is readily accessible in the clinic and can be used at the bedside. Operators can quickly image the heart from different directions by positioning the ultrasound probe accordingly. Each cardiac view is useful in examining the overall morphology of the heart, its ability to pump blood, and the condition of the heart valves. In addition, stenosis, hyper- or hypotrophy, and tumor growth can be detected with ultrasound.

Cardiac ultrasound images can also be processed to determine global and segmental longitudinal strain of the myocardium and assess regional wall motion abnormalities (RWMA), providing a direct measurement of the contractile performance of the heart. The development of RWMAs reflects myocardial segments that reduce in contractile function during dialysis as a consequence of regional ischemia. Assa *et al.* analysed echocardiography data from 105 patients and detected HD-induced RWMAs in 29 of them[169]. In a similar proportion of patients, Dubin *et al.* reported worsening RWMAs due to HD and found that patients with a previous diagnosis of heart failure had a higher risk of worsening RWMA during HD[131]. Since dialysis patients who

develop RWMAs during HD have a higher 1-year mortality, intradialytic echocardiography may be able to identify patients who are more vulnerable to complications associated with dialysis.

Measuring RWMAs with echocardiography could also be a useful metric for assessing physiologic response to interventions. An exploratory study by Penny et al., which investigated the effect of exercise for immediate cardio-protection against ischemia, demonstrated that intradialytic exercise is an effective preconditioning approach that significantly reduced the incidence of acute HD-induced cardiac injury, as quantified by a decrease in RWMAs[148].

LV ejection fraction and LV systolic function can also be quantified using echocardiography, providing a measurement of heart function. In addition, recent advancements in echocardiography have proven capable of acquiring myocardial perfusion information in real time with continuous intravenous administration of a contrast agent (e.g., microbubbles)[170]. Dynamic perfusion measurements provide invaluable information about the microvasculature abnormalities of the myocardium. However, perfusion imaging with myocardial contrast echocardiography has yet to be adopted in HD studies for several reasons. First, a very low mechanical index (related to the energy delivered by ultrasound) must be maintained to visualize the injected contrast. Second, echocardiography comes with an inherent limitation in image resolution. Third, image artefacts are common when imaging the heart as a result of its dynamic contractile movement, its positioning adjacent to the lungs, and its motion during respiration. Many other imaging modalities have overcome these limitations and will be discussed later on.

1.3.4 Principles of Computed Tomography Imaging

1.3.4.1 Coronary CT Angiography

Coronary angiography (CA) is not a tool for imaging acute dysfunction during HD. Rather, it is used to assess the chronic effects of renal impairment and dialysis on the coronary arteries to provide an assessment of flow limiting stenosis in the coronary circulation. Although traditionally performed with invasive cardiac catheterization, CA can be performed with different non-invasive imaging modalities, many of which enable three-dimensional acquisition of coronary angiograms in high resolution. Not only can CA assess the degree of luminal narrowing, but it can also detect areas of calcification within the wall of the coronary arteries themselves – first quantified by Agatston[171].

The use of CA in HD patients is considered clinically relevant as excess coronary artery calcification (CAC) is common in this patient population and is associated with high CV risk[172–177]. It is a common misconception that the origins of CV mortality in all stages of CKD are equivalent. In non-uremic CKD patients, arterial calcification is predominantly due to atheromatous plaques derived from the vessel intima[130,178]. For these patients, plaque burden is characteristically high and progresses rapidly. In patients with worsening degrees of CKD (and in particular those requiring dialysis, i.e. uremic CKD patients) the origin of the calcifications is different from that of non-uremic patients. Calcifications in uremic CKD patients commonly express bone-associated protein as well as the core-binding factor α-1, and arise from the arterial media rather than the intima[176,178]. CAC scoring used to assess the amount of calcium deposits in the arteries provides a measurement of intimal calcification (as a measure of plaque burden) and medial calcification (effecting arterial compliance). The CAC score is an essential measure for CV risk stratification as both of these entities contribute to increased CV risk.

Conventional cardiac CT angiography provides accurate assessment of coronary arterial calcifications (as compared to other imaging modalities such as intravascular ultrasound, fluoroscopy, and MRI)[179,180]. Contrast-enhanced CT angiography not only quantifies vascular calcifications, but also detects coronary artery stenoses which can put a patient at risk for HD-induced myocardial ischemia. However, conventional CT angiography provides no functional information on myocardial viability. To overcome this limitation, current studies have adopted new cardiac CT protocols that allow simultaneous acquisition of perfusion and angiography in a single dynamic heart scan. These protocols increase the amount of information we can obtain from the patient, while keeping radiation exposure low.

1.3.4.2 Overview of Myocardial CT Perfusion Imaging

In the recent decade, CT scanners have become widely used with the introduction of high slice system from 64 to 256, to even 320-slice scanners. The newer generation of scanners utilize faster gantry speed rotation, improved image reconstructive software, and a more sensitive detector to permit ultra-low dose cardiac imaging[181,182]. A faster gantry rotation speed can reduce cardiac and breathing motion artefact during a scan, while improved iterative and model based reconstructive software can significantly reduce the number of x-ray projections required for diagnostic quality thereby lessening the radiation dose. In addition to technological advancement of the scanner itself, new acquisition techniques have also been introduced with the goal of achieving clinical utilization of cardiac CT. So far, these techniques have yet to make their way into clinical practice but are available for research purposes.

As discussed previously, current clinically available imaging modalities are each individually useful in acquiring specific information about particular aspects of myocardial dysfunction. For patient assessment and CV research, multiple imaging modalities are usually used

in combination to obtain a more complete understanding of the pathophysiology at hand. This requires additional resources and time that often make the use of multi-modality imaging infeasible in the clinic and impractical in a research setting. In particular, using multiple imaging modalities during an HD session to assess intradialytic changes in myocardial function is very difficult to accomplish. However, an advanced CT system in parallel with novel imaging techniques that can acquire high quality information about multiple aspects of myocardial dysfunction in one rapid scanning session would be ideal for assessing the structural and functional changes of the heart in response to HD.

Dynamic contrast-enhanced (DCE)- CT is an x-ray imaging modality that quantifies the enhancement of tissue over time as a bolus of injected iodine contrast washes in and out of the tissue. A common concern with dynamic imaging is an increase in radiation exposure resulting from the frequent number of scans per imaging session. To overcome this, recent advancements in CT scanners have made prospective ECG-gating possible, allowing for the reduction of effective radiation dose to the patient from 12mSv to 3mSv. This is because images are acquired during a specific phase (often diastolic) of the cardiac cycle rather than over the whole cardiac cycle. A further benefit is that this approach also reduces the cardiac motion between each image slice. This is especially important because motion artefacts hinder the accuracy of perfusion measurements. To further reduce radiation exposure, there are approaches including decreasing the tube voltage or acquiring half the number of x-ray projections, but discussion of these techniques is beyond the scope of this article.

Following a dynamic scan, a tracer kinetic model that mathematically describes the delivery of contrast from the intravascular to the extravascular components of the tissue is applied to the DCE-CT image to generate functional maps of physiologic parameters such as myocardial

30

perfusion, blood volume, mean transit time, and extravascular contrast distribution volume (ECDV). Thus, a single dynamic scan can simultaneously provide valuable functional information about multiple aspects of myocardial dysfunction.

1.3.4.3 Dynamic CT Imaging for Myocardial Perfusion

Cardiac DCE-CT is a comprehensive imaging technique that can extract information on myocardial dysfunction, ischemia, tissue viability, fibrosis, edema, and coronary calcification from a single scan. It can also track changes in cardiac morphology during the progression of dialysis treatment. In the case of myocardial dysfunction during HD, it is well established that most treatment sessions introduce recurrent ischemic injury and stunning of myocardial segments. Following repeated treatment and recurring ischemic episodes, affected tissue will no longer be viable. With DCE-CT imaging, this can easily be identified as hypoperfused regions of interest in a myocardial perfusion map (Figure 1-6) that correspond to decreased blood volume. As the repetitively stunned myocardial tissue becomes irreversibly damaged over time, cell membranes within the region degenerate and become 'more permeable', allowing extravasation of iodine contrast to the intracellular space. To quantitatively distinguish viable from infarcted tissue, consideration of the intracellular compartment is necessary. To do this, So *et al.* developed the extended Johnson-Wilson-Lee tracer kinetic model and defined a new functional parameter, ECDV[183,184]. Quantitative measure of ECDV can also be used to detect myocardial fibrosis in HD as the same tracer kinetic model can be used to demonstrate an increased contrast distribution to the fibrotic tissue relative to normal tissue.
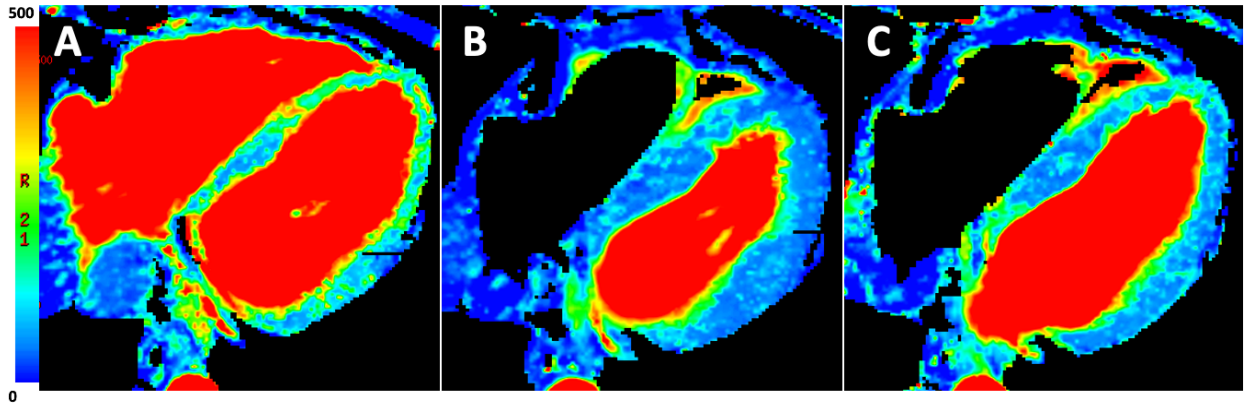
Figure 1-6 Morphological change in LV myocardium during an intradialytic CT imaging session. Perfusion images of HD patient at three time points: A) Before dialysis B) Peak dialysis; 225 minutes into HD C) Post dialysis. A decrease in global myocardial perfusion (ml/min/100g) is also demonstrated throughout the dialysis session. Adapted from *Current and novel imaging techniques to evaluate myocardial dysfunction during hemodialysis* by Hur and McIntyre, 2020.

Perfusion heterogeneity has been reported as a marker of endothelial dysfunction in the dialysis population. In 2018, Kharche and colleagues quantified myocardial perfusion heterogeneity in peritoneal dialysis patients using DCE-CT via fractal dimensions to test whether or not dialysis increased heterogeneity[185]. The same approaches can be applied to HD. Qualitatively, a case study demonstrated a significant increase in perfusion heterogeneity at peak- and post-HD relative to baseline (Figure 1-7). A patient with a prior history of peritoneal dialysis demonstrated an increase in perfusion heterogeneity during HD (Figure 1-8), consistent with previous studies that concluded HD stresses the myocardium more than PD.
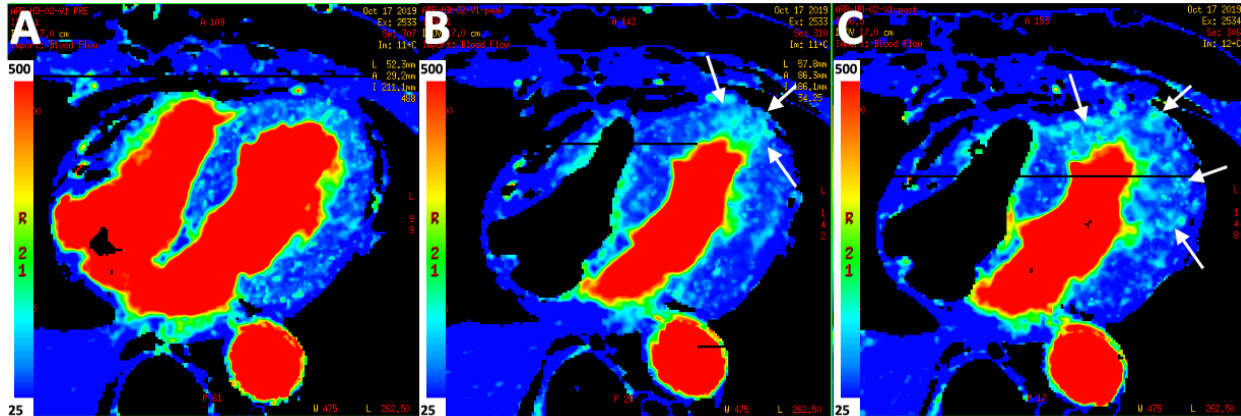
Figure 1-7 Myocardial CT perfusion (ml/min/100g) image of a HD patient at pre-dialysis (A), peak-dialysis (B), and post-dialysis (C). White arrows denoting increased perfusion heterogeneity throughout the left ventricular myocardium as the patient progresses through dialysis treatment. Adapted from *Current and novel imaging techniques to evaluate myocardial dysfunction during hemodialysis* by Hur and McIntyre, 2020.
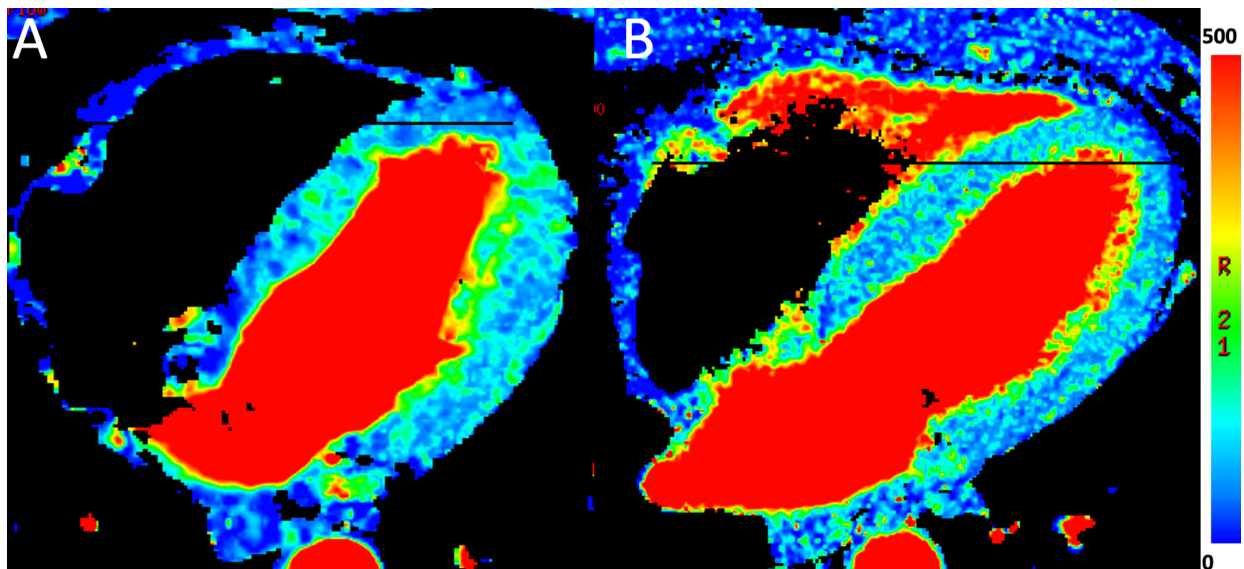
Figure 1-8 Myocardial CT perfusion (ml/min/100g) image of a single patient. Panel A during peritoneal dialysis and panel B during HD. It is qualitatively evident by the uneven, speckle-like perfusion effect seen in panel B that there is greater perfusion heterogeneity during HD treatment compared to peritoneal dialysis in the same subject. Adapted from *Current and novel imaging techniques to evaluate myocardial dysfunction during hemodialysis* by Hur and McIntyre, 2020.

There is a lot of potential for DCE-CT in terms of studying the hemodynamic effects of HD treatment and assessing HD patient responses. Not only can it measure multiple markers of myocardial dysfunction with high spatial resolution, it can do so in a rapid, single dynamic scan that allows patients to free-breathe. With the availability of these various radiation-reducing measures, the clinical benefit from the high-quality data provided by DCE-CT would outweigh the risks of radiation. The accessibility of CT and the short acquisition times offer additional advantages that enable increased clinical throughput. Multiple CT approaches (e.g. CT perfusion and CT angiography) can also be performed simultaneously to acquire even more complete morphological and functional information, as discussed previously. However, it is important to note one limitation to this technique. When generating functional maps such as perfusion, blood volume, and mean transit time maps, a tracer kinetic model must be used. This tracer kinetic model is selected based on the pathophysiology specific to a disease. In other words, different models are used for different pathophysiology, and selecting the correct model is essential for accurate quantification of functional data.

1.3.4.4   Risks Associated with CT Contrast Agents

Contrast-induced nephropathy has historically been an important concern for those with renal impairment. Most clinical research involving CT has therefore excluded participants with low residual renal function. However, recent studies investigating the effect of contrast agents on residual renal function found no evidence of contrast-induced nephropathy[186]. The benefits of contrast-enhanced imaging in patients with high CV mortality rate therefore outweigh the potential harm.

1.4 Motivation and Objectives of Thesis

The overarching goal of this thesis work is to study the acute effect of HD on the circulation at multiple levels—macrovascular, microvascular, and at the endothelial level—under conditions of intradialytic exercise and varying levels of dialysate sodium concentration. To address this overarching hypothesis, this thesis has been divided into three research projects (Chapters 2, 3, and 4) and the individual objectives are as follows:

Project 1: *The effect of coronary artery disease on myocardial perfusion and stunning response to HD treatment*

- o Examine how coronary artery disease affects global myocardial perfusion during HD

- o Examine how coronary artery disease affects segmental myocardial perfusion during HD

- o Examine the effects of coronary artery disease on myocardial stunning during HD

Project 2: *Investigating the role of dialysate sodium concentration on the endothelium and microcirculation during HD*

- o Examine endothelial injury and microvascular perfusion defect as a result of HD treatment

- o Study the effect of dialysate sodium on endothelial injury and microvascular perfusion

- o Explore the relationship between endothelial injury and microvascular perfusion with respect to dialysate sodium concentration

Project 3: *Assessment of intradialytic exercise for cardioprotection to HD-induced circulatory stress*

- Investigate the acute effect of intradialytic exercise on the endothelium during HD

- Examine how intradialytic exercise affects global myocardial perfusion during HD

- Assess whether or not intradialytic exercise improves ischemic tolerability of HD treatment through measures of myocardial stunning

1.5 References

1. Wallace MA. Anatomy and Physiology of the Kidney. *AORN J.* 1998;68(5):799-820. doi:10.1016/S0001-2092(06)62377-6

2. Moinuddin Z, Dhanda R. Anatomy of the kidney and ureter. *Anaesthesia and Intensive Care Medicine*. 2015;16(6):247-252. doi:10.1016/J.MPAIC.2015.04.001

3. Mahadevan V. Anatomy of the kidney and ureter. *Surgery (United Kingdom)*. 2019;37(7):359-364. doi:10.1016/J.MPSUR.2019.04.005

4. Leatherby RJ, Theodorou C, Dhanda R. Renal physiology: blood flow, glomerular filtration and plasma clearance. *Anaesthesia and Intensive Care Medicine*. 2021;22(7):439-442. doi:10.1016/J.MPAIC.2021.05.003

5. Biga LM, Dawson S, Harwell A, et al. Physiology of Urine Formation: Glomerular Filtration. In: OpenStax/Oregon State University; 2019.

6. Kaufman DP, Basit H, Knohl SJ. Physiology, Glomerular Filtration Rate. *StatPearls*. Published online July 18, 2022. Accessed August 14, 2022. https://www.ncbi.nlm.nih.gov/books/NBK500032/

7. Renkin EM, Robinson RR. Glomerular Filtration. *http://dx.doi.org/101056/NEJM197404042901408*. 2010;290(14):785-792. doi:10.1056/NEJM197404042901408

8. Makris K, Spanou L. *Acute Kidney Injury: Definition, Pathophysiology and Clinical Phenotypes*. Vol 37.; 2016.

9. Ronco C, Bellomo R, Kellum JA. Acute kidney injury. *The Lancet*. 2019;394(10212):1949-1964. doi:10.1016/S0140-6736(19)32563-2

10. Kellum JA, Romagnani P, Ashuntantang G, Ronco C, Zarbock A, Anders HJ. Acute kidney injury. *Nature Reviews*. 2021;7(52). doi:10.1038/s41572-021-00284-z

11. Sharfuddin AA, Molitoris BA. Pathophysiology of ischemic acute kidney injury. *Nat Rev Nephrol*. 2011;7:189-200. doi:10.1038/nrneph.2011.16

12. Webster AC, Nagler E v., Morton RL, Masson P. Chronic Kidney Disease. *The Lancet*. 2017;389(10075):1238-1252. doi:10.1016/S0140-6736(16)32064-5

13. Kalantar-Zadeh K, Jafar TH, Nitsch D, Neuen BL, Perkovic V. Chronic kidney disease. *The Lancet*. 2021;398(10302):786-802. doi:10.1016/S0140-6736(21)00519-5

14. Cockwell P, Fisher LA. The global burden of chronic kidney disease. *The Lancet*. 2020;395(10225):662-664. doi:10.1016/S0140-6736(19)32977-0

15. el Nahas AM, Bello AK. Chronic kidney disease: The global challenge. *Lancet*. 2005;365(9456):331-340. doi:10.1016/S0140-6736(05)17789-7

16. Kovesdy CP. Epidemiology of chronic kidney disease: an update 2022. *Kidney Int Suppl (2011)*. 2022;12(1):7-11. doi:10.1016/J.KISU.2021.11.003

17. United States Renal Data System. *USRDS Annual Data Report: Epidemiology of Kidney Disease in the United States*.; 2021. Accessed July 18, 2022. https://adr.usrds.org/2021/end-stage-renal-disease/6-mortality

18. Kumar P, Pradeep D, Dabla K. Renal function in diabetic nephropathy. Published online 2010. doi:10.4239/wjd.v1.i2.48

19. Thomas M, Brownlee M, Susztak K, et al. Diabetic kidney disease. *Nature Reviews*. 2015;1. doi:10.1038/nrdp.2015.18

20. Alicic RZ, Rooney MT, Tuttle KR, §|† ‡. Diabetic Kidney Disease Challenges, Progress, and Possibilities. *Clin J Am Soc Nephrol*. 2017;12:2032-2045. doi:10.2215/CJN.11491116

21. Hill NR, Fatoba ST, Oke JL, et al. Global Prevalence of Chronic Kidney Disease-A Systematic Review and Meta-Analysis. Published online 2016. doi:10.1371/journal.pone.0158765

22. Ku E, Lee BJ, Wei J, Weir MR. Hypertension in CKD: Core Curriculum 2019. *American Journal of Kidney Diseases*. 2019;74:120-131. doi:10.1053/j.ajkd.2018.12.044

23. Pugh D, Gallacher PJ, Dhaun · Neeraj. Management of Hypertension in Chronic Kidney Disease. 2019;79:365-379. doi:10.1007/s40265-019-1064-1

24. The Diabetes Control and Complications Research Group. Effect of intensive therapy on the development and progression of diabetic nephropathy in the Diabetes Control and Complications Trial. *Kidney Int*. 1995;47:1703-1720. doi:10.1038/ki.1995.236

25. Kjeldsen SE. Hypertension and cardiovascular risk: General aspects. *Pharmacol Res*. 2018;129:95-99. doi:10.1016/j.phrs.2017.11.003

26. Thurlow JS, Joshi M, Yan G, et al. Global Epidemiology of End-Stage Kidney Disease and Disparities in Kidney Replacement Therapy. *Am J Nephrol*. 2021;52(2):98-107. doi:10.1159/000514550

27. Vanholder R, Gryp T, Glorieux G. Urea and chronic kidney disease: the comeback of the century? (in uraemia research). doi:10.1093/ndt/gfx039

28. Zemaitis MR, Foris LA, Katta S, Bashir K. Uremia. *Urology at a Glance*. Published online July 18, 2022:57-60. doi:10.1007/978-3-642-54859-8_12

29. Rosner MH, Reis T, Husain-Syed F, et al. Classification of Uremic Toxins and Their Role in Kidney Failure. *CJASN*. 1918;16. doi:10.2215/CJN.02660221

30. Lau WL, Vaziri ND. Urea, a true uremic toxin: The empire strikes back. *Clin Sci*. 2017;131(1):3-12. doi:10.1042/CS20160203

31. Vaziri ND, Yuan J, Norris K. Role of Urea in Intestinal Barrier Dysfunction and Disruption of Epithelial Tight Junction in Chronic Kidney Disease. *Am J Nephrol*. 2013;37(1):1-6. doi:10.1159/000345969

32. Fleming GM. Renal replacement therapy review. *Organogenesis*. 2011;7(1):2-12. doi:10.4161/org.7.1.13997

33. Davenport A. Chronic Kidney Failure: Renal Replacement Therapy. *Kidney Transplantation - Principles and Practice*. Published online January 1, 2019:36-50. doi:10.1016/B978-0-323-53186-3.00003-6

34. Ku E, Mcculloch CE, Johansen KL. Starting Renal Replacement Therapy: Is It About Time? *Translational Research: Research Article Am J Nephrol*. 2019;50:144-151. doi:10.1159/000501510

35. Renal replacement therapy and conservative management. *Renal replacement therapy and conservative management*. Published online October 3, 2018. Accessed August 12, 2022. https://www.ncbi.nlm.nih.gov/books/NBK542264/

36. Lin ZH, Zuo L. When to initiate renal replacement therapy: The trend of dialysis initiation. Published online 2015. doi:10.5527/wjn.v4.i5.521

37. Johnson JP, McCauley CR, Copley JB. The quality of life of hemodialysis and transplant patients. *Kidney Int*. 1982;22(3):286-291. doi:10.1038/KI.1982.167

38. Chapman JR. The Recipient of a Renal Transplant. *Kidney Transplantation - Principles and Practice*. Published online January 1, 2019:51-68. doi:10.1016/B978-0-323-53186-3.00004-8

39. Redfield RR, Gupta M, Rodriguez E, Wood A, Abt PL, Levine MH. Graft and Patient Survival Outcomes of a Third Kidney Transplant. doi:10.1097/TP.0000000000000332

40. Poggio ED, Augustine JJ, Arrigain S, Brennan DC, Schold JD. Long-term kidney transplant graft survival—Making progress when most needed. *American Journal of Transplantation*. 2021;21(8):2824-2832. doi:10.1111/AJT.16463

41. Ghoneim MA, Bakr MA, Refaie AF, et al. Factors Affecting Graft Survival among Patients Receiving Kidneys from Live Donors: A Single-Center Experience. *Biomed Res Int*. 2013;2013. doi:10.1155/2013/912413

42. Foroutan F, Friesen EL, Clark KE, et al. Risk factors for 1-year graft loss after kidney transplantation systematic review and meta-analysis. *Clinical Journal of the American Society of Nephrology*. 2019;14(11):1642-1650. doi:10.2215/CJN.05560519/-/DCSUPPLEMENTAL

43. Ingsathit A, Avihingsanon Y, Rattanasiri S, et al. Different etiologies of graft loss and death in Asian kidney transplant recipients: A report from Thai transplant registry. *Transplant Proc*. 2010;42(10):4014-4016. doi:10.1016/J.TRANSPROCEED.2010.09.061

44. Tokgoz B. Clinical Advantages of Peritoneal Dialysis. *Peritoneal Dialysis Internatonal*. 2009;29. Accessed August 14, 2022. www.PDIConnect.com

45. Claudia M, Andreoli C, Totoli C. Peritoneal Dialysis. *REV ASSOC MED BRAS*. 2020;66(1):37-44. doi:10.1590/1806-9282.66.S1.37

46. Mehrotra R, Devuyst O, Davies SJ, Johnson DW. The Current State of Peritoneal Dialysis. *J Am Soc Nephrol*. 2016;27:3238-3252. doi:10.1681/ASN.2016010112

47. Teitelbaum I, Burkart J. Peritoneal Dialysis. *American Journal of Kidney Diseases*. 2003;42:1082-1096. doi:10.1053/S0272-6386(03)01123-5

48. Gokal R, Mallick NP. Peritoneal dialysis. *Lancet*. 1999;353(9155):823-828. doi:10.1016/S0140-6736(98)09410-0

49. Rabindranath KS, Adams J, Ali TZ, et al. Continuous ambulatory peritoneal dialysis versus automated peritoneal dialysis for end-stage renal disease. *Cochrane Database of Systematic Reviews*. 2007;(2). doi:10.1002/14651858.CD006515/INFORMATION/EN

50. Elliott DA. Hemodialysis. *Clin Tech Small Anim Pract*. 2000;15(3):136-148. doi:10.1053/SVMS.2000.18297

51. Himmelfarb J, Alp Ikizler T. *Hemodialysis*. Vol 19.; 2010.

52. Santoro D, Benedetto F, Mondello P, et al. Vascular access for hemodialysis: current perspectives. *Int J Nephrol Renovasc Dis*. Published online 2014:7-281. doi:10.2147/IJNRD.S46643

53. Hunter, J. P., & Gilbert, J. A. (n.d.). Access for Renal Replacement Therapy. In *Kidney Transplantation: Principles and Practice*.

54. Misra, M. (2005). The basics of hemodialysis equipment. *Hemodialysis International*, *9*, 30–36.

55. Barzegar H, Moosazadeh M, Jafari H, Esmaeili R. Evaluation of dialysis adequacy in hemodialysis patients: A systematic review. *Urology Journal* . 2016;13(4). Accessed August 14, 2022. https://journals.sbmu.ac.ir/urolj/index.php/uj/article/view/3314/1169

56. Depner TA. Assessing adequacy of hemodialysis: Urea modeling. *Kidney Int*. 1994;45(5):1522-1535. doi:10.1038/KI.1994.199

57. Hakim RM, Depner TA, Parker TF. Adequacy of Hemodialysis. *American Journal of Kidney Diseases*. 1992;20(2):107-123. doi:10.1016/S0272-6386(12)80538-5

58. Himmelfarb J. Hemodialysis Complications. Published online 2005. doi:10.1053/j.ajkd.2005.02.031

59. Assimon MM, Flythe JE. Definitions of Intradialytic Hypotension. *Semin Dial*. 2017;30(6):464-472. doi:10.1111/sdi.12626

60. Chou JA, Streja E, Nguyen D v, et al. Intradialytic hypotension, blood pressure changes and mortality risk in incident hemodialysis patients. *Nephrology Dialysis Transplantation*. 2018;33:149-159. doi:10.1093/ndt/gfx037

61. Sars B, van der Sande FM, Kooman JP. Advances in CKD 2020 Intradialytic Hypotension: Mechanisms and Outcome. *Blood Purif*. 2019;49:158-167. doi:10.1159/000503776

62. Stefánsson B v, Brunelli SM, Cabrera C, et al. Intradialytic Hypotension and Risk of Cardiovascular Disease. *Clinical Journal of the American Society of Nephrology*. Published online 2014. doi:10.2215/CJN.02680314

63. Sherman RA. Intradialytic hypotension: An overview of recent, unresolved and overlooked issues. *Semin Dial*. 2002;15(3):141-143. doi:10.1046/J.1525-139X.2002.00002.X

64. Sands JJ, Usvyat LA, Sullivan T, et al. Intradialytic hypotension: Frequency, sources of variation and correlation with clinical outcome. *Hemodialysis International*. 2014;18(2):415-422. doi:10.1111/HDI.12138

65. Flythe JE, Xue H, Lynch KE, Curhan GC, Brunelli SM. Association of Mortality Risk with Various Definitions of Intradialytic Hypotension. *J Am Soc Nephrol*. 2015;26:724-734. doi:10.1681/ASN.2014020222

66. Mcintyre CW, Salerno FR. Diagnosis and Treatment of Intradialytic Hypotension in Maintenance Hemodialysis Patients. *Clin J Am Soc Nephrol*. 2018;13:486-489. doi:10.2215/CJN.11131017

67. Kuipers J, Verboom LM, Ipema KJR, et al. The Prevalence of Intradialytic Hypotension in Patients on Conventional Hemodialysis: A Systematic Review with Meta-Analysis. *Translational Research: Research Article Am J Nephrol*. 2019;49:497-506. doi:10.1159/000500877

68. Kanbay M, Ertuglu LA, Afsar B, et al. An update review of intradialytic hypotension: concept, risk factors, clinical implications and management. *Clin Kidney J*. 2020;13(6):981-993. doi:10.1093/ckj/sfaa078

69. Rhee SY, Song JK, Hong SC, et al. Intradialytic exercise improves physical function and reduces intradialytic hypotension and depression in hemodialysis patients. *Korean Journal of Internal Medicine*. 2019;34(3):588-598. doi:10.3904/kjim.2017.020

70. Davenport A, Cox C, Thuraisingham R. Achieving blood pressure targets during dialysis improves control but increases intradialytic hypotension. *Kidney Int*. 2008;73(6):759-764. doi:10.1038/SJ.KI.5002745

71. Palmer BF, Henrich WL. Recent Advances in the Prevention and Management of Intradialytic Hypotension. Published online 2008. doi:10.1681/ASN.2007091006

72. Roumelioti ME, Unruh ML. Lower Dialysate Temperature in Hemodialysis: Is It a Cool Idea? *Clin J Am Soc Nephrol*. 2015;10:1318-1320. doi:10.2215/CJN.06920615

73. Ayoub A, Finlayson M. Effect of cool temperature dialysate on the quality and patients' perception of haemodialysis. *Nephrol Dial Transplant*. 2004;19:190-194. doi:10.1093/ndt/gfg512

74. Marants R, Qirjazi E, Grant CJ, Lee TY, Mcintyre CW. Renal Perfusion during Hemodialysis: Intradialytic Blood Flow Decline and Effects of Dialysate Cooling. Published online 2019. doi:10.1681/ASN.2018121194

75. Odudu A, Eldehni MT, McCann GP, McIntyre CIW. Randomized controlled trial of individualized dialysate cooling for cardiac protection in hemodialysis patients. *Clinical Journal of the American Society of Nephrology*. 2015;10(8):1408-1417. doi:10.2215/CJN.00200115

76. Selby NM, Burton JO, Chesterton LJ, McIntyre CW. Dialysis-induced regional left ventricular dysfunction is ameliorated by cooling the dialysate. *Clin J Am Soc Nephrol*. 2006;1(6):1216-1225. doi:10.2215/CJN.02010606

77. Inrig JK. Intradialytic Hypertension: A Less-Recognized Cardiovascular Complication of Hemodialysis. *Am J Kidney Dis*. 2010;55(3):580-589. doi:10.1053/j.ajkd.2009.08.013

78. Noel P, Buren V, Inrig JK. Mechanisms and Treatment of Intradialytic Hypertension. doi:10.1159/000441313

79. Gardano S, Bucharles E, Wallbach KKS, Proença De Moraes T, Pecoits-Filho R. Hypertension in patients on dialysis: diagnosis, mechanisms, and management. doi:10.1590/2175-8239-JBN-2018-0155

80. Pun PH. The interplay between CKD, sudden cardiac death, and ventricular arrhythmias. *Adv Chronic Kidney Dis*. 2014;21(6):480-488. doi:10.1053/j.ackd.2014.06.007

81. Jung HY, Choi H, Choi JY, et al. Dialysis modality-related disparities in sudden cardiac death: hemodialysis versus peritoneal dialysis. *Kidney Res Clin Pract*. 2019;38(4):490. doi:10.23876/J.KRCP.19.034

82. Makar MS, Pun PH. Sudden Cardiac Death Among Hemodialysis Patients. *American Journal of Kidney Diseases*. 2017;69(5):684-695. doi:10.1053/j.ajkd.2016.12.006

83. Franczyk-Skóra B, Gluba-Brzózka A, Wranicz JK, Banach M, Olszewski R, Rysz J. Sudden cardiac death in CKD patients. *Int Urol Nephrol*. 2015;47(6):971-982. doi:10.1007/s11255-015-0994-0

84. Kiuchi MG, Mion D. Chronic kidney disease and risk factors responsible for sudden cardiac death: A whiff of hope? *Kidney Res Clin Pract*. 2016;35(1):3-9. doi:10.1016/j.krcp.2015.11.003

85. Bleyer AJ, Russell GB, Satko SG. Sudden and cardiac death rates in hemodialysis patients. *Kidney Int*. 1999;55(4):1553-1559. doi:10.1046/j.1523-1755.1999.00391.x

86. Chiu DYY, Sinha S, Kalra PA, Green D. Sudden cardiac death in haemodialysis patients: Preventative options. *Nephrology*. 2014;19(12):740-749. doi:10.1111/nep.12337

87. Makar MS, Pun PH. Sudden Cardiac Death Among Hemodialysis Patients HHS Public Access. *American Journal of Kidney Disease*. 2017;69(5):684-695. doi:10.1053/j.ajkd.2016.12.006

88. Saravanan P, Davidson NC. Risk assessment for sudden cardiac death in dialysis patients. *Circ Arrhythm Electrophysiol*. 2010;3(5):553-559. doi:10.1161/CIRCEP.110.937888/FORMAT/EPUB

89. Banerjee D. Sudden cardiac death in haemodialysis: clinical epidemiology and mechanisms. *J Electrocardiol*. 2016;49(6):843-847. doi:10.1016/j.jelectrocard.2016.07.016

90. Koplan BA, Winkelmayer WC, Costea AI, et al. Implantable Loop Recorder Monitoring and the Incidence of Previously Unrecognized Atrial Fibrillation in Patients on Hemodialysis. *Kidney Int Rep*. 2022;7(2):189-199. doi:10.1016/J.EKIR.2021.10.001

91. Roy-Chaudhury P, Tumlin JA, Koplan BA, et al. Primary outcomes of the Monitoring in Dialysis Study indicate that clinically significant arrhythmias are common in hemodialysis patients and related to dialytic cycle. *Kidney Int*. 2018;93(4):941-951. doi:10.1016/j.kint.2017.11.019

92. Krüger-Genge A, Blocki A, Franke RP, Jung F. Vascular Endothelial Cell Biology: An Update. *Int J Mol Sci*. 2019;20(18). doi:10.3390/IJMS20184411

93. Endemann DH, Schiffrin EL. Endothelial Dysfunction. Published online 2004. doi:10.1097/01.ASN.0000132474.50966.DA

94. Malyszko J. Mechanism of endothelial dysfunction in chronic kidney disease. *Clinica Chimica Acta*. 2010;411(19-20):1412-1420. doi:10.1016/J.CCA.2010.06.019

95. Patterson EK, Cepinskas G, Fraser DD. Endothelial Glycocalyx Degradation in Critical Illness and Injury. *Front Med (Lausanne)*. 2022;0:1998. doi:10.3389/FMED.2022.898592

96. Cyr AR, Huckaby L v., Shiva SS, Zuckerbraun BS. Nitric Oxide and Endothelial Dysfunction. *Crit Care Clin*. 2020;36(2):307-321. doi:10.1016/j.ccc.2019.12.009

97. Tousoulis D, Kampoli AM, Tentolouris Nikolaos Papageorgiou C, Stefanadis C. The Role of Nitric Oxide on Endothelial Function. *Curr Vasc Pharmacol*. 2011;10(1):4-18. doi:10.2174/157016112798829760

98. Davignon J, Ganz P. Role of endothelial dysfunction in atherosclerosis. *Circulation*. 2004;109(23 SUPPL.). doi:10.1161/01.CIR.0000131515.03336.F8/FORMAT/EPUB

99. Mudau M, Genis A, Lochner A, Strijdom H. Endothelial dysfunction: the early predictor of atherosclerosis. *Cardiovasc J Afr*. 2012;23(4):222. doi:10.5830/CVJA-2011-068

100. Bonetti PO, Lerman LO, Lerman A. Endothelial dysfunction: A marker of atherosclerotic risk. *Arterioscler Thromb Vasc Biol*. 2003;23(2):168-175. doi:10.1161/01.ATV.0000051384.43104.FC/FORMAT/EPUB

101. Mahmud A, Feely J. Arterial stiffness and the renin-angiotensin-aldosterone system. *Journal of the Renin-Angiotensin-Aldosterone System*. 2004;5(3).

102. Aroor AR, Demarco VG, Jia G, et al. The role of tissue renin-angiotensin-aldosterone system in the development of endothelial dysfunction and arterial stiffness. Published online 2013. doi:10.3389/fendo.2013.00161

103. Sachse A, Wolf G. Angiotensin II-Induced Reactive Oxygen Species and the Kidney. Published online 2007. doi:10.1681/ASN.2007020149

104. Wang H, Wang AX, Aylor K, Barrett EJ. Nitric Oxide Directly Promotes Vascular Endothelial Insulin Transport. *Diabetes*. 2013;62(12):4030-4042. doi:10.2337/DB13-0627

105. Tessari P, Cecchet D, Cosma A, et al. Nitric Oxide Synthesis Is Reduced in Subjects With Type 2 Diabetes and Nephropathy. Published online 2010. doi:10.2337/db09-1772

106. Vlassara H, Palace MR. Diabetes and advanced glycation endproducts. *J Intern Med*. 2002;251(2):87-101. doi:10.1046/J.1365-2796.2002.00932.X

107. Tan KCB, Chow WS, Ai VHG, Metz C, Bucala R, Lam KSL. Advanced Glycation End Products and Endothelial Dysfunction in Type 2 Diabetes. *Diabetes Care*. 2007;30(10). Accessed August 14, 2022. http://diabetesjournals.org/care/article-pdf/25/6/1055/589729/dc0602001055.pdf

108. Uribarri J, Stirban A, Sander D, et al. Single Oral Challenge by Advanced Glycation End Products Acutely Impairs Endothelial Function in Diabetic and Nondiabetic Subjects. *Diabetes Care*. 2007;30(10):2579-2582. doi:10.2337/DC07-0320

109. Reitsma S, Slaaf DW, Vink H, van Zandvoort MAMJ, Oude Egbrink MGA. The endothelial glycocalyx: Composition, functions, and visualization. *Pflugers Arch*. 2007;454(3):345-359. doi:10.1007/S00424-007-0212-8/FIGURES/2

110. Beręsewicz A, Czarnowska E, Mączewski M. Ischemic preconditioning and superoxide dismutase protect against endothelial dysfunction and endothelium glycocalyx disruption in the postischemic guinea-pig hearts. *Molecular and Cellular Biochemistry 1998 186:1*. 1998;186(1):87-97. doi:10.1023/A:1006867214448

111. Padberg JS, Wiesinger A, di Marco GS, et al. Damage of the endothelial glycocalyx in chronic kidney disease. *Atherosclerosis*. 2014;234(2):335-343. doi:10.1016/j.atherosclerosis.2014.03.016

112. Dane MJC, Khairoun MR, Hyun Lee D, et al. Association of kidney function with changes in the endothelial surface layer. *Clinical Journal of the American Society of Nephrology*. 2014;9(4):698-704. doi:10.2215/CJN.08160813/-/DCSUPPLEMENTAL

113. Goligorsky MS. Oscillators in the microvasculature: glycocalyx and beyond. *https://doi.org/101152/ajpcell001702022*. 2022;323(2):C432-C438. doi:10.1152/AJPCELL.00170.2022

114. Jiang XZ, Goligorsky MS. Biomechanical properties of endothelial glycocalyx: An imperfect pendulum. *Matrix Biol Plus*. 2021;12. doi:10.1016/J.MBPLUS.2021.100087

115. Rafieian-Kopaei M, Setorki M, Doudi M, Baradaran A, Nasri H. *Atherosclerosis: Process, Indicators, Risk Factors and New Hopes*. Vol 5.; 2014. www.ijpm.ir

116. Schwarz U, Buzello M, Ritz E, et al. Morphology of coronary atherosclerotic lesions in patients with end-stage renal failure. *Nephrology Dialysis Transplantation*. 2000;15(2):218-223. doi:10.1093/NDT/15.2.218

117. Civilibal M, Caliskan S, Kurugoglu S, et al. Progression of coronary calcification in pediatric chronic kidney disease stage 5. *Pediatric Nephrology*. 2009;24(3):555-563. doi:10.1007/S00467-008-1038-0/TABLES/4

118. Oodman IGG, Onathan J, Oldin G, et al. Coronary-Artery Calcification in Young Adults with End-Stage Renal Disease Who Are Undergoing Dialysis. *https://doi.org/101056/NEJM200005183422003*. 2000;342(20):1478-1483. doi:10.1056/NEJM200005183422003

119. Preston E, Ellis MR, Kulinskaya E, Davies AH, Brown EA. Association between carotid artery intima-media thickness and cardiovascular risk factors in CKD. *American Journal of Kidney Diseases*. 2005;46(5):856-862. doi:10.1053/j.ajkd.2005.07.048

120. Valdivielso JM, Rodríguez-Puyol D, Pascual J, et al. Atherosclerosis in Chronic Kidney Disease. *Arterioscler Thromb Vasc Biol*. 2019;39(10):1938-1966. doi:10.1161/ATVBAHA.119.312705

121. Kawagishi T, Nishizawa Y, K0nishi T, Kawasaki K, Emoto M. High-resolution B-mode ultrasonography in evaluation of atherosclerosis in uremia. *Kidney Int*. 1995;48:820-826. doi:10.1038/ki.1995.356

122. Lindner A, Charra B, Sherrard DJ, Scribner BH. Accelerated Atherosclerosis in Prolonged Maintenance Hemodialysis. *http://dx.doi.org/101056/NEJM197403282901301*. 2010;290(13):697-701. doi:10.1056/NEJM197403282901301

123. Fathi R, Isbel N, Short L, Haluska B, Johnson D, Marwick TH. The effect of long-term aggressive lipid lowering on ischemic and atherosclerotic burden in patients with chronic kidney disease. *American Journal of Kidney Diseases*. 2004;43(1):45-52. doi:10.1053/J.AJKD.2003.09.012

124. Wojtaszek E, Oldakowska-Jedynak U, Kwiatkowska M, Glogowski T, Malyszko J. Uremic Toxins, Oxidative Stress, Atherosclerosis in ChronicKidney Disease, and Kidney Transplantation. Published online 2021. doi:10.1155/2021/6651367

125. Charytan D, Kuntz RE, Mauri L, Defilippi C. Distribution of Coronary Artery Disease and Relation to Mortality in Asymptomatic Hemodialysis Patients. *American Journal of Kidney Disease*. 2007;49(3):409-416. doi:10.1053/j.ajkd.2006.11.042

126. McIntyre CW. Effects of hemodialysis on cardiac function. *Kidney Int*. 2009;76(4):371-375. doi:10.1038/KI.2009.207

127. Yildiz A, Oflaz H, Pusuroglu H, et al. Left ventricular hypertrophy and endothelial dysfunction in chronic hemodialysis patients. *American Journal of Kidney Diseases*. 2003;41(3):616-623. doi:10.1053/AJKD.2003.50123

128. Niizuma S, Takiuchi S, Okada S, et al. Decreased coronary flow reserve in haemodialysis patients. *Nephrol Dial Transplant*. 2008;23:2324-2328. doi:10.1093/ndt/gfm954

129. Ragosta M, Samady H, Isaacs RB, Gimple LW, Sarembock IJ, Powers ER. Coronary flow reserve abnormalities in patients with diabetes mellitus who have end-stage renal disease and normal epicardial coronary arteries. Published online 2004. doi:10.1016/j.ahj.2003.07.029

130. Wenning C, Vrachimis A, Pavenstädt HJ, Reuter S, Schäfers M. Coronary artery calcium burden, carotid atherosclerotic plaque burden, and myocardial blood flow in patients with end-stage renal disease: A non-invasive imaging study combining PET/CT and 3D ultrasound. *Journal of Nuclear Cardiology*. Published online March 5, 2020. doi:10.1007/s12350-020-02080-w

131. Dubin RF, Beatty AL, Teerlink JR, et al. Determinants of hemodialysis-induced segmental wall motion abnormalities. *Hemodialysis International*. 2014;18(2):396-405. doi:10.1111/hdi.12111

132. Burton JO, Jefferies HJ, Selby NM, Mcintyre CW. Hemodialysis-Induced Repetitive Myocardial Injury Results in Global and Segmental Reduction in Systolic Cardiac Function. *Clin J Am Soc Nephrol*. 1925;4. doi:10.2215/CJN.04470709

133. Mcintyre CW, Burton JO, Selby NM, et al. Hemodialysis-Induced Cardiac Dysfunction Is Associated with an Acute Reduction in Global and Segmental Myocardial Blood Flow. *Clin J Am Soc Nephrol*. 2008;3:19-26. doi:10.2215/CJN.03170707

134. Park J, Soe •, Ann H, et al. Remote ischemic preconditioning in hemodialysis: a pilot study. doi:10.1007/s00380-013-0329-y

135. Salerno FR, Crowley LE, Odudu A, McIntyre CW. Remote Ischemic Preconditioning Protects Against Hemodialysis-Induced Cardiac Injury. *Kidney Int Rep*. 2020;5(1):99-103. doi:10.1016/J.EKIR.2019.08.016

136. Grigoriou SS, Giannaki CD, George K, et al. A single bout of hybrid intradialytic exercise did not affect left-ventricular function in exercise-naïve dialysis patients: a randomized, cross-over trial. *Int Urol Nephrol*. 2022;54(1):201-208. doi:10.1007/s11255-021-02910-x

137. Wodskou PM, Reinhardt SM, Andersen MB, Molsted S, Schou LH. Motivation, barriers, and suggestions for intradialytic exercise—A qualitative study among patients and nurses. *Int J Environ Res Public Health*. 2021;18(19). doi:10.3390/ijerph181910494

138. Momb BA, Headley SAE, Matthews TD, Germain MJ. Intradialytic exercise increases cardiac power index. *J Nephropathol*. 2020;9(1). doi:10.15171/jnp.2020.07

139. Salhab N, Alrukhaimi M, Kooman J, et al. Effect of intradialytic exercise on hyperphosphatemia and malnutrition. *Nutrients*. 2019;11(10). doi:10.3390/nu11102464

140. Chowdhury R, Jhamb M. Intradialytic exercise improves left ventricular mass in hemodialysis patients. *Kidney Int*. 2021;99(6):1272-1274. doi:10.1016/j.kint.2021.03.023

141. Seong EY. Acute intradialytic exercise and oxidative stress in hemodialysis patients. *Kidney Res Clin Pract*. 2015;34(1):1-3. doi:10.1016/j.krcp.2015.02.003

142. Momeni A, Nematolahi A, Nasr M. *Effect of Intradialytic Exercise on Echocardiographic Findings in Hemodialysis Patients*. Vol 8.; 2014. www.ijkd.org

143. Mcguire S, Horton EJ, Renshaw D, Jimenez A, Krishnan N, Mcgregor G. Hemodynamic Instability during Dialysis: The Potential Role of Intradialytic Exercise. *Biomed Res Int*. 2018;2018. doi:10.1155/2018/8276912

144. Kirkman DL, Scott M, Kidd J, Macdonald JH. The effects of intradialytic exercise on hemodialysis adequacy: A systematic review. *Semin Dial*. 2019;32(4):368-378. doi:10.1111/SDI.12785

145. Jeong JH, Biruete A, Fernhall B, Wilund KR. Effects of acute intradialytic exercise on cardiovascular responses in hemodialysis patients. *Hemodialysis International*. 2018;22(4):524-533. doi:10.1111/hdi.12664

146. Hart A, Johansen KL. Cardiovascular protection and mounting evidence for the benefits of intradialytic exercise. *Nephrology Dialysis Transplantation*. 2019;34(11):1816-1818. doi:10.1093/ndt/gfz038

147. Brown PDS, Rowed K, Shearer J, MacRae JM, Parker K. Impact of intradialytic exercise intensity on urea clearance in hemodialysis patients. *Applied Physiology, Nutrition and Metabolism*. 2018;43(1):101-104. doi:10.1139/apnm-2017-0460

148. Penny JD, Salerno FR, Brar R, et al. Intradialytic exercise preconditioning: An exploratory study on the effect on myocardial stunning. *Nephrology Dialysis Transplantation*. 2019;34(11):1917-1923. doi:10.1093/ndt/gfy376

149. Wilund KR, Tomayko EJ, Wu PT, et al. Intradialytic exercise training reduces oxidative stress and epicardial fat: A pilot study. *Nephrology Dialysis Transplantation*. 2010;25(8):2695-2701. doi:10.1093/ndt/gfq106

150. Greenwood SA, Koufaki P, Macdonald JH, et al. Randomized Trial—PrEscription of intraDialytic exercise to improve quAlity of Life in Patients Receiving Hemodialysis. *Kidney Int Rep*. 2021;6(8):2159-2170. doi:10.1016/j.ekir.2021.05.034

151. Rodríguez-Chagolla J, Cartas-Rosado R, Lerma C, et al. Low-Intensity Intradialytic Exercise Attenuates the Relative Blood Volume Drop Due to Intravascular Volume Loss during Hemodiafiltration. *Blood Purif*. 2021;50(2):180-187. doi:10.1159/000509273

152. Cooke AB, Ta V, Iqbal S, et al. The Impact of Intradialytic Pedaling Exercise on Arterial Stiffness: A Pilot Randomized Controlled Trial in a Hemodialysis Population. *Am J Hypertens*. 2018;31(4):458-466. doi:10.1093/ajh/hpx191

153. Dasselaar JJ, Slart RHJA, Knip M, et al. Haemodialysis is associated with a pronounced fall in myocardial perfusion. *Nephrology Dialysis Transplantation*. 2009;24(2):604-610. doi:10.1093/ndt/gfn501

154. Päivärinta J, Metsärinne K, Löyttyniemi E, et al. Myocardial perfusion reserve of kidney transplant patients is well preserved. *EJNMMI Res*. 2020;10(1). doi:10.1186/s13550-020-0606-6

155. Javed A, Yoon A, Cen S, Nayak KS, Garg P. Feasibility of coronary endothelial function assessment using arterial spin labeled CMR. *NMR Biomed*. 2020;33(2):1-10. doi:10.1002/nbm.4183

156. Zerhouni EA, Parish DM, Rogers WJ, Yang A, Shapiro EP. Human heart: tagging with MR imaging--a method for noninvasive assessment of myocardial motion. *Radiology*. 1988;169(1):59-63. doi:10.1148/radiology.169.1.3420283

157. Buchanan C, Mohammed A, Cox E, et al. Intradialytic cardiac magnetic resonance imaging to assess cardiovascular responses in a short-term trial of hemodiafiltration and hemodialysis. *Journal of the American Society of Nephrology*. 2017;28(4):1269-1277. doi:10.1681/ASN.2016060686

158. Moore CC, McVeigh ER, Zerhouni EA. Quantitative tagged magnetic resonance imaging of the normal human left ventricle. *Topics in Magnetic Resonance Imaging*. 2000;11(6):359-371. doi:10.1097/00002142-200012000-00005

159. Paknezhad M, Brown MS, Marchesseau S. Improved tagged cardiac MRI myocardium strain analysis by leveraging cine segmentation. *Comput Methods Programs Biomed*. 2020;184. doi:10.1016/j.cmpb.2019.105128

160. Odudu A, Francis ST, McIntyre CW. MRI for the assessment of organ perfusion in patients with chronic kidney disease. *Curr Opin Nephrol Hypertens*. 2012;21(6):647-654. doi:10.1097/MNH.0b013e328358d582

161. Schieda N, Blaichman JI, Costa AF, et al. Gadolinium-Based Contrast Agents in Kidney Disease: A Comprehensive Review and Clinical Practice Guideline Issued by the Canadian Association of Radiologists. *Can J Kidney Health Dis*. 2018;5. doi:10.1177/2054358118778573

162. Saeed M, Van TA, Krug R, Hetts SW, Wilson MW. Cardiac MR imaging: current status and future direction. *Cardiovasc Diagn Ther*. 2015;5(4):290-310. doi:10.3978/j.issn.2223-3652.2015.06.07

163. Edwards NC, Moody WE, Yuan M, et al. Diffuse interstitial fibrosis and myocardial dysfunction in early chronic kidney disease. *American Journal of Cardiology*. 2015;115(9):1311-1317. doi:10.1016/j.amjcard.2015.02.015

164. Graham-Brown MPM, March DS, Churchward DR, et al. Novel cardiac nuclear magnetic resonance method for noninvasive assessment of myocardial fibrosis in hemodialysis patients. *Kidney Int*. 2016;90(4):835-844. doi:10.1016/j.kint.2016.07.014

165. Mark PB, Johnston N, Groenning BA, et al. Redefinition of uremic cardiomyopathy by contrast-enhanced cardiac magnetic resonance imaging. *Kidney Int*. 2006;69(10):1839-1845. doi:10.1038/sj.ki.5000249

166. Aoki J, Hara K. Detection of pattern of myocardial fibrosis by contrast-enhanced MRI: Is redefinition of uremic cardiomyopathy necessary for management of patients? *Kidney Int*. 2006;69(10):1711-1712. doi:10.1038/sj.ki.5000259

167. Edwards NC, Moody WE, Chue CD, Ferro CJ, Townend JN, Steeds RP. Defining the natural history of uremic cardiomyopathy in chronic kidney disease: The role of cardiovascular magnetic resonance. *JACC Cardiovasc Imaging*. 2014;7(7):703-714. doi:10.1016/j.jcmg.2013.09.025

168. Rutherford E, Talle MA, Mangion K, et al. Defining myocardial tissue abnormalities in end-stage renal failure with cardiac magnetic resonance imaging using native T1 mapping. *Kidney Int*. 2016;90(4):845-852. doi:10.1016/j.kint.2016.06.014

169. Assa S, Hummel YM, Voors AA, et al. Hemodialysis-induced regional left ventricular systolic dysfunction: Prevalence, patient and dialysis treatment-related factors, and prognostic significance. *Clinical Journal of the American Society of Nephrology*. 2012;7(10):1615-1623. doi:10.2215/CJN.00850112

170. Porter TR, Xie F. Myocardial Perfusion Imaging With Contrast Ultrasound. *JACC Cardiovasc Imaging*. 2010;3(2):176-187. doi:10.1016/j.jcmg.2009.09.024

171. Agatston AS, Janowitz WR, Hildner FJ, Zusmer NR, Viamonte M, Detrano R. Quantification of coronary artery calcium using ultrafast computed tomography. *J Am Coll Cardiol*. 1990;15(4):827-832. doi:10.1016/0735-1097(90)90282-T

172. Cano-Megías M, Guisado-Vasco P, Bouarich H, et al. Coronary calcification as a predictor of cardiovascular mortality in advanced chronic kidney disease: A prospective long-term follow-up study. *BMC Nephrol*. 2019;20(1):1-9. doi:10.1186/s12882-019-1367-1

173. Bundy JD, Chen J, Yang W, et al. Risk factors for progression of coronary artery calcification in patients with chronic kidney disease: The CRIC study. *Atherosclerosis*. 2018;271:53-60. doi:10.1016/j.atherosclerosis.2018.02.009

174. Jansz TT, van Reekum FE, Özyilmaz A, et al. Coronary Artery Calcification in Hemodialysis and Peritoneal Dialysis. *Am J Nephrol*. 2018;48(5):369-377. doi:10.1159/000494665

175. Nishizawa Y, Higuchi C, Nakaoka T, et al. Compositional Analysis of Coronary Artery Calcification in Dialysis Patients in vivo by Dual-Energy Computed Tomography Angiography. *Therapeutic Apheresis and Dialysis*. 2018;22(4):365-370. doi:10.1111/1744-9987.12662

176. Veit Barreto D, Carvalho Barreto F, Barbosa Carvalho A, et al. Coronary calcification in hemodialysis patients: The contribution of traditional and uremia-related risk factors. *Kidney Int*. 2005;67(4):1576-1582. doi:10.1111/j.1523-1755.2005.00239.x

177. Kim ED, Parekh RS. Calcium and Sudden Cardiac Death in End-Stage Renal Disease. *Semin Dial*. 2015;28(6):624-635. doi:10.1111/sdi.12419

178. Chen NX, Moe SM. Vascular Calcification: Pathophysiology and Risk Factors. *Curr Hypertens Rep*. 2012;14(3):228-237. doi:10.1007/s11906-012-0265-8

179. Wang Y, Osborne MT, Tung B, Li M, Li Y. Imaging cardiovascular calcification. *J Am Heart Assoc*. 2018;7(13):1-15. doi:10.1161/JAHA.118.008564

180. Deng W, Peng L, Yu J, Shuai T, Chen Z, Li Z. Characteristics of coronary artery atherosclerotic plaques in chronic kidney disease: evaluation with coronary CT angiography. *Clin Radiol*. 2019;74(9):731.e1-731.e9. doi:10.1016/j.crad.2019.06.003

181. So A, Hsieh J, Li JY, Hadway J, Kong HF, Lee TY. Quantitative myocardial perfusion measurement using CT Perfusion: a validation study in a porcine model of reperfused acute myocardial infarction. *Int J Cardiovasc Imaging*. 2012;28(5):1237-1248. doi:10.1007/s10554-011-9927-x

182. So A, Lee TY. Quantitative myocardial CT perfusion: a pictorial review and the current state of technology development. *J Cardiovasc Comput Tomogr*. 2011;5(6):467-481. doi:10.1016/j.jcct.2011.11.002

183. So A, Wisenberg G, Teefy P, et al. Functional CT assessment of extravascular contrast distribution volume and myocardial perfusion in acute myocardial infarction. *Int J Cardiol*. 2018;266:15-23. doi:10.1016/j.ijcard.2018.02.101

184. Hur LYJ. *Functional CT Imaging for Myocardial Salvage in Acute Myocardial Infarction Management*. 2018.

185. McIntyre CW, Lee TY, Ellis C, et al. Computational Assessment of Blood Flow Heterogeneity in Peritoneal Dialysis Patients' Cardiac Ventricles. *Front Physiol*. 2018;9(May):1-16. doi:10.3389/fphys.2018.00511

186. Davenport MS, Perazella MA, Yee J, et al. Use of Intravenous Iodinated Contrast Media in Patients with Kidney Disease: Consensus Statements from the American College of Radiology and the National Kidney Foundation. *Radiology*. 2020;294(3):660-668. doi:10.1148/radiol.2019192094

1.6 Co-Authorship Statement

The material in Chapter 1 is published in Current Opinions in Nephrology and Hypertension in a manuscript entitled *Current and novel imaging techniques to evaluate myocardial dysfunction during hemodialysis*. Lisa Hur was the main contributor of the work that has been presented in this chapter—conducting the literature search and manuscript preparation. The co-authors of this chapter is Christopher W. McIntyre. Christopher McIntyre provided invaluable guidance in the interpretation of data, manuscript preparation, and manuscript revision.

Estimated percentage of the work for Chapter 1 conducted solely by Lisa Hur: 90%

<div align="center">Chapter 2</div>

2 Presence of coronary artery stenoses reduces segmental myocardial perfusion and is associated with myocardial stunning

A version of this chapter is in preparation for publication: Lisa Hur, Ali Islam, Jarrin Penny, Justin Dorie, Christopher W. McIntyre, "Presence of coronary artery stenoses reduces segmental myocardial perfusion and is associated with myocardial stunning," *In preparation*. Aug 2022.

Abstract Hemodialysis (HD) is associated with repetitive ischemia-reperfusion cardiac injury occurring during each treatment that accumulates with subsequent treatments. Conventional cardiovascular therapies effective in patients with atherosclerotic disease or myocardial infarction have been largely ineffective in treating HD-induced injuries. The objective of the present study was to use coronary CT angiography (CCTA), intradialytic CT perfusion and echocardiography imaging to noninvasively evaluate the myocardial perfusion and stunning response during HD in patients with and without coronary artery disease. CCTA images were acquired prior to HD (baseline) on thirteen patients and assessed by an experienced radiologist for clinically significant stenoses. In addition, dynamic contrast-enhanced CT scans (Revolution CT, GE) were conducted at baseline, peak HD stress, and 30 mins post HD. The dynamic CT images were analyzed using the Johnson-Wilson-Lee tracer kinetic model to quantify global myocardial perfusion (MP) of the left ventricular myocardium. Following each dynamic CT scan, apical 4-chamber and 2-chamber views of the heart were acquired with 2D echocardiography (Vivid Q, GE). The systolic function was evaluated by measuring segmental longitudinal strain (LS) using commercially available software (EchoPAC, GE). Myocardial segments demonstrating >20% reduction in LS compared to baseline were defined as regional wall motion abnormalities (RWMA). Three patients were identified with asymptomatic coronary artery disease (*CAD+*). In participants with stenoses, there were no significant intradialytic changes in global MP. HD participants with no identifiable stenoses lesions (*CAD-*) demonstrated a decrease in global MP from baseline to peak HD and a recovery of perfusion to baseline level at post HD timepoint. Furthermore, *CAD+* participants had elevated number of myocardial segments experiencing RWMA that remained elevated post HD. The presence of coronary artery disease alters myocardial perfusion and stunning response to HD treatment.

2.1 Introduction

Cardiovascular disease (CVD) is highly prevalent in end stage renal disease (ESRD) and is the major cause of morbidity and mortality[1–6]. Vascular dysfunction induced by uremia in ESRD is a potential underlying cause of these complication[7,8]. The interplay of uremic toxins such as guanidine compounds, advanced glycation end products, p-cresyl sulfate, indoxyl sulfate and asymmetric dimethylarginine promote the progression of atherosclerosis[9]. In an autopsy study, the intima-medial layer of the artery thickens with decreased renal function leading to arterial stiffness, a loss of vascular wall compliance[10]. The alteration in hemodynamics caused by arterial stiffening induces left ventricular hypertrophy associated with coronary hypoperfusion. Naturally, it can be assumed that a coronary perfusion compromise would alter myocardial perfusion producing ischemic regions in hypoperfused areas of the heart.

As part of the progression of atherosclerosis and arterial stiffening in uremic patients on hemodialysis (HD), vascular calcification of the intimal and medial layer is commonly seen[1]. The vascular calcification can be deleterious and have been shown to be associated with arterial stiffening and endothelial dysfunction[11,12]. This current study questions the effect of vascular dysfunction of the coronary arteries on the microvascular perfusion and cardiac function during HD.

During the HD treatment, multiple vascular beds experience ischemia and reduction in oxygen delivery, followed by reperfusion at the end of the dialysis treatment. A single episode of HD treatment exerts significant hemodynamic instability that can potentially lead to intradialytic hypotension, defined as greater than 20 to 30 mmHg decrease in systolic blood pressure[13–18]. This degree of circulatory stress and hypotension is associated with myocardial stunning and is due to the considerable reduction in intravascular volume as a result of the removal of large amounts of

fluid that is not adequately negated by plasma refill during dialysis[19]. Studies investigating the frequency of intradialytic hypotension and its association to clinical outcome have identified this significant reduction in systolic blood pressure in five to thirty percent of HD treatments, dependent on the set threshold[20–22]. Furthermore, the frequency of intradialytic hypotension was associated with increased patient mortality and hospitalization[16,23–25]. It is now common knowledge that the administration of HD results in recurrent circulatory stress.

In conjunction with the hemodynamic instability experienced with HD, the high prevalence of CVD and other comorbidities can further exacerbate the dialysis-induced ischemic injury[26–38]. ESRD patients with diabetes mellitus have reduced coronary flow reserve in the absence of angiographically evident coronary artery disease (CAD)[39]. Similarly, utilizing transthoracic doppler echocardiography, a study showed that HD patients without left anterior descending stenoses had significantly lower coronary flow reserve than compared to those with normal renal function[40]. These findings may be due to structural and functional cardiovascular abnormalities, such as left ventricular hypertrophy and increase in left ventricular mass resulting from hypertension that is commonly present in this cohort of patients[41–44]. Clinical studies using advanced imaging techniques to assess coronary flow have also demonstrated a reduction in myocardial perfusion in response to HD treatment, indicating that CAD is not a prerequisite for myocardial ischemia experienced with HD[37,45–47]. It is clear that HD patients have a higher risk for cardiovascular disease relative to the general population, which may be compounded by the presence of existing CAD and vascular dysfunction. Since HD induces challenges to tissue oxygenation due to perfusion anomalies and consequently induce myocardial stunning, it would be important to determine the effect CAD on perfusion during HD and evaluate whether or not asymptomatic CAD in HD patient should be intervened.

Therefore, the aim of this exploratory study was to identify flow restricting coronary artery lesions in HD participants with asymptomatic CAD and observe HD's effect on myocardial perfusion and stunning using serial multimodal imaging during HD. Coronary artery status was evaluated with coronary computed tomography (CT) angiography, myocardial perfusion was quantified with dynamic CT perfusion imaging, and myocardial stunning was assessed with echocardiography. It is hypothesized that HD is associated with an acute reduction in myocardial perfusion that is independent of coronary artery status. However, the coupling of flow limiting coronary artery lesions and HD-induced ischemia may affect the overall myocardial function, marked by the severity of myocardial stunning.

2.2 Methods

2.2.1 Study Design

This study aims to investigate the effect of coronary artery status on the myocardial response to HD. It is a single-centered cross-sectional study conducted on a cohort of ESRD patients requiring maintenance HD. Participants who agreed to participate in the study were asked to attend an intradialytic imaging session at St. Joseph Health Centre (London, Ontario, Canada). During the study, a series of dynamic contrast enhanced CT images, echocardiography, and blood samples were collected throughout the course of the dialysis treatment: prior to HD initiation (baseline), at maximal HD-induced circulatory stress (peak HD) and following the recovery phase after the return of blood (post HD). Collection of both blood and multimodal imaging enable the evaluation of myocardial perfusion and the presence of myocardial stunning in relation to intradialytic electrolyte changes.

2.2.2 Study Population

Fourteen participants, eighteen years of age or older, were recruited from the London Health Science Centre Renal Program (London, Ontario, Canada). Those recruited were required to have received HD for a minimum of three months prior to study enrollment and undergo HD at least thrice weekly. Prior to the initiation of the study, all participants enrolled provided informed consent. The HD participants enrolled in this study were at random and none were suspected of CAD. However, previous studies have suggested considerable plaque burden in this patient population that may be subclinical. The exclusion criterion for the involvement of this study included a history of chronic arrhythmia, being on anti-arrhythmic medications, and having implanted cardiac devices such as a pacemaker or cardioverter defibrillator. A single participant was removed from analysis as the coronary angiography image could not be acquired at the time of the study visit.

2.2.3 Demographic Information

At the time of enrollment, the following demographic information was collected from the participants: date of birth (month and year), biological sex, weight, height, ethnicity, and chronic kidney disease related patient information. From the provided information, additional demographics such as age and body mass index were calculated. Patient demographics are summarized in Table 2-1.

Table 2-1 Participant information and demographics

Characteristics	Prevalence
Ethnicity: Caucasian, n	10 (76%)
Men, n	8 (62%)
Age, yr	66 ± 13
BMI	33 (26-41)
Dialysis vintage (mo)	58 (20-141)
Hemodialysis vintage (mo)	50 (16-141)
*Charlson comorbidity index**	7.4 (4-12)
Congestive heart failure	4 (31%)
Primary renal diagnosis	
Hypertension	4 (31%)
Hypertensive nephrosclerosis	2 (15%)
Diabetic nephropathy	6 (46%)
Acute Interstitial Nephritis	1 (8%)
IgA nephropathy	2 (15%)
Current Smoker	1 (8%)
Medications	
ACEi/ARB	5 (38%)
β - blocker	7 (54%)
2+ antihypertensive agent	4 (31%)

2.2.4 Dialysis Treatment Information

The study visits were conducted midweek and dialysis treatments were delivered on the Fresenius 5008 dialysis machine using high-flux polysulfone dialyzers by a single operator (JP). HD treatment duration ranged from three to four hours. The dialysate composition was prescribed and delivered in accordance with the patient's individual prescription as summarized in Table 2-2: sodium range 135 to 140 mmol/L, potassium range 1.5 to 3.0 mmol/L, calcium range 1.25 to 1.5 mmol/L, and bicarbonate range 35 to 40 mmol/L. Dialysate flow ranged from 500 to 800 mL/min, with six patients using an arteriovenous fistula, a single patient dialyzing with an arteriovenous graft, and six dialyzing with a central line. Anticoagulation was achieved using low molecular weight heparin and the dialysate temperature was 36.5°C for all patients.

Table 2-2 Mean dialysis prescription (n=13)

Dialysis Prescription	Mean ± SD
Treatment Time (hr)	3.5 ± 0.7
Sodium (mmol/L)	139 ± 1.8
Calcium (mmol/L)	1.3 ± 0.1
Bicarbonate (mmol/L)	37.6 ± 2.3
Dialysis flow, Qd (ml/min)	546 ± 113
Vascular Access (AVF: AVG: CVC)*	6:1:6

*AVF = arteriovenous fistula; AVG = arteriovenous graft; CVC = central venous catheter

2.2.5 Assessment of Hemodynamic Stability

Intradialytic changes in systolic blood pressure were used as a marker of hemodynamic stability. Measurements were acquired upon participants arrival and then periodically throughout the dialysis session until thirty minutes following the end of HD treatment. Blood pressure measurements were made with patients seated upright on the dialysis chair.

2.2.6 Assessment of Coronary Artery Status

Coronary CT angiography was routinely collected at baseline before commencing dialysis for non-invasive anatomical assessment of coronary artery stenosis. To achieve the highest quality image of the coronary arteries, a smart prep feature allowing real time monitoring of the contrast agent as it enhances the descending aorta at low x-ray dose, was utilized to determine specific parameters that are personalized to the patient being scanned. Once the parameters were set, the prospectively ECG-gated scan was acquired at peak aortic enhancement of contrast during patient breath hold. The scanning parameters are as follows: display field of view = 25.0 cm; 75%-75% R-R interval; tube voltage = 100 kV; tube current = smart mA 600 – 700; detector coverage = 160mm; slice thickness = 0.625mm; gantry period = 0.28s. For contrast enhancement, iodine contrast (Isovue 370, 0.7 mL per kilogram of body weigh)t was administered intravenously at an infusion rate of 3 – 4 mL per second followed by a set 30 mL saline flush bolus at the same injection rate.

The images were retrospectively reconstructed on the scanner console using an adaptive statistical iterative reconstruction (ASiR) algorithm to further improve image quality and diagnostic value (Revolution, GE Healthcare). The slice thickness was maintained during the reconstruction and the processed images were transferred to a proprietary workstation for analysis (Advantage Workstation, GE Healthcare). An experienced radiologist (A.I) reviewed the coronary anatomy for clinically significant stenosis in the three major arteries: (1) right coronary artery (RCA), (2) left anterior descending (LAD) artery, (3) left circumflex (LCx) artery. As per literature, coronary arteries with greater than fifty percent narrowing of the vessel's diameter were identified to be stenosed lesions with potential hemodynamic significance. For each participant, the number of coronary arteries and the specific arteries with the stenosis were recorded. Based on the reported coronary artery status, the participants were divided into two arms. Individuals with one or more coronary artery stenoses were distinguished into the '*CAD+*' group while the remaining participants with no reports of stenosed lesions were distinguished into the '*CAD-*' group.

2.2.7 Dynamic Contrast Enhanced Computed Tomography

Prospectively ECG-gated, dynamic CT images of the heart were acquired at baseline, peak HD stress), and post HD treatment. To quantify perfusion, iodinated contrast agent (Isovue 370) was delivered during a series of axial scans that repeated every 1 to 2 heart beats (at approximately 1.5 seconds) was acquired. Participants were aligned on the CT bed in feet first-supine position. The scanner settings for all dynamic CT images acquired for this study were as follows: display field of view = 45.0 cm; 75%-75% R-R interval; tube voltage = 100 to 120 kV; tube current = 100mA; detector coverage = 160mm; slice thickness = 2.5mm; gantry period = 0.28s.

Retrospectively, the dynamic images collected at the three timepoints of HD treatment were reconstructed at 5mm slice thickness using the ASiR algorithm to increase the signal to noise ratio

(Revolution, GE Healthcare). Using a three-dimensional non-rigid registration algorithm, correction for residual cardiac and respiratory motion was then applied to the images on a proprietary workstation (GE proprietary software, advantage workstation, GE Healthcare).

Subsequently, the Johnson-Wilson-Lee model of tracer kinetics that characterizes the delivery of the contrast agent was applied to the motion corrected dynamic image to generate functional maps of the heart including absolute myocardial perfusion and blood volume. Maps were generated for each slice of the dynamic image set. For the purposes of this study, only the myocardial perfusion maps were examined.

2.2.8 Quantification of Global Myocardial Perfusion

The myocardial perfusion maps that were generated show the heart in the horizontal long axis view as defined by the American Heart Association's standardized myocardial nomenclature. Seven slices of the left ventricular myocardium taken parallel to the horizontal long axis view were selected (the mid slice, three slices posterior and three slices anterior to the selected mid slice) to measure global myocardial perfusion. This was completed for maps generated from the dynamic images acquired at baseline, peak HD stress, and following the end of HD.

2.2.9 Quantification of Segmental Myocardial Perfusion

The original perfusion images generated in the horizontal long axis view were rendered into a three-dimensional volume and reconstructed to produce a standard short axis view of the heart. Using the short axis view, the perfusion maps were segmented into sixteen myocardial segments as defined by criteria established by the American Heart Association. Myocardial perfusion was then quantified for each segment. Since the segments are anatomically defined, the

amount of myocardial perfusion corresponding to a particular coronary artery responsible for the supply of blood to the particular segments could be quantified.

2.2.10   Assessment of Regional Wall Motion Abnormality

Standard apical 4-chamber and 2-chamber views of the heart was imaged with echocardiography at baseline, peak HD stress, and post HD to study the effect of HD on myocardial stunning. Each cardiac view was imaged over three cardiac cycles identified using a built-in, three electrode ECG. A single cardiac cycle with the highest level of image quality was selected for calculation of longitudinal strain. Using an offline two-dimensional speckle tracking proprietary software (EchoPac, GE Healthcare), segmental longitudinal strain values were calculated for twelve myocardial segments visualized in the 4-chamber and 2-chamber views. This was completed for all intradialytic timepoints (baseline, peak HD stress, post HD treatment).

Calculating segmental longitudinal strain allowed the identification of segments exhibiting regional wall motion abnormalities (RWMAs). RWMAs are defined by a decrease in longitudinal strain during HD relative to the baseline strain values, representing a loss of contractile function and indicating myocardial stunning. For each of the twelve myocardial segments, percent change in longitudinal strain relative to baseline was calculated at peak HD and post HD. Of the twelve myocardial segments, those with greater than twenty percent reduction in longitudinal strain change from baseline were considered to have experienced RWMAs. For each participant, the number of segments experiencing RWMAs at the peak HD and post HD timepoints were counted.

2.2.11   Statistical Analysis

All statistical analyses presented in this paper were performed in GraphPad Prism 9 software (GraphPad Software, La Jolla, California, United States of America).

2.2.11.1 Participant Demographics and Dialysis Treatment Information

Demographic and dialysis treatment information for the thirteen participants are summarized with descriptive statistics (minimum value, maximum value, mean and standard deviation) in Tables 1 and 2.

2.2.11.2 Assessment of Hemodynamic Stability

Hemodynamic stability was assessed using systolic blood pressure measurements. Systolic blood pressure measurements acquired at baseline, peak HD stress, and post HD were analyzed using a repeated measure one-way ANOVA. The Geisser-Greenhouse correction was applied to correct for the sphericity of the data. Pos-hoc testing was completed with Tukey's correction for multiple comparison to determine differences in systolic blood pressure between the intradialytic timepoints.

To determine differences in systolic blood pressure between the *CAD+* and *CAD-* arm, grouped analysis was performed. A repeated measure two-way ANOVA with group (stenosed or non-stenosed), timepoint (baseline, peak HD, or post HD), and group-by-timepoint as fixed effects was performed for the systolic blood pressure measurements. A Geisser-Greenhouse correction was applied. If any of the fixed effects were statistically significant, post-hoc tests were performed with Sidak's correction for multiple comparisons to determine systolic blood pressure differences between intradialytic timepoints and between groups.

2.2.11.3 Laboratory Testing

Intradialytic changes in electrolyte concentrations measured from the blood samples were assessed using linear mixed models. Specifically, levels of ionized calcium, sodium, potassium, chloride, bicarbonate, anion gap, creatinine, and calcium were analyzed using linear mixed models

with intradialytic timepoint as the fixed effect and participant as the repeated effect. A maximum likelihood algorithm was used to estimate variance parameters. The Geisser-Greenhouse correction was applied to correct for the sphericity of the data. If there was a significant effect of timepoint, post-hoc testing was completed with Tukey's correction for multiple comparison to identify differences in electrolyte between timepoints. A linear mixed model was used for these data, as some participants did not have measures of all electrolytes at all timepoints.

In contrast, intradialytic changes in urea, albumin, magnesium, phosphate, parathyroid hormone, cardiac troponin T, hemoglobin, C-reactive protein, and hematocrit levels were measured for all participants at all timepoints. As such, these data were analyzed using repeated measures one-way ANOVA. The Geisser-Greenhouse correction was applied to correct for the sphericity of the data. If the ANOVA was statistically significant, post-hoc testing with Tukey's correction for multiple comparison was completed to determine differences between timepoints.

Grouped analysis was performed for cardiac troponin T and C-reactive protein measurements. A repeated measure two-way ANOVA test with intradialytic timepoint and group (*CAD+* or *CAD-*) as fixed effects were performed with the Geisser-Greenhouse correction for sphericity. If any fixed effect was statistically significant, post-hoc testing was completed with Sidak's correction for multiple comparisons to determine differences between groups and between timepoints.

2.2.11.4 Global Myocardial Perfusion

First, the global myocardial perfusion values were assessed to identify outliers using the robust regression and outlier (ROUT) removal method. One participant's perfusion measurement of a single timepoint was identified as an outlier and that data point was removed from further

analysis. The remaining global myocardial perfusion measurements were analyzed using a linear mixed model with intradialytic timepoint (baseline, peak HD, and post HD) as the fixed effect. Restricted maximum likelihood estimation was used. If there was a significant effect of intradialytic timepoint, post-hoc testing with Tukey's correction for multiple comparisons was performed to identify the differences in myocardial perfusion between timepoints.

A separate grouped analysis was performed to investigate the effect of CAD on global myocardial perfusion during dialysis. A linear mixed model with group (*CAD+* or *CAD-*) and intradialytic timepoint as fixed effects was performed with restricted maximum likelihood estimation and the Geisser-Greenhouse correction. Post-hoc testing with Tukey's correction for multiple comparison was performed to identify differences in myocardial perfusion within and between groups.

2.2.11.5 Segmental Myocardial Perfusion

Segmental myocardial perfusion measurements from all participants were pooled for analysis. Myocardial segments perfused by coronary arteries identified with greater than 50% stenoses were grouped together while myocardial segments perfused by non-stenosed coronary arteries composed another group. In total, 156 myocardial segments received their blood supply from normal coronary arteries ('unaffected' group) and 39 myocardial segments were supplied by coronary arteries that had stenosed lesions ('affected' group). At each individual timepoint (baseline, peak HD, post HD), a parametric unpaired two-tailed t-test was performed to determine statistical significance in myocardial perfusion between the unaffected and affected group.

The number of myocardial segments with greater than thirty percent reduction in perfusion relative to baseline perfusion values was determined at peak HD and post HD[45]. A repeated

measure two-way ANOVA test with intradialytic timepoint and group (*CAD+* and *CAD-*) as fixed effects was performed with the Geisser-Greenhouse correction for sphericity. If any fixed effect was statistically significant, post-hoc testing was completed with Sidak's correction for multiple comparison to determine differences between groups and between timepoints.

2.2.11.6   Regional Wall Motion Abnormality

The number of myocardial segments experiencing RWMAs was analyzed with a repeated measure one-way ANOVA. If the ANOVA demonstrated statistical significance, a post-hoc testing was completed with Tukey's correction for multiple comparisons to identify differences between intradialytic timepoints.

Additionally, a grouped analysis was performed to investigate the effect of clinically significant stenoses on the number of myocardial segments experiencing RWMAs during dialysis. A repeated measure two-way ANOVA was conducted with group (*CAD+* and *CAD-*) and intradialytic timepoint as fixed effects and the participant as the repeated effect. A Geisser-Greenhouse correction was applied for this analysis. If any of the fixed effects were significant, post-hoc tests were completed with Tukey's correction for multiple comparisons to identify differences in the number of myocardial segments experiencing RWMAs within and between groups.

2.3 Results

2.3.1 Participants

Of the fourteen participants enrolled, thirteen had a complete set of coronary CT angiography, dynamic CT perfusion, and echocardiography image data. A coronary CT angiography image was not successfully acquired for one participant and that participant was

excluded from all analyses. All thirteen participants included for assessment in this study completed laboratory testing at baseline, peak HD, and post HD. In our analysis of RWMA, one participant from the *CAD-* arm was excluded due to the poor image quality of the echocardiograph. The participants demographic information reflects the general HD population and is summarized in Table 2-1.

2.3.2 Dialysis Treatment

The dialysis treatment is summarized in Table 2-3 and includes weight +gain/-loss, pre-systolic blood pressure (SBP), pre-diastolic blood pressure (DBP), SBP nadir, DBP nadir, Kt/V, minimum relative blood volume (RBV), mean ultrafiltration rate (UFR), mean UFR relative to pre-HD weight, and total fluid removed during the HD treatment session.

Table 2-3 Intradialytic clinical information

	Mean $\pm$ SD
Weight +gain/-loss (kg $\pm$ SD)	1.4 $\pm$ 0.7
Pre HD SBP (mmHg $\pm$ SD)	147 $\pm$ 20
Pre HD DBP (mmHg $\pm$ SD)	62 $\pm$ 18
SBP nadir (mmHg $\pm$ SD)	103 $\pm$ 19
DBP nadir (mmHg $\pm$ SD)	52 $\pm$ 14
Kt/V $\pm$ SD	1.48 $\pm$ 0.3
Min RBV (% $\pm$ SD)	85.0 $\pm$ 3.5
Mean UFR (mL/hr $\pm$ SD)	666 $\pm$ 203
Mean UFR/pre weight (mL/kg/hr $\pm$ SD)	7.57 $\pm$ 2.7
Total fluid removed (mL $\pm$ SD)	2548 $\pm$ 816

*SBP = systolic blood pressure; DBP = diastolic blood pressure; RBV = relative blood volume; UFR = ultrafiltration rate

2.3.3 Laboratory Testing

Electrolytes that were measured at baseline, peak HD, and post HD included sodium, calcium, potassium, chloride, phosphate, magnesium, and bicarbonate (Table 2-4). Linear mixed

modelling and post-hoc multiple comparison test demonstrated expected changes in sodium, potassium, chloride, bicarbonate, and calcium resulting from dialysis (Supplementary Figure 2-1, Panel B, C, D, E, and J, respectively). Repeated measure one-way ANOVA and post-hoc testing showed expected decrease in levels of potassium and magnesium electrolytes with dialysis. (Supplementary Figure 2-1, Panel C and K, respectively). Similarly, analyses of serum creatinine and urea displayed decrease in concentration of these electrolytes due to dialysis (Supplementary Figure 2-1, Panel G and H, respectively). Repeated measure one-way ANOVA test showed a significant intradialytic change in hemoglobin levels ($F_{(1.686, 20.23)}$=19.91, $p < 0.0001$, Supplementary Figure 2-1, Panel O), Post-hoc testing showed that hemoglobin increased significantly from the start of dialysis to peak HD stress (100.9 ± 9.4 to 110.9 g/L ± 11.1, $p = 0.0002$), followed by a decrease at post HD (107.4 ± 10.6 g/L, $p = 0.03$), while remaining elevated compared to the start of dialysis ($p = 0.01$).

Table 2-4 Mean plasma electrolyte concentration of those with significant changes as a response to hemodialysis treatment

Electrolyte (Conc. ± SD)	Control (n=13)		
	Baseline	Peak HD	Post HD
Ionized Calcium (mmol/L)	1.09± 0.1	1.05 ± 0.1	1.04 ± 0.1
Potassium (mmol/L)	4.62 ± 0.8	3.33 ± 0.4	3.35 ± 0.4
Bicarbonate (mmol/L)	24.5 ± 2.5	30.1 ± 2.2	30.1 ± 2.1
Anion Gap (mmol/L)	16.0 ± 3.7	12.6 ± 2.5	12.1 ± 2.5
Creatinine (umol/L)	732 ± 190	260 ± 86	254 ± 98
Urea (mmol/L)	18.0 ± 4.7	5.06 ± 1.6	4.85 ± 1.7
Albumin (g/L)	36.3 ± 3.8	41.5 ± 4.6	40.1 ± 4.6
Calcium (mmol/L)	2.25 ± 0.3	2.28 ± 0.2	2.21 ± 0.2
Magnesium (mmol/L)	1.07 ± 0.2	0.94 ± 0.2	0.92 ± 0.2
Phosphate (mmol/L)	1.77 ± 0.5	0.71 ± 0.1	0.78 ± 0.2
Hemoglobin (g/L)	101 ± 9.4	111 ± 11	107 ± 11
C-Reactive Protein (mg/L)	10.2 ± 10.1	11.5 ± 11.2	11.0 ± 10.8
Hematocrit (L/L)	0.31 ± 0.03	0.34 ± 0.04	0.33 ± 0.03

Biomarkers of cardiac injury and inflammation analyzed were cardiac troponin T (cTnT) and C-reactive protein (CRP). A one-way ANOVA analysis did not show a statically significant effect of timepoints on the levels of cTnT (F (1.019, 12.22) = 3.178, p=0.09, Supplementary Figure 2-1, Panel N). Two-way ANOVA analysis with group designation (*CAD+* and *CAD-*) as fixed effect revealed a significant group effect (F (1,11) = 18.34, p = 0.0013, Figure 2-1A), but no significant effect of timepoint were seen (F (1.023, 11.25) = 0.5215, p = 0.4889). Post-hoc testing showed increased cTnT signal in the *CAD+* group relative to *CAD-* group at peak HD (t (2.755) = 4.485, p = 0.0723) and post HD (t (2.605) = 4.434, p = 0.0831) timepoints.

In the thirteen participants, a one-way ANOVA analysis showed a statistically significant effect of timepoint on levels of CRP (F (1.407, 16.88) = 13.75, p = 0.0008, Supplementary Figure 2-1, Panel P). Post-hoc testing showed that the levels of CRP were significantly higher at peak HD (11.5 ± 11.2 mg/L) compared to baseline (10.2 ± 10.1 mg/L, p = 0.0041) that remained elevated post HD relative to baseline (11.0 ± 10.7 vs. 10.2 ± 10.1 mg/L, p = 0.011). Two-way ANOVA analysis with group designation (*CAD+* and *CAD-*) as a fixed effect revealed a significant effect of timepoint (F (1.441, 15.85) = 12.95, p = 0.0011, Figure 2-1B), but no significant group effect (F (1, 11) = 1.677, p = 0.2218). Post-hoc testing showed an increase in CRP level from baseline to peak HD (8.3 ± 7.2 vs. 9.4 ± 8.1 mg/L, p = 0.0167) that remained elevated post HD in the *CAD-* group, although insignificant (9.0 ± 7.7 mg/L, p = 0.0671).
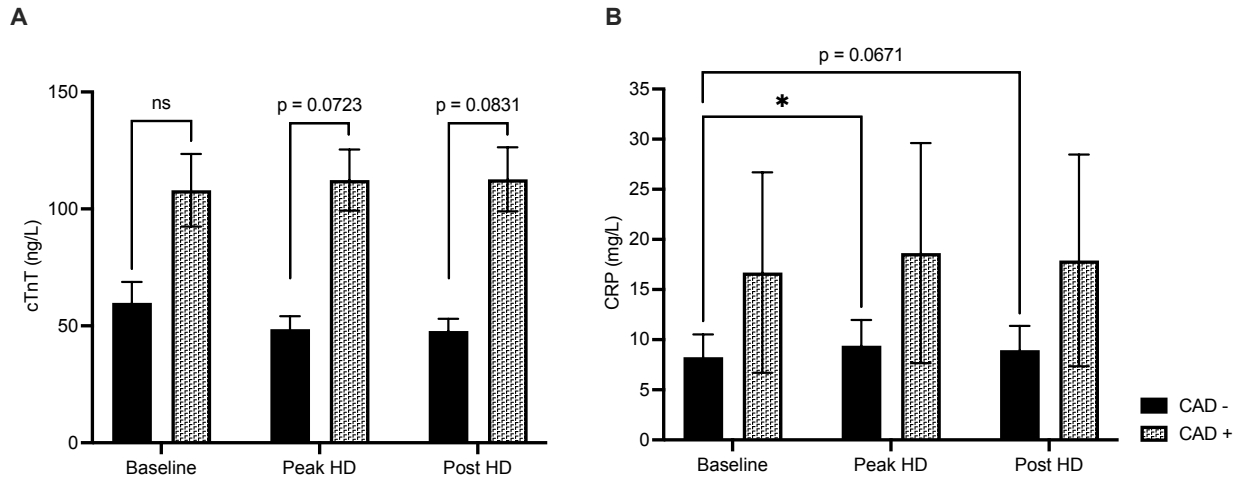
Figure 2-1 Mean cardiac troponin T (panel A) and C-reactive protein (panel B) in *CAD*- (n=10) and *CAD*+ arm (n=3) at baseline, peak HD stress, and post HD. Error bars represent the standard error of the mean. * Denote $p < 0.0332$.

2.3.4 Systolic Blood Pressure for Hemodynamic Stability

The repeated measure one-way ANOVA demonstrated a significant effect of timepoint ($F_{(1.614, 19.3)} = 8.963$, $p = 0.003$). The post-hoc testing showed that systolic blood pressure was significantly lower at peak HD in comparison to baseline (119.5 ± 24.15 mmHg vs. 145.2 ± 24.92 mmHg, $p = 0.019$, Figure 2-2). Systolic blood pressure post HD (121.9 ± 21.70 mmHg), was not significantly different from peak HD ($p = 0.886$) but was significantly reduced relative to baseline ($p = 0.012$).

In the grouped analysis with the *CAD*+ and *CAD*- arms, two-way ANOVA showed a significant effect of intradialytic timepoint ($F_{(1.523, 16.75)} = 5.161$, $p = 0.0246$). Post-hoc testing revealed no differences in systolic blood pressure between the *CAD*+ and *CAD*- groups at individual HD timepoints. However, only the *CAD*- group demonstrated a statistically significant

reduction in mean systolic pressure at peak HD (p = 0.0362, Figure 2-3) relative to baseline, followed by a partial recovery to baseline values at post HD (p = 0.0727, Figure 2-3).
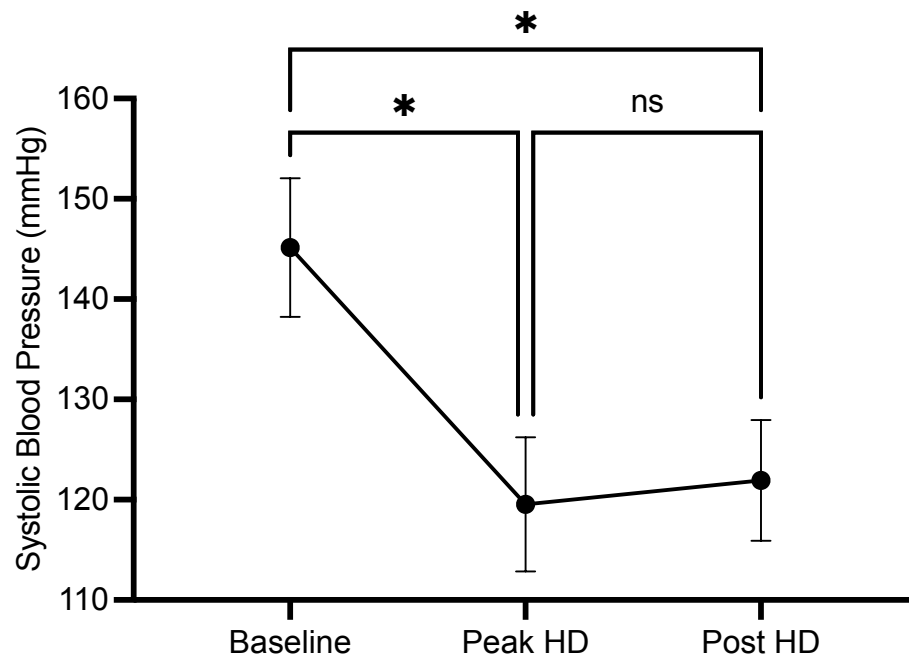
Figure 2-2 Mean systolic blood pressure (n=13) at baseline, peak HD stress, and post HD. Error bars represent the standard error of the mean. * Denote p < 0.0332.
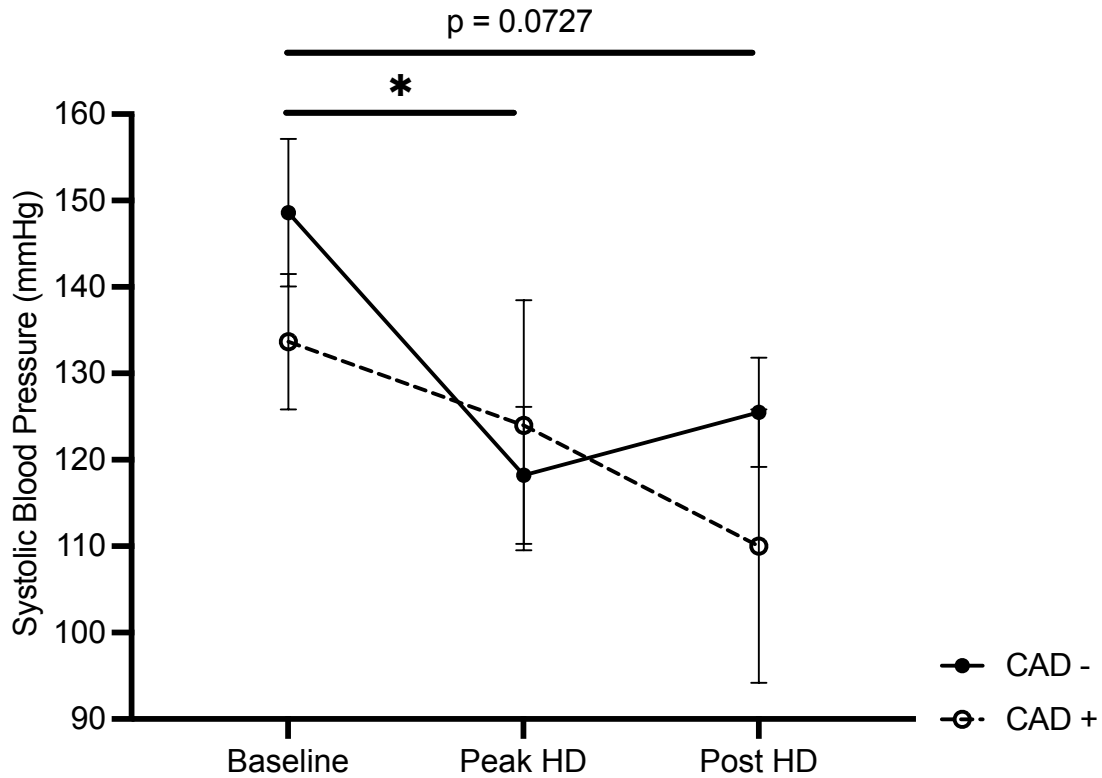
Figure 2-3 Mean systolic blood pressure in *CAD-* (n=10) and *CAD+* arm (n=3) at baseline, peak HD stress, and post HD. Error bars represent the standard error of the mean. Solid significance bar is based on the post hoc test performed on the non-stenosed group. * Denote $p < 0.0332$.

2.3.5 Coronary Artery Status

Coronary angiography findings of the thirteen participants are summarized in Table 2-5. Of the thirteen participants, three were identified to have multivessel CAD with stenoses greater than fifty percent. The LCx artery was identified to be the most commonly stenosed in this participant group. One *CAD+* participant had stenosed lesions in all three of the coronary arteries and was also evaluated with a high calcification score. Ten participants showed no hemodynamically significant lesions that were greater than fifty percent stenosed and one of the participants in this group had high calcification scoring. In total, thirty-nine coronary arteries were

imaged across thirteen participants. Of these, three were not evaluable due to poor image quality and were removed from further analysis. Amongst the three participants with CAD, seven coronary arteries had stenosed lesions with potential for hemodynamic significance (2 RCA, 2 LAD, 3 LCx).

Table 2-5 Descriptive analysis of coronary artery status of individual patients. (+) denote lesions with > 50 % stenoses in the respective coronary artery and (-) indicate no stenosed lesions or stenosis ≤ 50 %.

Participant #	RCA	LAD	LCx	Highly Calcified
1	-	-	-	-
2	-	+	+	-
3	-	-	-	-
4	-	-	-	-
5	NE	-	-	-
6	-	-	-	-
7	+	+	+	+
8	-	-	-	+
9	-	-	-	-
10	+	NE	+	-
11	-	-	-	-
12	NE	-	-	-
13	-	-	-	-
Total Lesions (%)	15	15	23	15

*RCA = right coronary artery; LAD = left anterior descending artery; LCx = left circumflex artery; NE = not evaluable

2.3.6 Global Myocardial Perfusion

Linear mixed modelling revealed a statistically significant fixed effect of timepoint (Figure 2-4, p = 0.0115). Post-hoc testing showed that global myocardial perfusion was significantly lower at peak HD compared to baseline (79.18 ± 21.00 ml/min/100g vs. 94.14 ± 18.01 ml/min/100g, p = 0.0001) before normalizing back to baseline levels at post HD (90.35 ± 17.76 ml/min/100g, p = 0.37, Figure 2-4). When including the group designation (*CAD+* vs. *CAD-*) in the linear mixed model, there were no significant effect of group (F (1,11) = 0.021, p = 0.8874). However, there

was a trend towards an effect of timepoint (F (1.416,14.86) = 3.375, p = 0.07). Figure 2-5 qualitatively demonstrates the effect of timepoint on a single participant. Post-hoc multiple comparison testing showed a reduction in global myocardial perfusion in the *CAD-* participant group from baseline to peak HD (97.25 ± 18.13 ml/min/100g vs. 78.65 ± 17.89 ml/min/100g, p <0.0001, Figure 2-6), and perfusion recovery from peak HD to post HD (78.65 ± 17.89 ml/min/100g vs. 94.81 ± 16.49 ml/min/100g, p = 0.0029, Figure 2-6). There were no significant changes in intradialytic global myocardial perfusion measurements in the *CAD+* participant group (Figure 6).
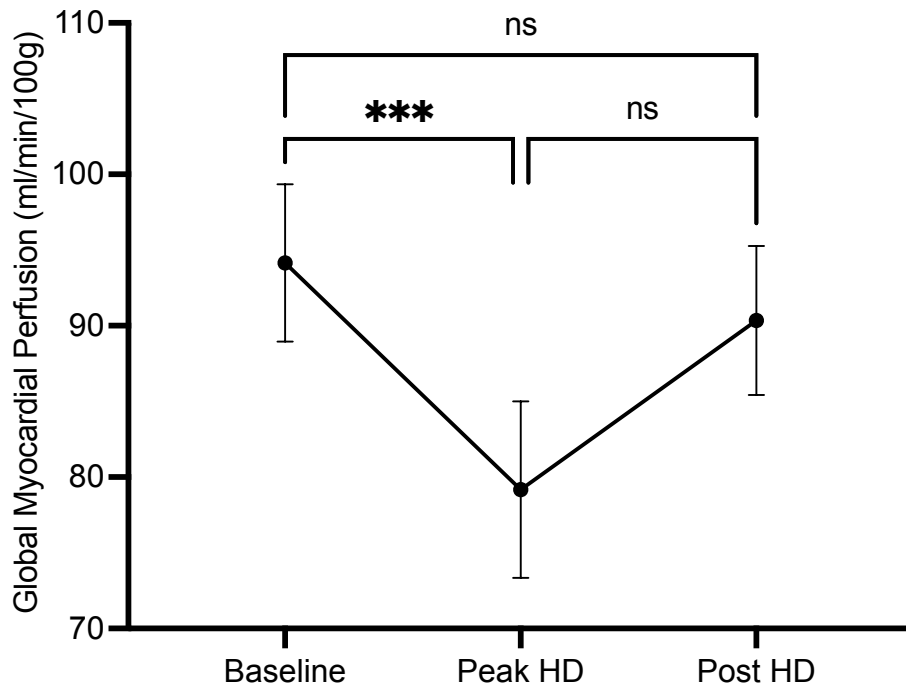
Figure 2-4 Mean global myocardial perfusion in all participants (n=13) at baseline, peak HD stress, and post HD. Error bars represent the standard error of the mean. *** Denote p < 0.0002.
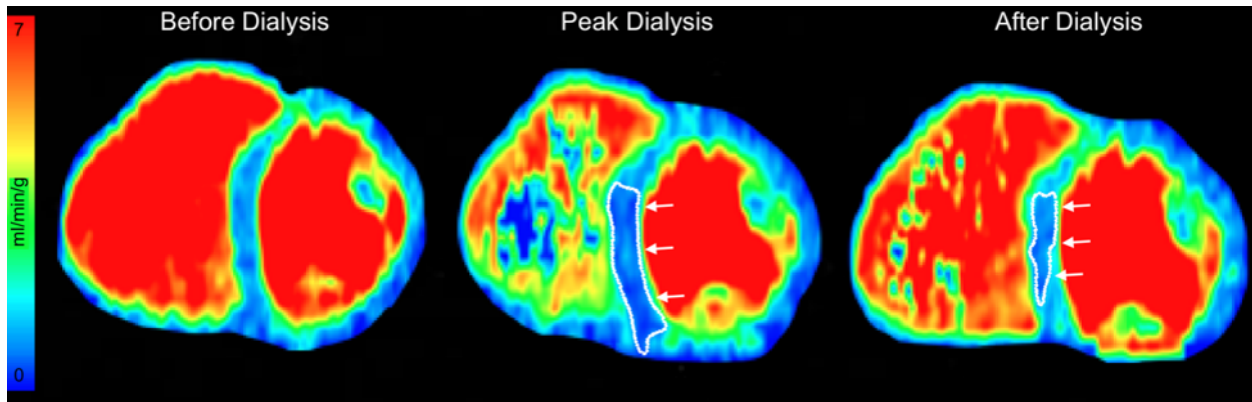
Figure 2-5 Qualitative assessment of changes in myocardial perfusion through dialysis of a single participant, in the absence of coronary artery stenosis. Cardiac image in of a short axis view and the regions outlined in white and identifiable by the white arrows represent myocardial regions with perfusion reduction.
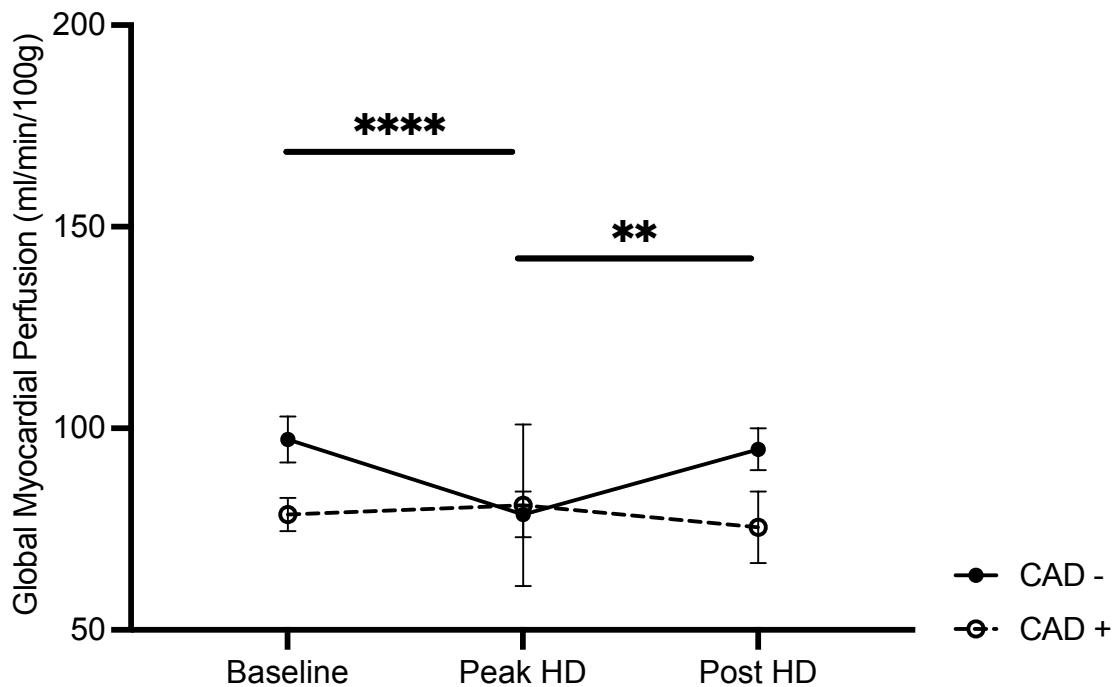
Figure 2-6 Mean global myocardial perfusion in *CAD-* (n=10) and *CAD+* (n=3) participants. Error bars represent the standard error of the mean. Significance bar for pairwise comparison reflect that within the non-stenosed group. ** Denote $p < 0.0021$ and **** denote $p < 0.0001$.

2.3.7 Segmental Myocardial Perfusion

At baseline (Figure 2-7A), the segmental myocardial perfusion measurements were not significantly different between the affected and unaffected group (t (193) = 1.587, p = 0.1142). Similarly, the segmental perfusion measurements were not different between groups at peak HD (Figure 2-7B, t (193) = 0.9012, p = 0.369). However, at post HD timepoint (Figure 2-7C), the mean segmental myocardial perfusion in the affected group was significantly lower compared to the unaffected group (70.02 ± 21.59 ml/min/100g vs. 92.19 ± 39.48 ml/min/100g, t (193) = 3.380, p = 0.0009).

The number of myocardial segments with greater than thirty percent reduction in perfusion were quantified (Figure 2-8). Two-way ANOVA showed no significance in the interaction between timepoint and group (F (1, 11) = 0.2362, p = 0.6365). There was a signal for an effect of intradialytic timepoint (F (1,11) = 4.217, p = 0.0646), warranting further testing. Post-hoc testing showed that fewer myocardial segments experienced greater than thirty percent reduction in perfusion at post HD compared to peak HD in *CAD-* participant group (p = 0.045). In participants with *CAD+*, no statistical difference between the timepoints was seen (p = 0.629).
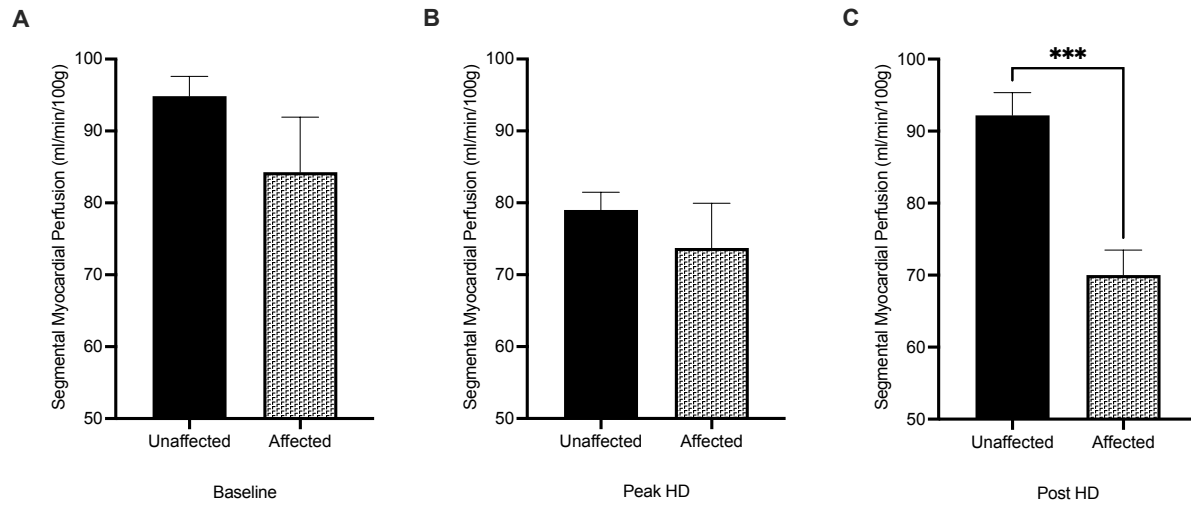
Figure 2-7 Mean myocardial perfusion in unaffected segments (n=156) and affected segments (n=39) at (A) baseline, (B) peak HD stress, and (C) post HD. Error bars represent the standard error of the mean. *** Denote significance of $p < 0.0002$.
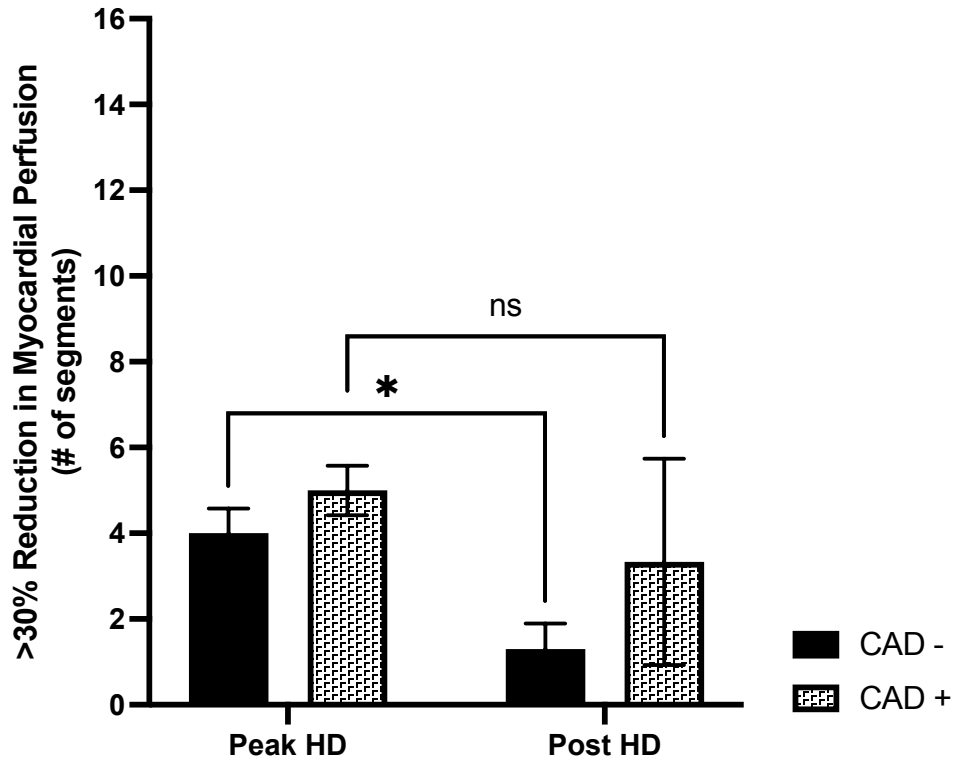
Figure 2-8 Mean number of myocardial segments with greater than 30% reduction in myocardial perfusion at peak HD stress and post HD relative to baseline myocardial perfusion. Error bars represent standard error of the mean. * Denote $p < 0.0332$.

2.3.8 Regional Wall Motion Abnormality

In the twelve participants with viable echocardiography data, one-way ANOVA analysis showed a statistically significant effect of timepoint on the number of myocardial segments experiencing RWMAs (F $(1.875,20.62) = 31.16$, $p = 0.0115$, Figure 2-9). Post-hoc testing showed that the number of segments experiencing RWMAs were significantly higher at peak HD compared to baseline (5.5 ± 2.9 segments, $p = 0.0001$). This remained elevated at post HD relative to baseline (4.7 ± 2.6 segments, $p = 0.0002$). Two-way ANOVA analysis with group designation (*CAD+* vs. *CAD-*) as a fixed effect revealed a significant effect of timepoint (F $(1.844,18.44) = 28.67$, $p < 0.0001$), but no significant group effect (F $(1,10) = 1.717$, $p = 0.2193$, Figure 2-10). Post-hoc testing showed an increase in segments experiencing RWMAs in the *CAD-* participant

group from baseline to peak HD (5.1 ± 3.2 segments, p = 0.003), that is reduced post HD compared to at peak HD (4.0 ± 2.5 segments, p = 0.003). In the *CAD+* group, there was a similar increase in segments experiencing RWMAs at peak HD (6.7 ± 1.5 segments, p = 0.031). A trend towards increased segments experiencing RWMA at post HD relative to baseline (6.7 ± 2.1 segments, p = 0.056) was also detected for the *CAD+* group.
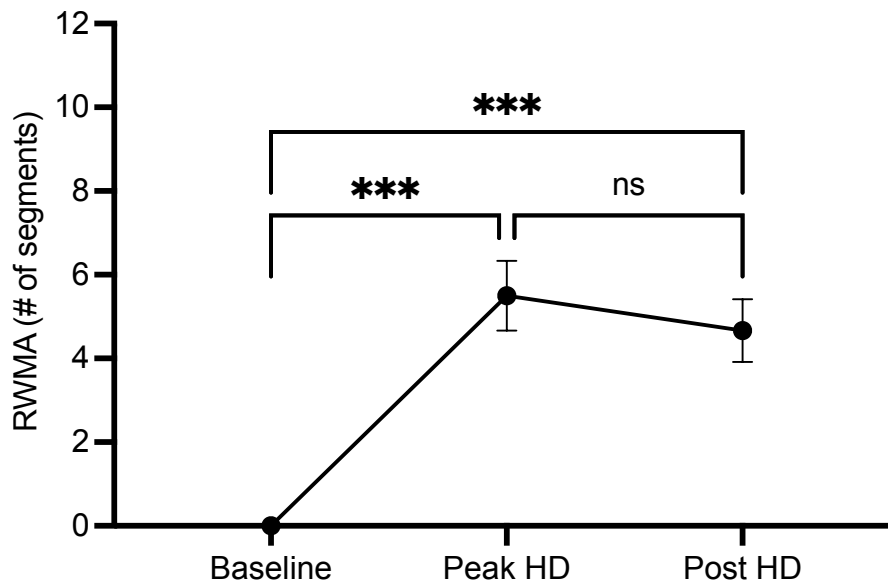
Figure 2-9 Mean myocardial segments with regional wall motion abnormalities (n=12). Error bars represent the standard error of the mean. *** Denote p < 0.0002.
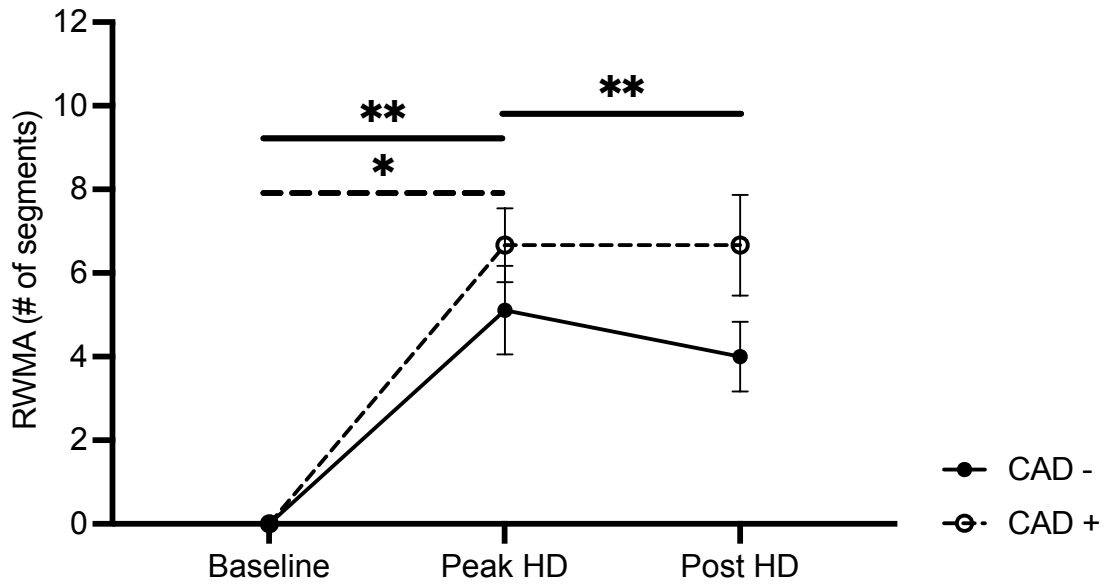
Figure 2-10 Mean regional wall motion abnormality in *CAD-* (n=9) and *CAD+* (n=3) participants. Error bars represent the standard error of the mean. Solid significance bars for pairwise comparison performed in the non-stenosed group. Dotted significance bar for pairwise comparison completed for the stenosed arm. * Denote $p < 0.0332$ and ** denote $p < 0.0021$.

2.4 Discussion

This study demonstrated HD-induced circulatory stress as measured by a reduction in myocardial perfusion and elevation in myocardial stunning that was independent of CAD. In our study population, where none of the patients had symptomatic CAD, it was revealed that almost a quarter of this population had considerable plaque burden that were flow limiting. These flow-limiting stenoses exacerbated perfusion anomalies in myocardial segments to which it supplied blood, leading to myocardial stunning that could not be recuperated following the end of HD treatment.

Participant without CAD experienced a significant rise in myocardial stunning during HD treatment which appears to be related to the reduction in myocardial perfusion. This is in line with previous findings from our lab as well as others, demonstrating intradialytic reduction in organ

perfusion during HD. Marants et al. conducted an intradialytic CT perfusion study to explore HD effects on renal perfusion, and was able to show acute decrease in renal perfusion during HD treatment[48]. Many studies looked into the effects of HD on the brain and similarly concluded that HD induced reduction in cerebral blood flow. This was confirmed using transcranial doppler, CT, magnetic resonance imaging, and near infrared spectroscopy[49–54]. As all vascular beds originate from a single contiguous endothelial surface, it is expected that during an ischemic insult such as the one experienced during HD, the reduction in blood flow occurs in multiple vascular beds. The heart is also a vascular bed that experiences HD ischemic injury. McIntyre et al. demonstrated a reduction in regional myocardial perfusion throughout dialysis using positron emission tomography, with its lowest mean perfusion measurement at four hours from commencing dialysis[45]. They also determined that myocardial segments identified to have RWMAs were significantly associated with greater reduction in myocardial perfusion from baseline compared to normal segments[45]. This study also identified a greater than thirty percent reduction in perfusion from baseline as the perfusion threshold associated with regional wall motion abnormality[45]. It is evident from our current study that with HD, there is a general reduction in global myocardial perfusion and an increased number of myocardial segments experiencing regional wall motion abnormality or myocardial stunning in participants with no CAD. Shortly after the end of HD treatment, global myocardial perfusion is recovered and stunned myocardial segments are partially salvaged upon reperfusion.

The addition of CAD appears to be associated with worsened response to HD treatment as evidenced by the consistently hypoperfused myocardium and prolong stunning that does not recover following the end of HD treatment. We have shown that unlike the traditional perfusion response seen with HD, participants with CAD showed no intradialytic perfusion changes,

however, the mean perfusion measurements tended to be lower at baseline and post HD timepoint compared to those without known CAD. The modest level of global myocardial perfusion in the *CAD+* arm at baseline may be the result of the flow limiting epicardial artery stenoses that have been identified through coronary angiography. In all intradialytic timepoints, myocardial segments corresponding to coronary arteries with stenosed lesions greater than fifty percent demonstrated trends of lower perfusion, indicating that these identified stenoses were in fact flow-limiting. The reduction in perfusion in the myocardial segment affected by CAD was most evident after the end of HD treatment. This suggests that reperfusion of these segments affected my flow-limited stenoses may take longer to return to baseline perfusion levels, which is also evident through the lack of improvement in the number of myocardial segments with greater than 30% reduction in perfusion in *CAD+* arm. With this in mind, it is interesting to see that with the extended duration of ischemic-reperfusion injury associated with CAD, the number of stunned myocardial segments remained elevated and persistent from peak HD to post HD. These findings suggest that the CAD plays a significant role in the recovery phase of HD treatment (post HD).

The two laboratory measurements that have been important predictors of CAD in HD patients include cTnT and CRP. A rise in cTnT has been used as a marker of myocardial cell injury in clinically suspected myocardial ischemia[55]. There continues to be controversy regarding the clinical usefulness of measuring cardiac troponin levels to diagnosis acute ischemic injury continues in the chronic HD population, as its levels are frequently higher at baseline without evidence of injury[56–64]. In our current study, there were no evident intradialytic changes in mean cTnT levels in the thirteen HD participants, despite its higher-than-normal levels. The three participants with CAD showed trends of increased cTnT at baseline relative to the *CAD-* arm, that remained higher at peak HD and post HD timepoints. The elevated levels of cTnT at baseline in

the *CAD+* arm may represent the existence of a prior silent infarct or subclinical myocardial ischemia where the stenoses constructs the delivery of blood and ultimately, oxygen to the myocardial cells, causing injury. The presence of a coronary stenoses may potentially have an additive effect on cTnT levels in those with chronic HD. The lack of change in troponin levels throughout dialysis in the *CAD+* arm may be a response to the increased ischemia experienced in these participants when HD-induced and stenoses effects are combined.

In a study completed on a HD population, it was concluded that the probability of cardiovascular disease almost doubles when the serum CRP levels are greater than 0.6md/dL[65]. CRP shows trends of higher concentration in the blood stream of the *CAD+* group than the non-stenosed. Generally, CRP > 3.0mg/L is a major risk factor for heart disease[66]. In this study, the mean CRP levels at baseline was greater than 3.0 mg/L in HD with no CAD. This elevation in CRP in *CAD-* HD participant can be a result of the chronic inflammation associated with HD, that is most evident with significant intradialytic changes in CRP. The mean CRP levels are approximately doubled in participants on HD with CAD. CRP levels has shown to be a possible biomarker of vascular inflammation in coronary artery disease[67–69]. The excessive levels of CRP we see in the *CAD+* arm may be an indication of vascular inflammation and vessel damage localized to the affected artery.

This study was a retrospective exploratory study with a limited number of HD participants; data should be interpreted with this in mind. Despite the small number of participants, the effect sizes of the reported results in the present study are large. Cohen's d was calculated for the primary outcomes of global myocardial perfusion and RMWAs. The calculated Cohen's d value for global myocardial perfusion between the two arms at baseline, peak HD, and post HD were 1.38, 0.08, and 1.21, respectively. The calculated Cohen's d value for regional wall motion abnormality

between the two arms at peak HD and post HD were 0.62 and 1.16, respectively. Generally, a Cohen's d value greater than 0.8 is considered to be a large effect size. While the number of patients studied was small, it was able to demonstrate the circulatory and function cardiac changes to HD with respect to the coronary artery health. It is important to also note that as a result of the small sample size, it is unlikely that other variables presented in this work were powered to detect change.

2.5 Conclusion

HD treatment induces ischemic injury to the heart causing myocardial stunning that is not specific to the presence or absence of CAD. In a limited number of participants with no clinical evidence or symptoms of CAD, this study has shown that the cardiac response (perfusion and stunning) to HD is exacerbated with the addition of stenosed lesions in the coronary artery. Patients with severe and unresolved intradialytic stunning may warrant screening for CAD with CT angiography for intervention to improve tolerability of HD treatment. Further work is required, and we acknowledge that a larger randomized clinical trial would be beneficial in providing a complete summary of varying degrees of CVD on patient's cardiac response to HD. This would further allow personalized treatment methods for patients undergoing HD.

2.6 Acknowledgements

2.7 References

1. Mathew RO, Bangalore S, Lavelle MP, et al. Diagnosis and management of atherosclerotic cardiovascular disease in chronic kidney disease: a review. *Kidney Int*. 2017;91(4):797-807. doi:10.1016/j.kint.2016.09.049

2. Foley RN, Parfrey PS, Sarnak MJ. Clinical epidemiology of cardiovascular disease in chronic renal disease. *American Journal of Kidney Diseases*. 1998;32(5):S112-S119. doi:10.1053/AJKD.1998.V32.PM9820470

3. Li H, Wang S. Cardiovascular Disease in Hemodialysis Patients. *Hemodialysis*. Published online 2013:3-19. doi:10.5772/53071

4. Cozzolino M, Mangano M, Stucchi A, Ciceri P, Conte F, Galassi A. Cardiovascular disease in dialysis patients. *Nephrology Dialysis Transplantation*. 2018;33:iii28-iii34. doi:10.1093/ndt/gfy174

5. Foley RN. CLINICAL EPIDEMIOLOGY OF CARDIOVASCULAR DISEASE IN CHRONIC KIDNEY DISEASE. *J Ren Care*. 2010;36:4-8. doi:10.1111/j.1755-6686.2010.00171.x

6. Aoki J, Ikari Y. Cardiovascular Disease in Patients with End-Stage Renal Disease on Hemodialysis. *Ann Vasc Dis*. 2017;10(4):327-337. doi:10.3400/avd.ra.17-00051

7. Su JB. Vascular endothelial dysfunction and pharmacological treatment. *World J Cardiol*. 2015;7(11):719. doi:10.4330/WJC.V7.I11.719

8. Bonetti PO, Lerman LO, Lerman A. Endothelial dysfunction: A marker of atherosclerotic risk. *Arterioscler Thromb Vasc Biol*. 2003;23(2):168-175. doi:10.1161/01.ATV.0000051384.43104.FC/FORMAT/EPUB

9. Brunet P, Gondouin B, Duval-Sabatier A, et al. Does Uremia Cause Vascular Dysfunction? Published online 2011. doi:10.1159/000327131

10. Schwarz U, Buzello M, Ritz E, et al. Morphology of coronary atherosclerotic lesions in patients with end-stage renal failure. *Nephrology Dialysis Transplantation*. 2000;15(2):218-223. doi:10.1093/NDT/15.2.218

11. Huang PH, Chen LC, Leu HB, et al. Enhanced coronary calcification determined by electron beam CT is strongly related to endothelial dysfunction in patients with suspected coronary artery disease. *Chest*. 2005;128(2):810-815. doi:10.1378/chest.128.2.810

12. Raggi P, Bellasi A, Ferramosca E, Islam T, Muntner P, Block GA. Association of pulse wave velocity with vascular and valvular calcification in hemodialysis patients. *Kidney Int*. 2007;71(8):802-807. doi:10.1038/SJ.KI.5002164

13. Mcintyre CW, Salerno FR. Diagnosis and Treatment of Intradialytic Hypotension in Maintenance Hemodialysis Patients. *Clin J Am Soc Nephrol*. 2018;13:486-489. doi:10.2215/CJN.11131017

14. Palmer BF, Henrich WL. Recent Advances in the Prevention and Management of Intradialytic Hypotension. Published online 2008. doi:10.1681/ASN.2007091006

15. Sars B, van der Sande FM, Kooman JP. Advances in CKD 2020 Intradialytic Hypotension: Mechanisms and Outcome. *Blood Purif*. 2019;49:158-167. doi:10.1159/000503776

16. Sands JJ, Usvyat LA, Sullivan T, et al. Intradialytic hypotension: Frequency, sources of variation and correlation with clinical outcome. *Hemodialysis International*. 2014;18(2):415-422. doi:10.1111/HDI.12138

17. Assimon MM, Flythe JE. Definitions of Intradialytic Hypotension. *Semin Dial*. 2017;30(6):464-472. doi:10.1111/sdi.12626

18. Kanbay M, Ertuglu LA, Afsar B, et al. An update review of intradialytic hypotension: concept, risk factors, clinical implications and management. *Clin Kidney J*. 2020;13(6):981-993. doi:10.1093/ckj/sfaa078

19. Mcintyre C, Crowley L. Dying to Feel Better: The Central Role of Dialysis-Induced Tissue Hypoxia. *Clin J Am Soc Nephrol*. 2016;11:549-551. doi:10.2215/CJN.01380216

20. Kuipers J, Verboom LM, Ipema KJR, et al. The Prevalence of Intradialytic Hypotension in Patients on Conventional Hemodialysis: A Systematic Review with Meta-Analysis. *Translational Research: Research Article Am J Nephrol*. 2019;49:497-506. doi:10.1159/000500877

21. Davenport A, Cox C, Thuraisingham R. Achieving blood pressure targets during dialysis improves control but increases intradialytic hypotension. *Kidney Int*. 2008;73(6):759-764. doi:10.1038/SJ.KI.5002745

22. Sherman RA. Intradialytic hypotension: An overview of recent, unresolved and overlooked issues. *Semin Dial*. 2002;15(3):141-143. doi:10.1046/J.1525-139X.2002.00002.X

23. Chou JA, Streja E, Nguyen D v, et al. Intradialytic hypotension, blood pressure changes and mortality risk in incident hemodialysis patients. *Nephrology Dialysis Transplantation*. 2018;33:149-159. doi:10.1093/ndt/gfx037

24. Stefánsson B v, Brunelli SM, Cabrera C, et al. Intradialytic Hypotension and Risk of Cardiovascular Disease. *Clinical Journal of the American Society of Nephrology*. Published online 2014. doi:10.2215/CJN.02680314

25. Flythe JE, Xue H, Lynch KE, Curhan GC, Brunelli SM. Association of Mortality Risk with Various Definitions of Intradialytic Hypotension. *J Am Soc Nephrol*. 2015;26:724-734. doi:10.1681/ASN.2014020222

26. Mcintyre CW. Effects of hemodialysis on cardiac function. *Kidney Int*. 2009;76:371-375. doi:10.1038/ki.2009.207

27. McIntyre CW. Haemodialysis-Induced Myocardial Stunning in Chronic Kidney Disease – A New Aspect of Cardiovascular Disease. *Blood Purif*. 2010;29(2):105-110. doi:10.1159/000245634

28. Mcintyre CW. Recurrent Circulatory Stress: The Dark Side of Dialysis. *Semin Dial*. 2010;23(5):449-451. doi:10.1111/j.1525-139X.2010.00782.x

29. Hur L, McIntyre CW. Current and novel imaging techniques to evaluate myocardial dysfunction during hemodialysis. *Curr Opin Nephrol Hypertens*. 2020;29(6). doi:10.1097/MNH.0000000000000645

30. McIntyre CW, Odudu A. Hemodialysis-associated cardiomyopathy: A newly defined disease entity. *Semin Dial*. 2014;27(2):87-97. doi:10.1111/sdi.12197

31. Selby NM, McIntyre CW. The Acute Cardiac Effects of Dialysis. *Semin Dial*. 2007;20(3):220-228. doi:10.1111/j.1525-139X.2007.00281.x

32. Odudu A, Francis ST, McIntyre CW. MRI for the assessment of organ perfusion in patients with chronic kidney disease. *Curr Opin Nephrol Hypertens*. 2012;21(6):647-654. doi:10.1097/MNH.0b013e328358d582

33. Burton JO, Jefferies HJ, Selby NM, Mcintyre CW. Hemodialysis-Induced Repetitive Myocardial Injury Results in Global and Segmental Reduction in Systolic Cardiac Function. *Clin J Am Soc Nephrol*. 1925;4. doi:10.2215/CJN.04470709

34. Burton JO, Jefferies HJ, Selby NM, Mcintyre CW. Hemodialysis-Induced Cardiac Injury: Determinants and Associated Outcomes. *Clin J Am Soc Nephrol*. 2009;4:914-920. doi:10.2215/CJN.03900808

35. Jefferies HJ, Virk B, Schiller B, Moran J, Mcintyre CW. Frequent Hemodialysis Schedules Are Associated with Reduced Levels of Dialysis-induced Cardiac Injury (Myocardial Stunning). *Clin J Am Soc Nephrol*. 2011;6:1326-1332. doi:10.2215/CJN.05200610

36. Dasselaar JJ, Slart RHJA, Knip M, et al. Haemodialysis is associated with a pronounced fall in myocardial perfusion. *Nephrol Dial Transplant*. 2009;24:604-610. doi:10.1093/ndt/gfn501

37. Buchanan C, Mohammed A, Cox E, et al. Intradialytic Cardiac Magnetic Resonance Imaging to Assess Cardiovascular Responses in a Short-Term Trial of Hemodiafiltration and Hemodialysis. *J Am Soc Nephrol*. 2017;28:1269-1277. doi:10.1681/ASN.2016060686

38. Buchanan C, Mohammed A, Cox E, et al. Intradialytic cardiac magnetic resonance imaging to assess cardiovascular responses in a short-term trial of hemodiafiltration and hemodialysis. *Journal of the American Society of Nephrology*. 2017;28(4):1269-1277. doi:10.1681/ASN.2016060686

39. Ragosta M, Samady H, Isaacs RB, Gimple LW, Sarembock IJ, Powers ER. Coronary flow reserve abnormalities in patients with diabetes mellitus who have end-stage renal disease and normal epicardial coronary arteries. Published online 2004. doi:10.1016/j.ahj.2003.07.029

40. Niizuma S, Takiuchi S, Okada S, et al. Decreased coronary flow reserve in haemodialysis patients. *Nephrol Dial Transplant*. 2008;23:2324-2328. doi:10.1093/ndt/gfm954

41. Dohi K, Matsuo H, Machida H, et al. Echocardiographic Assessment of Cardiac Structural and Functional Abnormalities in Patients With End-Stage Renal Disease Receiving Chronic Hemodialysis. *Circulation Journal*. 2018;82:586-595. doi:10.1253/circj.CJ-17-0393

42. Chirakarnjanakorn S, Navaneethan SD, Francis GS, Wilson Tang WH. Cardiovascular impact in patients undergoing maintenance hemodialysis: Clinical management considerations. Published online 2017. doi:10.1016/j.ijcard.2017.01.015

43. Meeus F, Kourilsky O, Guerin AP, Gaudry C, Marchais SJ, London GM. Pathophysiology of cardiovascular disease in hemodialysis patients. *Kidney Int Suppl*. 2000;58(76). doi:10.1046/J.1523-1755.2000.07618.X

44. Ahmadmehrabi S, Wilson Tang | W H, Tang WHW. Hemodialysis-induced cardiovascular disease. Published online 2018. doi:10.1111/sdi.12694

45. Mcintyre CW, Burton JO, Selby NM, et al. Hemodialysis-Induced Cardiac Dysfunction Is Associated with an Acute Reduction in Global and Segmental Myocardial Blood Flow. *Clin J Am Soc Nephrol*. 2008;3:19-26. doi:10.2215/CJN.03170707

46. Hothi DK, Rees L, Marek J, Burton J, Mcintyre CW. Pediatric Myocardial Stunning Underscores the Cardiac Toxicity of Conventional Hemodialysis Treatments. *Clin J Am Soc Nephrol*. 2009;4:790-797. doi:10.2215/CJN.05921108

47. Odudu A, Eldehni MT, McCann GP, McIntyre CIW. Randomized controlled trial of individualized dialysate cooling for cardiac protection in hemodialysis patients. *Clinical Journal of the American Society of Nephrology*. 2015;10(8):1408-1417. doi:10.2215/CJN.00200115

48. Marants R, Qirjazi E, Grant CJ, Lee TY, Mcintyre CW. Renal Perfusion during Hemodialysis: Intradialytic Blood Flow Decline and Effects of Dialysate Cooling. Published online 2019. doi:10.1681/ASN.2018121194

49. Postiglione A, Faccenda F, Gallotta G, Rubba P, Federico S. Changes in middle cerebral artery blood velocity in uremic patients after hemodialysis. *Stroke*. 1991;22(12):1508-1511. doi:10.1161/01.STR.22.12.1508

50. Hata R, Matsumoto M, Handa N, Terakawa H, Sugitani Y, Kamacta T. Effects of hemodialysis on cerebral circulation evaluated by transcranial Doppler ultrasonography. *Stroke*. 1994;25(2):408-412. doi:10.1161/01.STR.25.2.408

51. Metry G, Spittle M, Rahmati S, et al. Online Monitoring of Cerebral Hemodynamics During Hemodialysis. Published online 2002. doi:10.1053/ajkd.2002.36333

52. Metry G, Bj¨ B, Wikstr¨om B, et al. Effect of Normalization of Hematocrit on Brain Circulation and Metabolism in Hemodialysis Patients. *J Am Soc Nephrol*. 1998;8:1132.

53. Wolfgram DF. Intradialytic Cerebral Hypoperfusion as Mechanism for Cognitive Impairment in Patients on Hemodialysis. *REVIEW www.jasn.org JASN*. 2017;30:2052-2058. doi:10.1681/ASN.2019050461

54. Polinder-Bos HA, Willem Elting JJ, Aries MJ, et al. Changes in cerebral oxygenation and cerebral blood flow during hemodialysis-A simultaneous near-infrared spectroscopy and positron emission tomography study. *Journal of Cerebral Blood Flow & Metabolism*. 2020(2). doi:10.1177/0271678X18818652

55. Welsh P, Preiss D, Hayward C, et al. Cardiac Troponin T and Troponin i in the General Population: Comparing and Contrasting Their Genetic Determinants and Associations with Outcomes. *Circulation*. 2019;139(24):2754-2764. doi:10.1161/CIRCULATIONAHA.118.038529/FORMAT/EPUB

56. Mahajan VS, Jarolim P. How to interpret elevated cardiac troponin levels. *Circulation*. 2011;124(21):2350-2354. doi:10.1161/CIRCULATIONAHA.111.023697/FORMAT/EPUB

57. Hung SY, Hung YM, Fang HC, et al. Cardiac Troponin I and Creatine Kinase Isoenzyme MB in Patients with Intradialytic Hypotension. *Blood Purif*. 2004;22:338-343. doi:10.1159/000079188

58. Maresca B, Manzione A, Moioli A, et al. Prognostic value of high-sensitive cardiac troponin I in asymptomatic chronic hemodialysis patients. *J Nephrol*. 2020;33:129-136. doi:10.1007/s40620-019-00610-5

59. Breidthardt T, Burton JO, Odudu A, Eldehni MT, Jefferies HJ, Mcintyre CW. Troponin T for the Detection of Dialysis-Induced Myocardial Stunning in Hemodialysis Patients. *Clin J Am Soc Nephrol*. 2012;7:1285-1292. doi:10.2215/CJN.00460112

60. Breidthardt T, Burton JO, Odudu A, Eldehni MT, Jefferies HJ, Mcintyre CW. Troponin T for the Detection of Dialysis-Induced Myocardial Stunning in Hemodialysis Patients. *Clin J Am Soc Nephrol*. 2012;7:1285-1292. doi:10.2215/CJN.00460112

61. Breidthardt T, Burton JO, Odudu A, Eldehni MT, Jefferies HJ, Mcintyre CW. Troponin T for the Detection of Dialysis-Induced Myocardial Stunning in Hemodialysis Patients. *Clin J Am Soc Nephrol*. 2012;7:1285-1292. doi:10.2215/CJN.00460112

62. Sun L, Ji Y, Wang Y, et al. High-sensitive cardiac troponin T: a biomarker of left-ventricular diastolic dysfunction in hemodialysis patients. *J Nephrol*. 2018;31:967-973. doi:10.1007/s40620-018-0540-0

63. Ünlü S, Şahinarslan A, Sezenöz B, et al. High-sensitive troponin T increase after hemodialysis is associated with left ventricular global longitudinal strain and ultrafiltration rate. *Cardiol J*. 2020;27(4):376-383. doi:10.5603/CJ.A2018.0118

64. Assa S, Gansevoort RT, Westerhuis R, et al. Determinants and prognostic significance of an intra-dialysis rise of cardiac troponin I measured by sensitive assay in hemodialysis patients. doi:10.1007/s00392-013-0551-8

65. Heidari B. *C-Reactive Protein and Other Markers of Inflammation in Hemodialysis Patients*.

66. Polyakova EA, Mikhaylov EN. The prognostic role of high-sensitivity C-reactive protein in patients with acute myocardial infarction. *Journal of Geriatric Cardiology*. 2020;17:379-383. doi:10.11909/j.issn.1671-5411.2020.07.007

67. Sproston NR, Ashworth JJ. Role of C-Reactive Protein at Sites of Inflammation and Infection. *Front Immunol*. 2018;9(APR):754. doi:10.3389/FIMMU.2018.00754

68. Inoue N. Vascular C-Reactive Protein in the Pathogenesis of Coronary Artery Disease:Role of Vascular Inflammation and Oxidative Stress. *Cardiovascular & Hematological Disorders-Drug Targets*. 2012;6(4):227-231. doi:10.2174/187152906779010719

69. Mazer SP, Rabbani LE. *Evidence for C-Reactive Protein's Role in (CRP) Vascular Disease: Atherothrombosis, Immuno-Regulation and CRP*. Vol 17. Kluwer Academic Publishers; 2004.

2.8 Co-Authorship Statement

The material in Chapter 2 is in preparation for publication at the Kidney International Journal. Some materials presented in this chapter submitted for a presentation at the American Society of Nephrology International Conference (November 5, 2022; SA-PO374; poster presentation). Lisa Hur is the main contributor of the work that has been presented in this chapter including the designing of the study, data acquisition, data processing, statistical analysis of the data, and manuscript preparation. Co-authors of this chapter were Ali Islam, Jarrin Penny, Justin Dorie, and Christopher W. McIntyre. Ali Islam assessed the coronary CT angiography images for data analysis. Jarrin Penny and Justin Dorie were responsible for the delivery of hemodialysis and exercise, ensuring the safety of the participants during the study visits. Christopher McIntyre provided clinical and logistical oversight, as well as invaluable guidance in terms of the study design, interpretation of data, and manuscript preparation.

Estimated percentage of the work for Chapter 2 conducted solely by Lisa Hur: 85%

2.9 Supplementary Figures
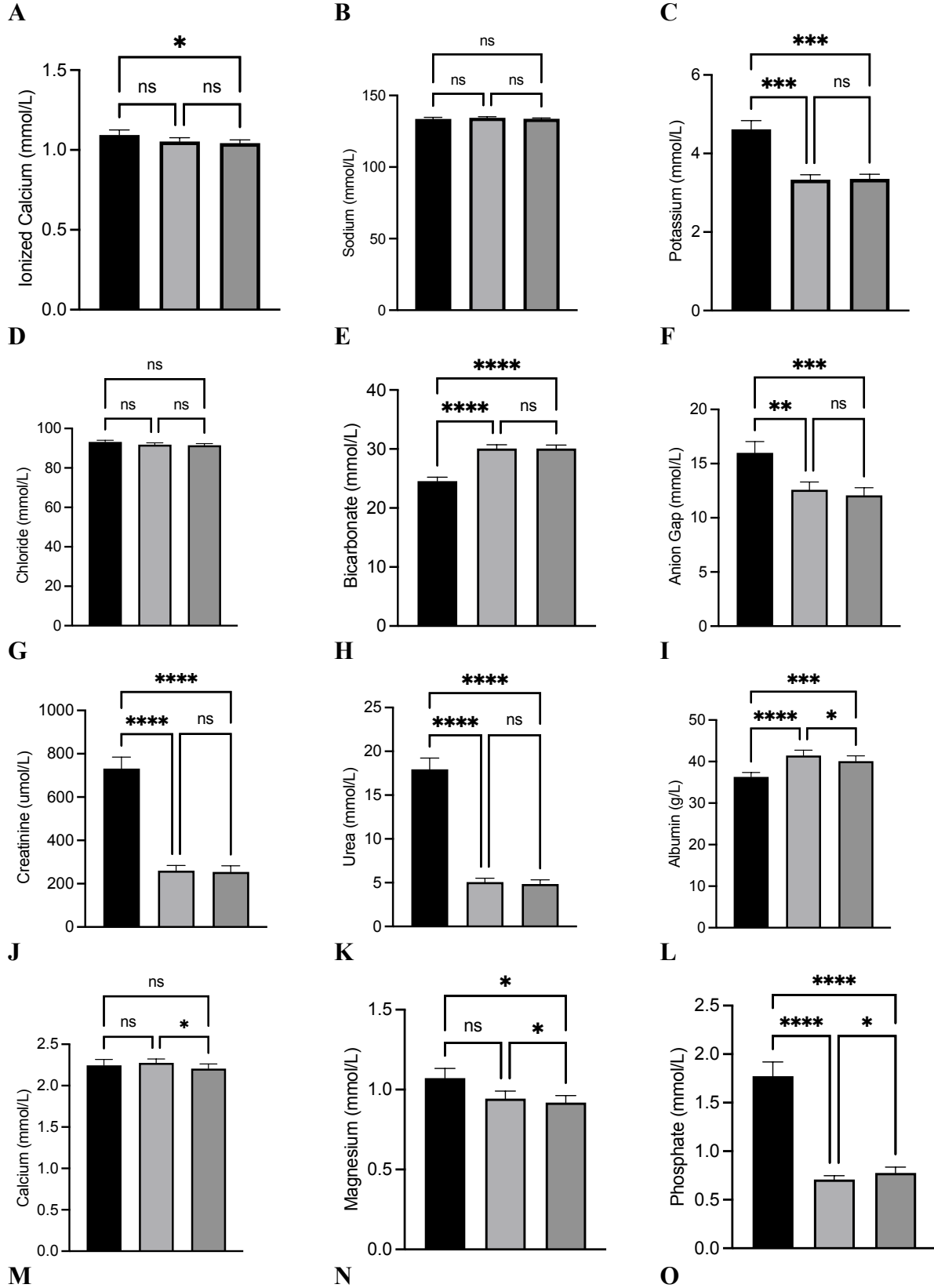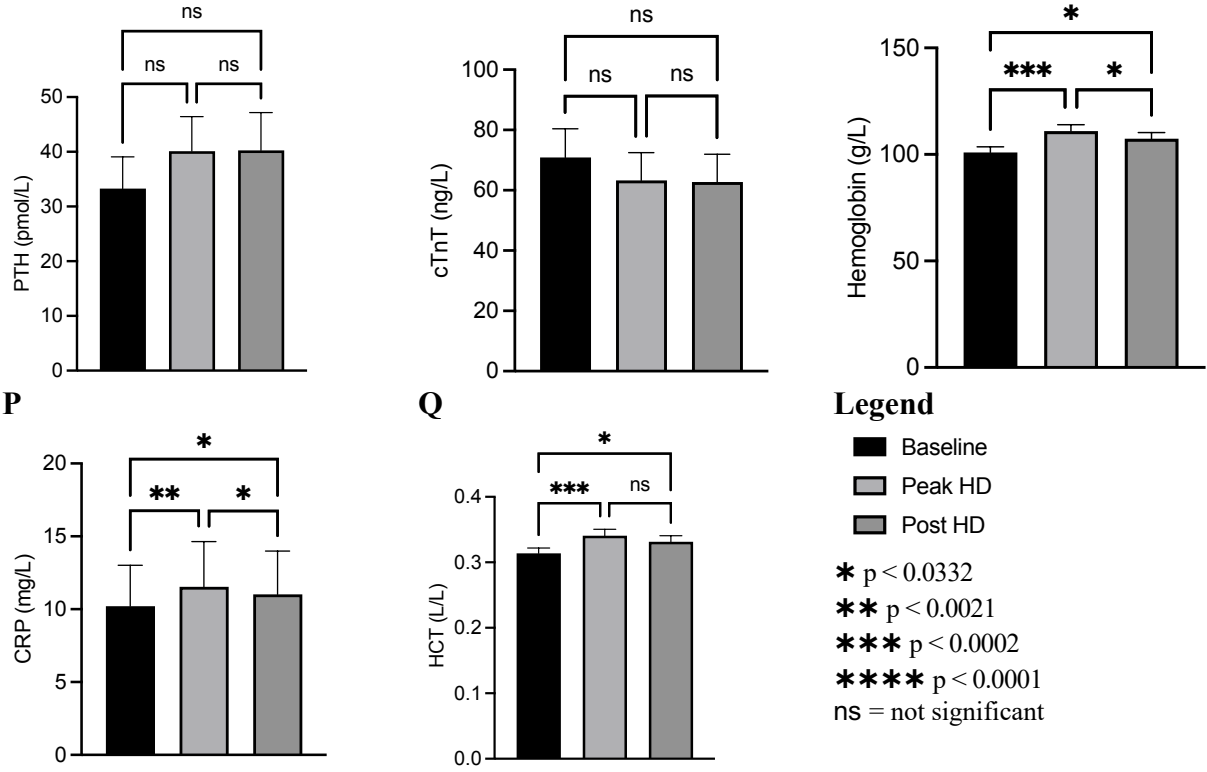
Supplementary Figure 2-1. Intradialytic changes in serum electrolyte and protein levels. Error bars represent standard error of the mean

Chapter 3

3 The effect of dialysate sodium on endothelial injury and microcirculatory dysfunction

A version of this chapter is in preparation for publication: Lisa Hur, Yanmin Zhang, Barry Janssen, Christopher W. McIntyre, "The effect of dialysate sodium on endothelial injury and microcirculatory dysfunction," *In preparation*. Aug 2022.

Abstract Each episode of hemodialysis (HD) treatment causes injury to the glycocalyx which induces shedding of syndecan-1 (syn-1), a transmembrane heparan sulfate proteoglycan. This damage results from hemodynamic stress of HD itself and injury caused by oncotic shifts in the presence of additional sodium (Na+) during HD. The glycocalyx binds Na+, buffering sudden serum Na+ shifts, and can be damaged with acute changes in Na+ concentration. The aim of this study is to use a preclinical platform to investigate the effects of Na+ dialysate concentration on endothelial cell injury and microcirculatory dysfunction during HD. We hypothesize that changes in plasma Na+ concentration will result in the direct injury to the glycocalyx and reduce microcirculatory perfusion. Twenty-seven healthy male Wistar Kyoto rats underwent HD: eight were exposed to dialysate Na+ concentration at typical rat plasma Na+ level (isonatric, 140mM), ten were exposed to dialysate Na+ below typical rat plasma Na+ level (hyponatremic, 130mM), and nine were exposed to dialysate Na+ above typical rat plasma Na+ level (hypernatremic, 150mM). Throughout HD, intravital microscopy (IVM) was used to image the microvasculature at baseline, during extracorporeal circulation with no dialysate flow ("Sham"), at 1 hr into HD, at 2 hrs into HD, and post HD ("Final"). The IVM images were processed to derive the number of identified intersecting points, a metric quantifying microcirculatory blood flow, to observe the change in perfusion index at each timepoint. Blood samples were collected at the same timepoints corresponding to the IVM image acquisitions to measure syn-1 and quantify glycocalyx shedding during HD. Blood pressure of the animal were acquired continually throughout the experiment. Blood pressure between the three groups were comparable. The findings demonstrate a gradual increase in syn-1 concentration in blood plasma throughout the duration of the experiment in the isonatric, hyponatremic, and the hypernatremic groups. The percent change in syn-1 of the hypernatremic group doubled that of the isonatric and hyponatremic group by 2hrs into HD. The experimental groups demonstrated a consistent trend of lower perfusion index throughout the duration of the experiment. A single HD session can possibly elevate syn-1 and reduce microvascular perfusion, indicating HD-associated endothelial injury and microcirculatory dysfunction. As well, the damage to the glycocalyx may be more pronounced with hypernatremic effects.

3.1 Introduction

The therapeutic aim of hemodialysis (HD) is to artificially remove the interdialytic sodium load accumulated between dialysis sessions that cannot be eliminated efficiently by the kidney in individuals with end stage renal disease (ESRD). Failure to effectively remove sodium from the body results in interdialytic fluid gain, hypertension and exacerbated ischemic injury as a result of the unfavorably high ultrafiltration requirement to achieve target weight[1–5]. This can be explained by the need to intake fluid to maintain sodium-water balance in our body after the ingestion of sodium rich content which in turn increases interdialytic weight gain. Furthermore, sodium that was not cleared through dialysis is deposited in the skin and muscle (including the myocardium)[6]; the storage capacity of sodium in the tissue is limited and the buffer capacity of the vasculature for interdialytic circulating serum sodium is variable amongst individuals[7]. Excess serum sodium concentration directly results in injury to the endothelial glycocalyx (discussed below) and aggravates ischemic vulnerability to the circulatory stress induced during HD. However, excessive sodium depuration during HD could cause hypotension and circulatory collapse owing to the lack of maintenance of plasma tonicity and refill.

Currently, the manipulation of dialysate sodium concentration is the principle approach in achieving sodium homeostasis in HD patients. Low dialysate sodium concentration has been shown to reduce sodium deposition in the tissue using sodium MR imaging while minimizing interdialytic weight gain[6]. Despite these advantages of low dialysate sodium concentration, sodium dialysate concentration cannot be prescribed as a one size fits all approach. As discussed earlier, one of the detrimental effects of low sodium is hypotension and circulatory collapse; patients predisposed to these symptoms would experience worsening HD-associated cardiovascular injury when treated with low sodium dialysate concentration. Hence, it is difficult to determine the most

optimal dialysate sodium concentration based on the limitations in our knowledge relating to the mechanism of HD-induced circulatory dysfunction in the presence of sodium. One of the common non-invasive methods of assessing tolerability to HD treatment is through quantification of myocardial stunning, a surrogate marker of regional ischemia[8–14]. The observed variation in myocardial stunning during HD is mostly attributed to factors relating to hemodynamic stress including hypovolemia, hypotension, tissue ischemia, and arrythmias[15]. Investigation of other non-hemodynamic stress factors such as osmotic shift and changes in electrolyte may potentially shed light on other approaches to improving tolerability to HD treatment.

The recent findings of endothelial damage with acute rise of plasma sodium during dialysis raised the possibility that investigation of sodium may be important[16]. Syndecan-1 is a transmembrane heparan sulfate proteoglycan and a component of the glycocalyx layer on the luminal side of the endothelial cell[17]. With endothelial dysfunction, syndecan-1 sheds from the cell surface into the bloodstream. Consequences of a damaged endothelium include the loss of vascular integrity (i.e. inability to control dilation and constriction) and increases in vascular permeability[18,19]. The earlier study investigating changes in plasma sodium during HD suggested that the stability of the endothelium was influenced by the plasma sodium concentration exceeding the buffering capacity of the glycocalyx. The hemodynamic stress of HD itself in addition to the injury caused by the acute oncotic shift in the presence of excess sodium during HD may explain the endothelial vulnerability and damage seen in the HD population. With damage to the endothelium, we expect to consequently see dysfunction in the vasculature. Microvascular dysfunction results in the maldistribution of blood flow or irregular microcirculation within arterioles, venules, and capillaries[20]. This transpires with maintenance HD treatment; there is inadequate perfusion to the

tissue due to microvascular dysfunction, causing irreversible ischemic damage and reaching organ failure with time [21–24].

The question we aim to address in this research paper is whether or not sodium is a contributor of HD-induced endothelial injury, making the patient more vulnerable to microvascular dysfunction and ischemia. Our lab has previously created a small-animal hemodialysis system to study the effect of hemodialysis on the microcirculation in a small animal model[24]. Using intravital video microscopy on surgically exposed muscle tissue, changes in microvascular blood flow were measured and quantified while the animal was be dialyzed. The purpose of this current study was to use this established preclinical model to investigate the effects of sodium dialysate concentration on endothelial cell injury and microcirculatory dysfunction during HD. It is hypothesized that changes in plasma sodium concentration will result in the direct injury to the glycocalyx, affecting the degree of microcirculatory perfusion during HD.

3.2 Methods

3.2.1 Experimental Animals

The experiments conducted in this study followed the Canadian Council of Animal Care and the ARRIVE guidelines and regulations. This work has been approved by the Animal Care and Use Committee of Western University (London, Ontario Canada).

Thirty-one male Wistar-Kyoto rats (approximately 250 – 300g in weight, SPF, Charles River, Wilmington, MA, United States of America) were group-housed in standard conditions, at room temperature. The animals were fed without restriction and were exposed to 12-hour periods of light-dark cycle per day. Interaction with cage-mates were unrestricted. Upon arrival from the

supplier, animals had a minimum of 72 hours to acclimatize to the new environment before proceeding with experiment procedures.

3.2.2 Surgical Procedure for Muscle Microvasculature Imaging

Prior to muscular surgery, the animals were anaesthetized with a mixture of four percent isoflurane and one percent oxygen. To ensure the maintenance of anesthesia while minimizing its effect on blood pressure, two percent isoflurane was delivered continuously through a facemask ventilator fitted for small animals. A rectal temperature probe was used for continuous monitoring of the core body temperature throughout experimental procedure (TCAT-2 Temperature Controller, Physitemp Instruments LLC, Clifton, NJ, United States of America). The body temperature was maintained at 36.5°C with an infrared lamp. For continuous monitoring of the animal blood pressure, a catheter was inserted into the carotid artery and connected to a pressure transducer that measured the mean arterial blood pressure and heart rate (DMSI-400, Micro-Med INC, Louisville, Kentucky, United States of America). Heparinized dialysate (2U/mL) was used periodically to ensure the carotid artery catheter did not occlude.

The extensor digitorum longus (EDL) muscle of the animal's right hind leg was exposed for intravital microscopy according to the surgical procedure outlined by Tyml and Budreau[25]. After the exposure, the EDL muscle was left open to air for thirty minutes prior to the visualization of the circulation under the intravital microscopy. Microvascular perfusion behaviors were observed using an inverted microscope (Nikon Eclipse-Ti, Nikon Instruments, Melville, New York, United States of America) with a modified microscope stage, a 100-watt xenon light source (PTI LPS 220, Horiba Scientific, Piscataway, New Jersey, United States of America) and an optical light guide (Thorlabs, Newton, New Jersey, United States of America). To prevent tissue damage, a 400-550nm bandpass filter was used to restrict the frequencies of light used for tissue

imaging. For better visualization of the red blood cells, an additional 450nm/20nm bandpass filter was placed directly on the camera.

3.2.3 Small-Animal Dialyzer Unit

The small-animal dialyzer units used in this study were assembled in-house using 75 fiber parts of an existing conventional polysulphone dialyzer (FX 600 Helixone, Fresenius, Canada). Following the designs of the dialyzers utilized clinically, the fibers were encapsulated in a polycarbonate tube (Figure 3-1). The internal volume of the microdialyzer was 290μL. The dialyzer had an external bypass line connected from one end to the other, holding the equivalent volume of fluid as the dialyzer itself, and enabling study of the effects of the change in systemic blood volume that occurs during dialysis but in the absence of dialysate flow.
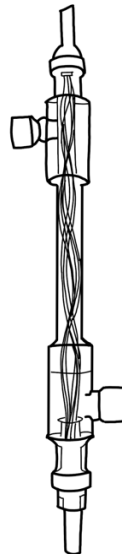
Figure 3-1 Small animal dialysis unit

3.2.4 Dialysate Composition

To study the effects of dialysate sodium concentration on the microvasculature, fresh dialysate fluid of specific sodium concentration was prepared for each experiment. The first group

was the isonatric (control) group; animals in this arm were exposed to dialysate fluid of 140mM

sodium concentration that is comparable to their baseline plasma sodium level. The second was

the hyponatremic group, whose dialysate fluid was of lower sodium concentration (130mM).

Lastly, the third arm was the hypernatremic group, exposed to high levels of sodium (150mM). To

assess accuracy of the dialysate prescription, samples of the dialysate fluid were collected, and

levels of sodium were measured. The dialysate sodium concentration for the isonatric group were

determined based on our previous rodent study that showed plasma sodium concentration ranging

between 139 and 140 mmol/L at baseline[24]. To ensure variability in the delivered sodium dialysate

concentration, the sodium concentration chosen for the hypo- and hypernatremic group were ± 10

mM of the isonatric group.

3.2.5 In-vivo Hemodialysis Experiment

In the left hind limb, the limb without EDL muscle exposure, two catheters were inserted

to establish extracorporeal blood flow (Figure 3-2). A catheter was placed in the left femoral artery

for blood outflow to the dialyzer, and a second catheter was inserted within the left femoral vein

for the return of filtered blood from the dialyzer to the systemic circulation of the animal. The

catheters were securely connected to the dialyzer, and the extracorporeal circulation of blood was

initiated using a peristaltic pump (P720, Instech Lab., Plymouth Meeting, Pennsylvania, United

States of America). Immediately after initiation, 'baseline' blood samples and intravital

microscopy images were acquired. The blood was then circulated through the dialysis circuit for

one hour. After one hour, blood samples and intravital microscopy images were collected for the

'sham' timepoint. Subsequently, the blood flow was directed to pump through the dialyzer for two

hours at a rate of 2ml/kg/hr. For dialysate flow, two peristaltic infusion pumps (Sigma Spectrum

V8 Infusion System, Baxter, Deerfield, Illinois, United States of America) were used at 1ml/min,

with continuous adjustment throughout the experiment depending on the hematocrit level. Blood

samples and intravital microscopy images were repeated at 1hr and 2hrs into HD treatment.
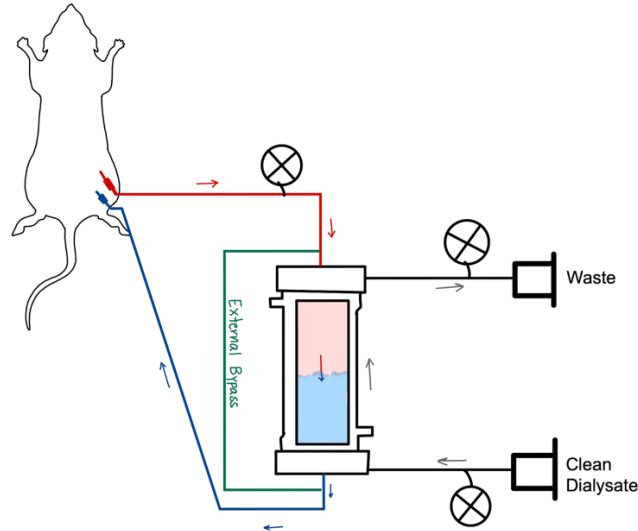
Figure 3-2 Small animal hemodialysis experimental set-up

3.2.6 Acquisition of Experimental Blood Work

At baseline, sham, 1hr HD, and 2hr HD, 200μL of blood were sampled from the animals,

directly through the dialyzer unit. Of the 200μL, 100μL of the sample was added to the iStat EC8+

cartridge (Abbot, Princeton, New Jersey, United States of America) for analysis of sodium,

potassium, chloride, glucose, blood urea nitrogen, hematocrit and hemoglobin levels. Creatinine

levels were measured with the remaining blood sample (100μL) with the iStat Crea cartridge

(Abbot, Princeton, New Jersey, United States of America). The cartridges were processed using a

VetStat point of care blood gas analyzer (VetScan i-STAT-1 Handheld Analyzer, Abaxis, Union

City, California, United States of America.

3.2.7 Intravital Microscopy: Quantification of Microvascular Perfusion

The acquisition of the dynamic (sequence of 60 seconds at 30 frames per second) microvascular perfusion images at baseline, sham, 1hr HD, and 2hr HD were completed using a multispectral multicamera system (MSMC-23-1-A, Spectral Device Inc., London, Canada). At baseline, multiple adjacent fields of views are selected for recording. In the subsequent imaging timepoints, the microvascular perfusion of previously selected fields of views are acquired, allowing the quantification of the observed change in microvascular perfusion throughout the experiment.

The intravital images were post-processed using in-house software written in Matlab (Matlab 2020a, the Matworks Inc, Natrick, Massachusetts, United States of America)[26,27]. The software applies an algorithm to identify perfused vessels within the field of view captured based on the active flow of the red blood cells. This is completed by assessing the change in light intensity caused by the movement of the red blood cell within the pixels of interest. From this information, a sum of absolute intensity difference image is generated for each field of view at each experimental imaging timepoints (baseline, sham, 1hr HD, and 2hr HD), allowing the user to visualize the perfused vessels. An additional processing step follows for the quantification of the number of perfused vessels: a ten-by-ten grid is mapped onto the sum of absolute intensity difference image, where a separate two-step machine learning algorithm is applied to identify points within the grid with observed perfusion. The number of identifiable points of intersection between the grid and the regions of vessel perfusion are added to represent the perfusion index of the specific field of view and experiment timepoint.

3.2.8 Plasma Sampling: Quantification of Syndecan-1

At baseline, sham, 1hr HD, and 2hr HD, 150µL of blood were obtained from the animal, directly through the dialyzer unit. Shortly after the end of HD, a final set of blood samples were collected from the animal. This served as the endpoint for the animals. The acquired blood samples were centrifuged for thirty minutes at 2500 RCF in 4°C to extract the plasma layer. The plasma samples collected in thirty-one animals were stored in a -80°C freezer before processing. A commercially available ELISA kit was used to quantify rodent syndecan-1 levels (Novus Biologicals, NBP2-76611, Littleton, Colorado, United States of America). ELISA experiments were performed in accordance with the manufacturers' instruction manual. The reference standards were within the limits of detection and were fitted to a 4-parameter logistic model. This model was then used to estimate absolute concentration of syndecan-1. To assess the damage of the glycocalyx and endothelium, the percent change in syndecan-1 concentration at sham, 1hr HD, 2hr HD, and final were calculated in reference to the baseline.

3.2.9 Statistical Analysis

All statistical analyses described in this section were completed using GraphPad Prism 9 software (GraphPad Software, La Jolla, California, United States of America).

3.2.9.1   Dialysate Composition

Ordinary one-way ANOVA was performed to compare the dialysate sodium levels between the experimental groups (isonatric, hyponatremic, and hypernatremic). In the case the one-way ANOVA test demonstrated statistical significance, post-hoc tests were completed with Tukey's correction for multiple comparison. The means and standard deviations were also recorded following a descriptive statistical analysis.

3.2.9.2 Experimental Blood Work

Levels of sodium, potassium, chloride, glucose, blood urea nitrogen, creatine, hematocrit, and hemoglobin were recorded at baseline, sham, 1hr HD, and 2hr HD. For each of these measurements, a repeated measure two-way ANOVA with group (hyponatremic, isonatric, hypernatremic) and timepoint (baseline, sham, 1hr HD, 2hr HD) as the fixed effect was performed to enable comparison between timepoints as well as between experimental groups. A Geisser-Greenhouse correction was applied. If a fixed effect was statistically significant, post-hoc testing was performed with Tukey's correction for multiple comparison.

3.2.9.3 Mean Arterial Pressure for Assessment of Hemodynamic Stability

Hemodynamic stability throughout the experiment was assessed via continuous monitoring of mean arterial pressure. The mean arterial pressure was recorded for analysis at baseline, sham, 1hr HD, and 2hr HD. To analyze the mean arterial pressure data between the three experimental groups across the timepoints, a linear mixed model analysis was completed with group (hyponatremic, isonatric, hypernatremic) and timepoint (baseline, sham, 1hr HD, 2hr HD) as the fixed effects. Residual maximum likelihood estimation was used and a Geisser-Greenhouse correction for sphericity was applied. If a fixed effect was statistically significant, post-hoc testing with Tukey's correction for multiple comparison was completed.

In addition, a Pearson correlation analysis was performed on the pooled data of all animals across at all available timepoints to assess the association between the percent change in syndecan-1 measurements and the microvascular perfusion index.

3.2.9.4   Microvascular Perfusion Index through Intravital Microscopy

The changes in microvascular perfusion index throughout the experiment were analyzed with a repeated measure two-way ANOVA with timepoints (sham, 1hr HD, 2hr HD) and group (hyponatremic, isonatric, hypernatremic) as the fixed effects. The Geisser-Greenhouse correction was applied. If any of the fixed effects were statistically significant, post-hoc testing was completed with Tukey's correction for multiple comparisons to identify statistically significant differences.

3.2.9.5   Syndecan-1 as a Marker of Endothelial Injury

The percent change throughout the experiment of syndecan-1 relative to baseline was analyzed using a repeated measure two-way ANOVA with group (hyponatremic, isonatric, hypernatremic) and timepoints (sham, 1hr HD, 2hr HD, final) as the fixed effects. The Geisser-Greenhouse correction was applied. If any fixed effect was statistically significant, additional post-hoc testing was completed with Tukey's correction for multiple comparisons to identify statistically significant differences.

In addition, a Pearson correlation analysis was performed on the pooled data of all animals across at all available timepoints to assess the association between percent change in syndecan-1 and microvascular perfusion index.

3.3 Results

Of the thirty-one animals, four were excluded from analysis due to death, two from the isonatric arm and two from the hypernatremic arm. In total, there were eight animals in the isonatric group, ten animals in the hyponatremic group, and nine animals in the hypernatremic group.

3.3.1 Dialysate Composition

Ordinary one-way ANOVA analysis showed a significant effect of group ($F_{(2, 24)} = 211.3$, $p < 0.0001$), indicating statistically significant differences in sodium dialysate composition between isonatric, hyponatremic, and hypernatremic groups. Post-hoc testing showed the expected statistically significant differences in sodium levels between the hyponatremic and isonatric (131.6 ± 2.0 mmol/L vs 139.8 ± 2.6 mmol/L, $p < 0.0001$), isonatric and hypernatremic (139.8 ± 2.6 mmol/L vs. 150.2 ± 1.2, $p < 0.0001$), and hyponatremic and hypernatremic arms (131.6 ± 2.0 mmol/L vs. 150.2 ± 1.2, $p < 0.0001$). The prescribed sodium dialysate and the actual experimental sodium dialysate concentration are summarized in Table 3-1.

Table 3-1 Dialysate composition for isonatric, hyponatremic, and hypernatremic experimental arms. Values represent the mean ± standard deviation. Statistical significance performed to isonatric group.

Sodium Conc. (mmol/L)	Isonatric	Hyponatremic	p - value	Hypernatremic	p - value
Prescribed	140.0	130.0		150.0	
Experimental	139.8 ± 2.6	131.6 ± 2.0	< 0.0001	150.2 ± 1.2	< 0.0001

3.3.2 Experimental Blood Work

The blood work obtained at baseline, sham, 1 hr HD, and 2 hr HD included serum sodium, potassium, chloride, glucose, blood urea nitrogen, creatinine, hematocrit and hemoglobin levels. Repeated two-way ANOVA showed a significant effect of timepoint-by-group effect for both plasma sodium ($F_{(6,72)} = 63.13$, $p < 0.0001$) and chloride ($F_{(6,72)} = 113.8$, $p < 0.0001$). Post-hoc testing showed no differences in plasma sodium and chloride levels between the isonatric, hyponatremic, and hypernatremic groups at the baseline and sham timepoints (Figure 3-1A,C).

After 1 hr of commencing HD, the plasma sodium level was significantly different between groups. Specifically, plasma sodium level was higher in the hypernatremic group (142.4 ± 2.0 mmol/L) and reduced in the hyponatremic group (133.0 ± 0.8 mmol/L), relative to the isonatric group ($p < 0.0001$ and $p = 0.0004$, respectively). At 2 hrs into HD treatment, there remained a significant difference between the three groups with the mean sodium level remaining elevated in the hypernatremic group (141.6 ± 2.7 mmol/L, $p = 0.0071$) and low in the hyponatremic group (132.6 ± 0.8 mmol/L, $p < 0.0001$), relative to the isonatric group.

Repeated two-way ANOVA showed no statistically significant group effect for potassium, glucose, blood urea nitrogen, creatinine, hematocrit, and hemoglobin levels. However, significant effect in timepoint was revealed in levels of potassium, glucose, blood urea nitrogen creatinine, hematocrit, and hemoglobin. Table 3-2 reports the results of the post-hoc tests for the isonatric group over the duration of the experiment. In the standard isonatric arm, the mean potassium increased from baseline to sham (4.5 ± 0.2 mmol/L vs. 4.7 ± 0.3 mmol/L, $p = 0.0375$) but was reduced with 1 hr and 2 hr dialysis compared to baseline values (3.2 ± 0.1 mmol/L, $p < 0.0001$ and 3.4 ± 0.1 mmol/L, $p < 0.0001$, respectively). In this group, there was a trend of increasing plasma glucose from baseline (184 ± 22.4 mg/dL) to sham (197 ± 19.5 mg/dL, $p = 0.06$), followed by a significant reduction in glucose at 1 hr and 2 hr after initiating HD relative to baseline measurements (122 ± 4.6 mg/dL, $p = 0.0005$ and 106 ± 16.3 mg/dL, $p = 0.0005$, respectively). Relative to baseline levels, the blood urea nitrogen was elevated at the time of sham (24.9 ± 2.7 mg/dL, $p = 0.0022$), but declined at 1 hr HD (10.5 ± 2.2 mg/dL, $p = 0.0002$) and 2 hr HD (12.9 ± 2.7 mg/dL, $p = 0.0038$). Similarly, relative to baseline, creatinine levels elevated at the time of sham (0.49 ± 0.06 mg/dL, $p = 0.0068$), but declined at 1 hr HD (0.23 ± 0.05 mg/dL, $p = 0.0105$)

before recovering to baseline levels at 2 hr HD (0.33 ± 0.14 mg/dL, p = 0.6551). Hematocrit and hemoglobin levels in the blood were not significantly different throughout the experiment. Similar changes in blood work were seen in the hyponatremic and hypernatremic groups as summarized in Table 3-3 and 3-4. These results have been graphically presented in Figure 3-1.

Table 3-2 Concentration of basic electrolyte at baseline, sham, 1 hr- and 2 hr- into hemodialysis for to isonatric group (n=8). Values represent the mean ± standard deviation. Statistical significance test represents comparison of timepoints to the baseline timepoint.

Electrolyte	Baseline	Sham	p-value	1 hr into HD	p-value	2 hr into HD	p-value
Sodium (mmol/L)	137.8 ± 0.5	137.5 ± 0.5	0.85	137.8 ± 1.4	>0.9999	137.8 ± 1.5	>0.9999
Potassium (mmol/L)	4.49 ± 0.22	4.74 ± 0.17	0.0375	3.21 ± 0.10	<0.0001	3.39 ± 0.13	<0.0001
Chloride (mmol/L)	97.8 ± 1.75	98.9 ± 1.13	0.0569	92.9 ± 2.2	0.0003	93.1 ± 1.7	0.0005
Glucose (mg/dL)	184 ± 22.4	197 ± 19.5	0.0603	122 ± 4.6	0.0005	106 ± 16.3	0.0005
BUN (mg/dL)	19.4 ± 2.8	24.9 ± 2.7	0.0022	10.5 ± 2.2	0.0002	12.9 ± 2.5	0.0038
Creatinine (mg/dL)	0.38 ± 0.07	0.49 ± 0.06	0.0068	0.23 ± 0.05	0.0105	0.33 ± 0.14	0.6551
Hematocrit (%PCV)	33.5 ± 2.62	34.8 ± 2.32	0.6388	33.9 ± 4.79	0.9972	32.8 ± 3.45	0.9615
Hemoglobin (g/dL)	11.4 ± 0.89	11.8 ± 0.79	0.6571	11.5 ± 1.64	0.9981	11.1 ± 1.17	0.9572

Table 3-3 Concentration of basic electrolyte at baseline, sham, 1 hr- and 2 hr- into hemodialysis for to hyponatremic group (n=10). Values represent the mean ± standard deviation. Statistical significance test represents comparison of timepoints to the baseline timepoint.

Electrolyte	Baseline	Sham	p-value	1 hr into HD	p-value	2 hr into HD	p-value
Sodium (mmol/L)	137.5 ± 1.2	137.3 ± 1.2	0.48	133.0 ± 0.8	<0.0001	132.6 ± 0.8	<0.0001
Potassium (mmol/L)	4.56 ± 0.34	4.92 ± 0.34	0.0062	3.07 ± 0.21	<0.0001	3.20 ± 0.28	<0.0001
Chloride (mmol/L)	97.5 ± 1.90	99.1 ± 1.20	0.0087	87.8 ± 1.03	<0.0001	87.7 ± 1.06	<0.0001
Glucose (mg/dL)	183 ± 28.1	192 ± 26.8	0.2599	118 ± 13.5	<0.0001	98.2 ± 24.6	<0.0001
BUN (mg/dL)	18.8 ± 2.3	24.1 ± 1.7	0.0001	12.0 ± 8.1	0.0646	12.8 ± 3.9	0.0045
Creatinine (mg/dL)	0.39 ± 0.07	0.51 ± 0.11	0.0009	0.28 ± 0.06	0.0141	0.37 ± 0.13	0.9675
Hematocrit (%PCV)	33.2 ± 3.23	34.2 ± 1.75	0.7128	33.2 ± 1.75	>0.9999	33.3 ± 2.63	0.9997
Hemoglobin (g/dL)	11.3 ± 1.10	11.6 ± 0.48	0.6877	11.3 ± 0.59	>0.9999	11.3 ± 0.89	0.9998

Table 3-4 Concentration of basic electrolyte at baseline, sham, 1 hr- and 2 hr- into hemodialysis for to hypernatremic group (n=9). Values represent the mean ± standard deviation. Statistical significance test represents comparison of timepoints to the baseline timepoint.

Electrolyte	Baseline	Sham	p-value	1 hr into HD	p-value	2 hr into HD	p-value
Sodium (mmol/L)	137.4 ± 131	136.9 ± 1.6	0.18	142.4 ± 2.0	0.0001	141.6 ± 2.7	0.0074
Potassium (mmol/L)	4.37 ± 0.23	4.52 ± 0.26	0.2047	3.58 ± 0.17	<0.0001	3.78 ± 0.24	0.0014
Chloride (mmol/L)	98.1 ± 0.60	98.9 ± 1.05	0.1542	100.3 ± 1.22	0.0086	101.4 ± 0.88	0.0002
Glucose (mg/dL)	188 ± 22.7	201 ± 19.1	0.0390	133 ± 3.17	0.0003	114 ± 16.0	0.0001
BUN (mg/dL)	18.2 ± 0.8	23.2 ± 2.9	0.0026	13.1 ± 2.7	0.0006	16.2 ± 3.2	0.2252
Creatinine (mg/dL)	0.38 ± 0.07	0.48 ± 0.07	0.0121	0.26 ± 0.05	0.0002	0.41 ± 0.15	0.7538
Hematocrit (%PCV)	31.8 ± 2.39	33.9 ± 1.69	0.0186	31.4 ± 3.75	0.9568	29.8 ± 4.87	0.3274
Hemoglobin (g/dL)	10.8 ± 0.81	11.5 ± 0.58	0.0192	10.7 ± 1.28	0.9602	10.1 ± 1.66	0.3318
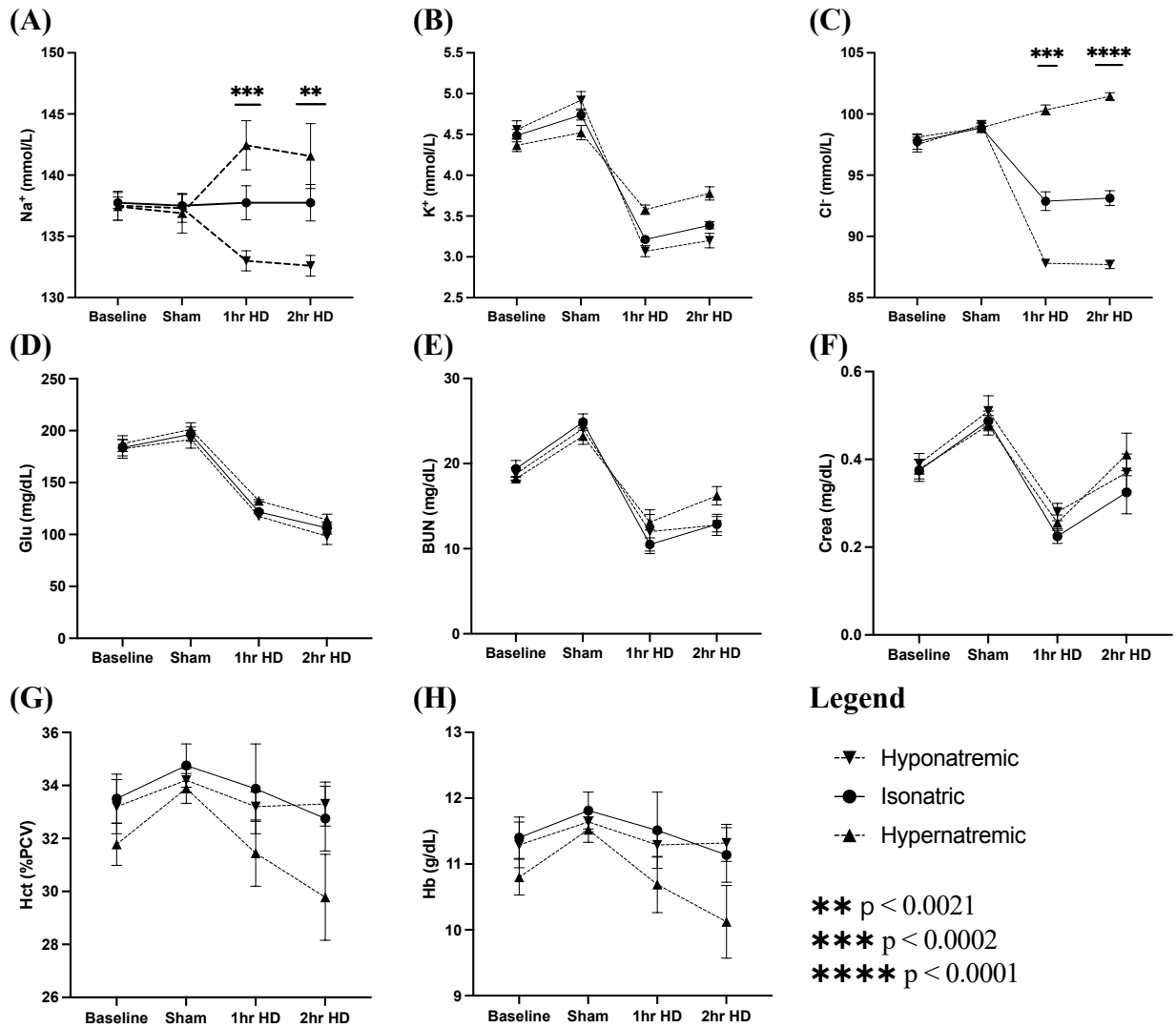
Figure 3-3 Mean serum electrolyte levels throughout the experimental procedure timepoint in hyponatremic (n=10), isonatric (n=8), and hypernatremic (n=9) arms. Error bars represent standard error of the mean. Statistical significance bars denote significant differences between groups at individual timepoints.

3.3.3 Levels of Syndecan-1

Two-way ANOVA analysis of syndecan-1 levels showed statistically significant effect of timepoint (F (1.383, 33.19) = 88.30, p <0.0001, Figure 3-2), but no group effect (F (2, 24) = 0.9408, p = 0.4042). Post-hoc testing revealed increases in percent change in syndecan-1 between sham and 2 hr HD in the isonatric (42.6 ± 39.2% vs. 113.9 ± 64.5%, p = 0.0030), hyponatremic (27.8 ± 30.6% vs. 85.9 ± 48.2%, p = 0.0034), and hypernatremic (51.3 ± 56.6% vs. 178.2 ± 108.1%, p = 0.0024) groups. Elevation in percent change in syndecan-1 was also evident from 2 hr HD to the final experimental timepoint as assessed by post-hoc testing in the isonatric (113.9 ± 64.5% vs. 228.3 ± 135.9%, p < 0.0155), hyponatremic (85.9 ± 48.2% vs. 237.7 ± 90.9%, p < 0.0001), and hypernatremic (178.2 ± 108.1% vs. 265.6 ± 155.5%, p = 0.0270) groups. The percent change in syndecan-1 at 2hr HD were assessed by post-hoc testing. The isonatric and hyponatremic group showed comparable levels of syndecan-1 in the blood (113.9 ± 64.5% vs. 85.9 ± 48.2%, p = 0.5780). However, the percent change in syndecan-1 nearly doubled in the hypernatremic group (178.2 ± 108.1%) compared to the hyponatremic group at 2hr HD (p = 0.0896).
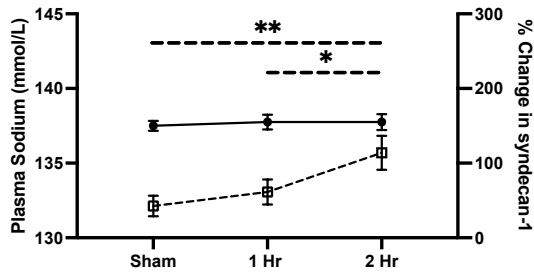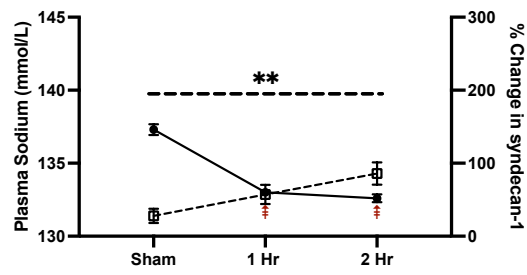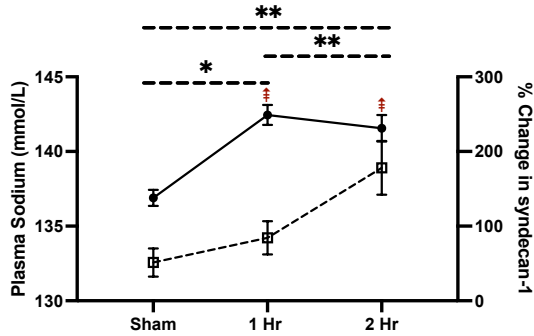
Figure 3-4 Mean plasma sodium levels (left y-axis) throughout the experimental procedure timepoint in isonatric (A), hyponatremic (B), and hypernatremic (C) arms. Mean percent change in syndecan-1 concentration (right y-axis) throughout the experimental procedure timepoint in isonatric (A), hyponatremic (B), and hypernatremic (C) arms. Error bars represent standard error of the mean. Dotted statistical significance bars denote significant differences in % change in syndecan-1 between experimental timepoints.

3.3.4 Microvascular Perfusion

The absolute microvascular perfusion index measured as the number of identified points using intravital microscopy was compared using a two-way ANOVA. The two-way ANOVA demonstrated a significant effect of time ($F_{(2.033, 46.76)} = 19.38$, $p < 0.0001$, Figure 3-3), but no significant effect of group. Post-hoc testing showed a trend towards a decreased microvascular perfusion index at 2hr HD compared to baseline in the isonatric group (116.7 ± 48.8 points vs. 154.1 ± 60.0 points, $p = 0.0889$). A trend towards a decreased microvascular perfusion index at 2hr HD compared to sham in the hyponatremic group (111.8 ± 55.7 points vs. 145.2 ± 42.2 points,

p = 0.0982) was also observed. The hypernatremic group demonstrated a statistically significant reduction in the microvascular perfusion index from baseline (208.9 ± 68.9 points) and sham (166.5 ± 46.0 points) to 2 hr HD (119.9 ± 39.7 points) ($p = 0.0098$ and $p < 0.0103$, respectively). A trend towards a decreased microvascular perfusion index at 1hr HD compared to baseline in the hypernatremic group (146.5 ± 36.9 points vs. 208.9 ± 68.9 points, $p = 0.0622$) was also observed.
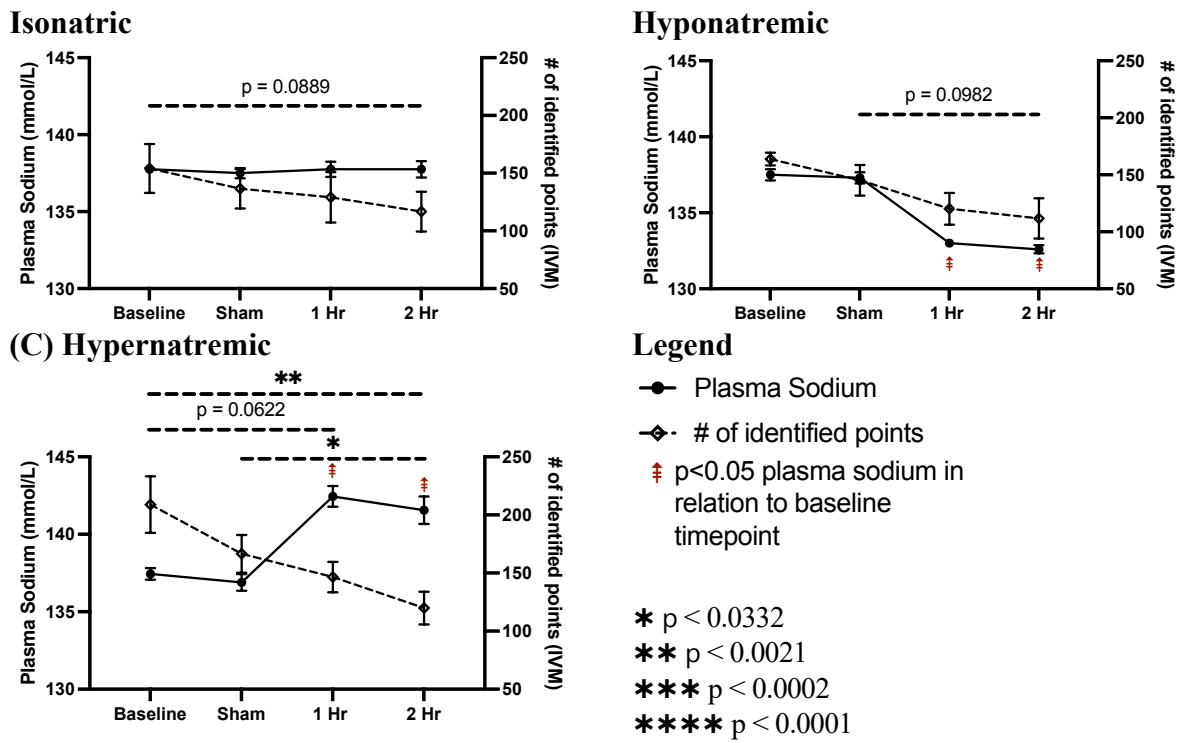
Figure 3-5 Mean plasma sodium levels (left y-axis) throughout the experimental procedure timepoint in isonatric (A), hyponatremic (B), and hypernatremic (C) arms. Mean number of identified points (right y-axis) throughout the experimental procedure timepoint in isonatric (A), hyponatremic (B), and hypernatremic (C) arms. Error bars represent standard error of the mean. Dotted statistical significance bars denote significant differences in identified points between experimental timepoints.

3.3.5 Relationship between Microvascular Perfusion and Syndecan-1

A Pearson correlation analysis demonstrated a negative association between percent change in syndecan-1 and the microvascular perfusion index measured by the number of identified points ($R^2 = 0.13$, Pearson r = -0.36, p = 0.0012). In other words, a greater change in syndecan-1 from baseline levels was associated with decreased number of identified perfusion points (Figure 3-4).
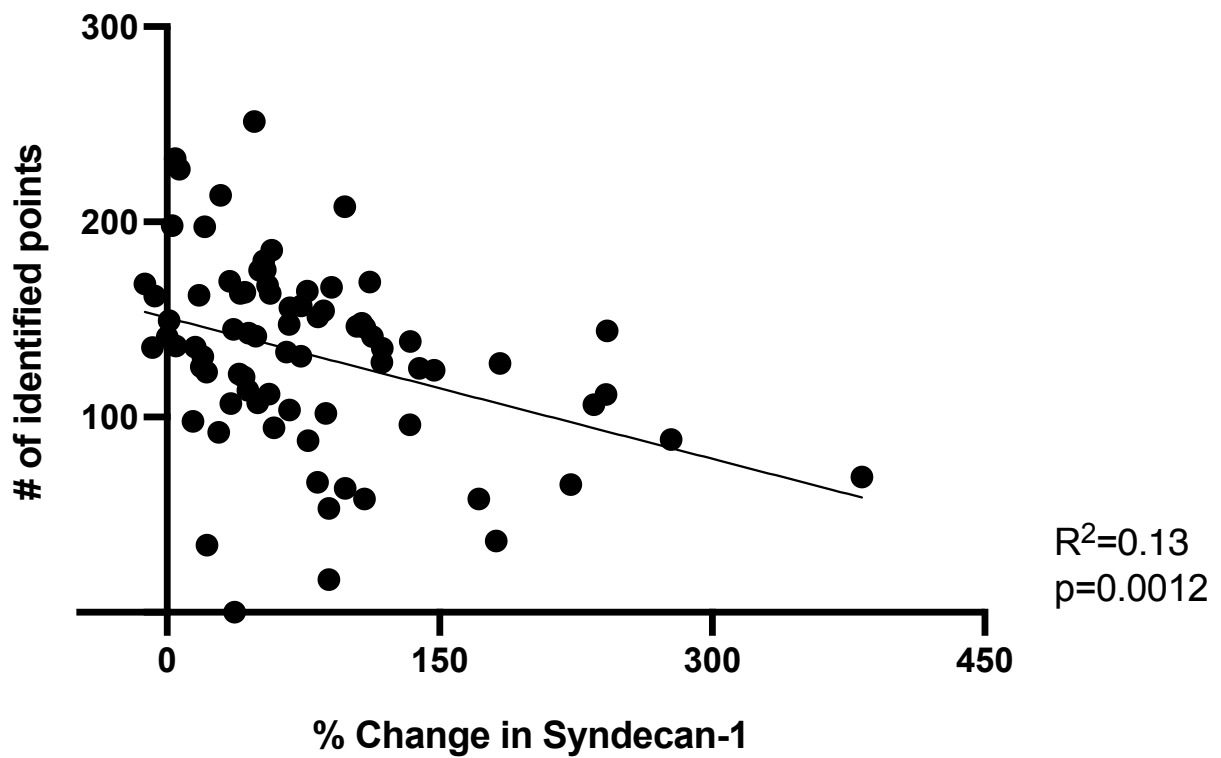
Figure 3-6 Correlation in number of identified perfusion points and percent change in syndecan-1 in all subjects (n=27).

3.3.6 Mean Arterial Pressure

Linear mixed model analysis of mean arterial pressure for assessment of hemodynamic stability showed a significant effect of experimental timepoint ($F_{(2.642, 61.65)} = 93.53$, $p < 0.0001$). Post-hoc testing showed that, in the standard isonatric group, the mean arterial pressure did not change from baseline to sham (88.6 ± 10.5 mmHg and 87.1 ± 9.9 mmHg, $p = 0.9843$). However, in the hyponatremic and hypernatremic groups, there was a trend towards decreasing mean arterial pressure from baseline to sham. At baseline, the mean arterial pressure was 85.3 ± 2.1 mmHg at baseline and reduced to 81.0 ± 4.5 mmHg in the hyponatremic group at sham ($p = 0.0694$) with one hour of extracorporeal circuit in the absence of dialysate flow. In the hypernatremic group, the mean arterial pressure was 85.8 ± 8.2 mmHg at baseline and reduced to 75.5 ± 8.1 mmHg at sham ($p = 0.0825$). Compared to baseline, post-hoc testing showed that the mean arterial blood pressure was significantly lower at 1 hr HD and 2 hr HD in all three experimental groups as shown in Figure 3-5A. The mean arterial pressure did not recover to baseline levels during the remainder of the experiment. Post-hoc testing revealed no significant differences in mean arterial pressure between the experimental groups.

3.3.7 Relationship between Mean Arterial Pressure and Syndecan-1

A Pearson correlation analysis demonstrated a negative association between percent change in syndecan-1 and mean arterial pressure ($R^2 = 0.07$, Pearson r = -0.2645, $p = 0.019$). In other words, a larger change in syndecan-1 from baseline levels was associated with lower levels of mean arterial pressure (Figure 3-5B).

(A)

(B)
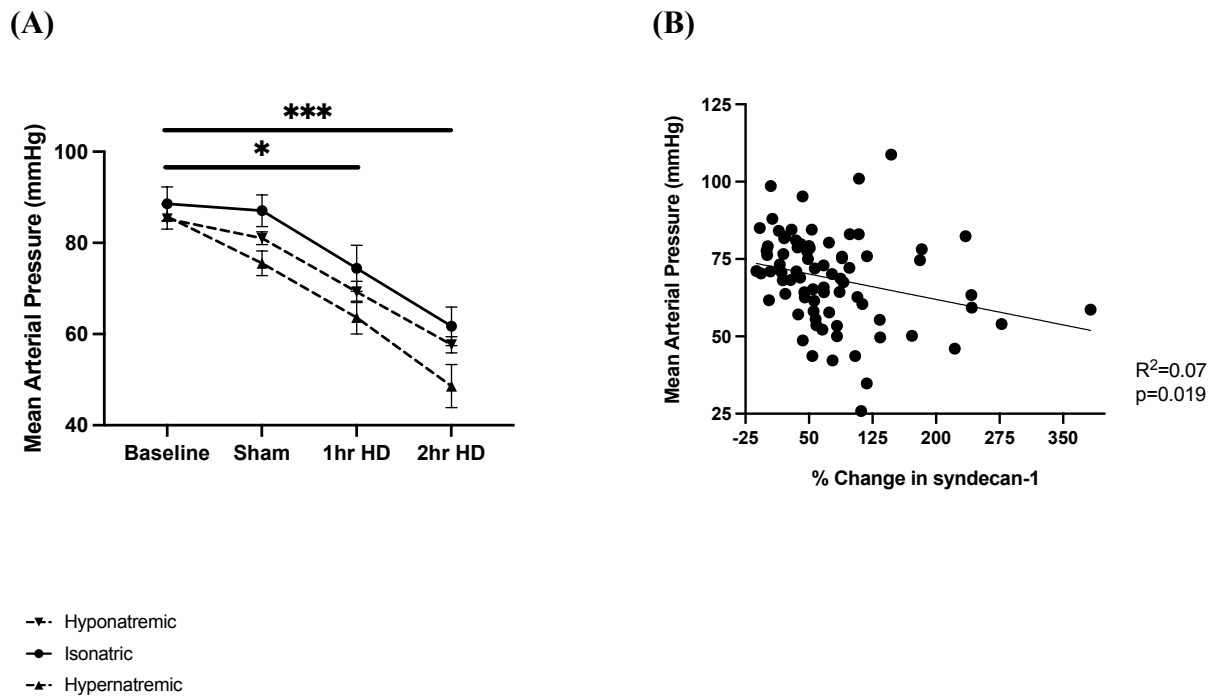
Figure 3-7 (A) Experimental changes in mean arterial pressure in the isonatric (n=8), hyponatremic (n=10), and hypernatremic (n=9) groups. Error bars represent standard error of the mean. Statistical significance bars denote significant differences mean arterial pressure between experimental timepoints. (B) Correlation in mean arterial pressure and percent change in syndecan-1 in all subjects (n=27).

3.4 Discussion

The objective of this study was to study hemodialysis-induced endothelial injury with the specific question of whether acute changes in plasma sodium during dialysis were a contributor. First, the results of this study confirmed that HD directly led to endothelial damage. Plasma syndecan-1 levels increased over the course of dialysis in all animals, regardless of whether they were members of the hypernatremic, isonatric, or hyponatremic groups. This replicates prior studies in human subjects demonstrating increasing levels of syndecan-1 that is associated with

HD treatment [28,29]. Animals also demonstrated a marked reduction in mean arterial pressure throughout dialysis, while mean arterial pressure remained consistent throughout the sham procedure (removal of volume via an extracorporeal circuit without dialysis), confirming that HD induces hypotension, and replicating the well-demonstrated phenomenon of intradialytic hypotension and hemodynamic circulatory stress that occurs during HD [1,2,30–40] Interestingly, we showed an association between the mean arterial pressure and the percent change in syndecan-1, with low mean arterial pressure being associated with high levels of plasma syndecan-1. This suggests that increased hemodynamic instability during dialysis is associated with increased endothelial dysfunction. In other words, hypotension and circulatory stress can lead to endothelial injury.

The results of our study also show that HD-induced endothelial injury is significant with respect to microvascular dysfunction and microcirculatory perfusion. Using the microvascular perfusion index derived from intradialytic intravital microscopy, statistical analysis showed a significant effect of time, suggesting that, across the entire cohort of animals, perfusion decreased over the course of dialysis. This is consistent with prior work done by our group, which showed a significant reduction in microvascular perfusion from baseline to 2hr into HD in animals exposed to standard dialysate with 140 mM of sodium[24]. In the present study, a pattern of microvascular perfusion index decrease was seen in the isonatric group in the same timepoints in post-hoc analysis adjusted for the additional multiple comparison tests required to compare the experimental groups over time with changes in plasma sodium. However, when perfusion trends for the standard sodium level group was assessed separately with an ordinary one-way ANOVA, the result was replicated, with a statistically significant reduction of perfusion from baseline to 2hr HD. Together, the simultaneous intradialytic increase in syndecan-1 and intradialytic decrease in microvascular

perfusion index suggests that HD-induced endothelial injury is significant with respect to perfusion. Indeed, a significant association between plasma syndecan-1 levels and microvascular perfusion index was demonstrated, with higher levels of syndecan-1 associated with a lower microvascular perfusion index.

Plasma sodium levels during dialysis appear to mediate the HD-induced endothelial injury and microvascular hypoperfusion. In the hypernatremic group, cumulative syndecan-1 shedding tended to be higher than in the isonatric and hyponatremic groups. Post-hoc analyses of microvascular perfusion index demonstrated a significant reduction in microvascular perfusion index with dialysis in the hypernatremic group but not in the isonatric and hyponatremic groups. These results suggest that increased plasma sodium levels during dialysis secondary to a higher sodium dialysate prescription aggravates endothelial injury and exacerbates microvascular perfusion. This is consistent with human studies looking at acute sodium changes and endothelial injury. In one study by Koch et al., where hemocontrol hemodialysis was employed, plasma sodium levels were manipulated during dialysis and plasma syndecan-1 levels were measured; plasma syndecan-1 levels tracked with plasma sodium levels increased with acute rise in plasma sodium[16]. In general, these results lend support to the view that lower dialysate sodium concentrations may be the way forward and that supra-physiological dialysate sodium concentrations should be avoided. Not only can lower dialysate sodium concentrations lead to more modest intradialytic weight gain and reduced tissue deposition of sodium[41], it may also lower the severity of HD-induced endothelial injury.

As this study's primary objective was to study the effects of dialysate sodium in HD-induced injuries, it was important to ensure that sodium concentration delivered to the animals matched the prescribed dialysate sodium and to show that sodium levels were successfully

manipulated with the dialysate used. Indeed, the mean sodium dialysate levels were the same within group, but significantly different between isonatric, hyponatremic, and hypernatremic groups. This is often a point of concern in human studies, with a recent study conducted by Shendi et al. showing discrepancies between the prescribed dialysate sodium and the sodium concentration that was delivered to the patient through dialysis[42].

This study had its limitations. This was an exploratory study, and its primary objective was to investigate the effects of sodium dialysate on endothelial cell injury and microvascular perfusion. For this purpose, healthy animals with normal kidney function were used to eliminate confounding factors associated with kidney failure. To holistically understand the mechanism of sodium induced injury in HD, future studies should be conducted on chronic kidney disease model of animals. A major limitation of utilizing a small animal experimental platform is the availability of blood. Based on the IACUC guideline, the total blood volume of a 300g rat is estimated to be 17 to 21mL. Increasing the number of times blood is sampled can lead to harmful hemodynamic instability in a study that is already removing large volume of blood into the extracorporeal circuit. Hence, we were limited with the amount of blood that could be sampled during this experiment. Because of the nature of the preclinical platform in this current study, including the surgical exposure of tissue for intravital microscopy, animals were sacrificed at the end of the HD treatment preventing a cross-over design that has been used in human studies[16] to enable a paired comparison analysis that eliminates covariates in the relationship between plasma sodium and syndecan-1.

3.5 Conclusion

In this study, we demonstrate that during a single HD session, there are marked elevations in levels of syndecan-1 that is associated with the reduction in microvascular perfusion. Through the small animal model of healthy rats, we conclude that HD treatment itself induce endothelial

injury and microcirculatory dysfunction. As well, the degree of damage to the glycocalyx may be more pronounced with hypernatremic effects of high sodium dialysate leading to structural and function changes to the microvasculature.

The optimal dialysate sodium concentration to deliver during HD is not known. Lower dialysate sodium is ideal considering the deleterious effects of high sodium levels on the endothelium, exacerbating HD-induced circulatory dysfunction and ischemia to the extent of worsening myocardial stunning. However, sodium level must be sufficient enough to avoid inducing intradialytic hypotension and hemodynamic injury. Clinically, dialysate sodium concentration should be manipulated and individualized to each patient's needs and further refined through iterative evaluation of intradialytic weight gain, hemodynamic stability, sodium deposition in the tissue and symptoms of intolerability.

3.6 Acknowledgement

3.7 References

1. Davenport A. Audit of the Effect of Dialysate Sodium Concentration on Inter-Dialytic Weight Gains and Blood Pressure Control in Chronic Haemodialysis Patients. *Nephron Clin Pract*. 2006;104(3):c120-c125. doi:10.1159/000094544

2. Davenport A, Cox C, Thuraisingham R. Achieving blood pressure targets during dialysis improves control but increases intradialytic hypotension. *Kidney Int*. 2008;73(6):759-764. doi:10.1038/SJ.KI.5002745

3. McIntyre CW, Burton JO, Selby NM, et al. Hemodialysis-induced cardiac dysfunction is associated with an acute reduction in global and segmental myocardial blood flow. *Clinical Journal of the American Society of Nephrology*. 2008;3(1):19-26. doi:10.2215/CJN.03170707

4. Mcintyre CW, Burton JO, Selby NM, et al. Hemodialysis-Induced Cardiac Dysfunction Is Associated with an Acute Reduction in Global and Segmental Myocardial Blood Flow. *Clin J Am Soc Nephrol*. 2008;3:19-26. doi:10.2215/CJN.03170707

5. Buchanan C, Mohammed A, Cox E, et al. Intradialytic Cardiac Magnetic Resonance Imaging to Assess Cardiovascular Responses in a Short-Term Trial of Hemodiafiltration and Hemodialysis. *J Am Soc Nephrol*. 2017;28:1269-1277. doi:10.1681/ASN.2016060686

6. Qirjazi E, Salerno FR, Akbari A, et al. Tissue sodium concentrations in chronic kidney disease and dialysis patients by lower leg sodium-23 magnetic resonance imaging. *Nephrology Dialysis Transplantation*. Published online April 6, 2020. doi:10.1093/ndt/gfaa036

7. Oberleithner H. Vascular endothelium: a vulnerable transit zone for merciless sodium. *Nephrol Dial Transplant*. 2014;29(2):440-446. doi:10.1093/NDT/GFT461

8. Guaricci AI, Bulzis G, Pontone G, et al. Current interpretation of myocardial stunning. *Trends Cardiovasc Med*. 2018;28(4):263-271. doi:10.1016/J.TCM.2017.11.005

9. Dorairajan S, Chockalingam A, Misra M. Myocardial stunning in hemodialysis: What is the overall message? *Hemodialysis International*. 2010;14(4):447-450. doi:10.1111/J.1542-4758.2010.00495.X

10. Zuidema MY, Dellsperger KC. Myocardial Stunning with Hemodialysis: Clinical Challenges of the Cardiorenal Patient. *Cardiorenal Med*. 2012;2:125-133. doi:10.1159/000337476

11. Hothi DK, Rees L, Marek J, Burton J, Mcintyre CW. Pediatric Myocardial Stunning Underscores the Cardiac Toxicity of Conventional Hemodialysis Treatments. *Clin J Am Soc Nephrol*. 2009;4:790-797. doi:10.2215/CJN.05921108

12. Jefferies HJ, Lemoine S, Mcintyre CW. High magnesium dialysate does not improve intradialytic hemodynamics or abrogate myocardial stunning. *Hemodialysis International*. 2020;24:506-515. doi:10.1111/hdi.12863

13. Selim Guler H, Cansin |, Kaya T, et al. Acute stunning effect of hemodialysis on myocardial performance: A three-dimensional speckle tracking echocardiographic study. *Artif Organs*. 2020;44:1081-1089. doi:10.1111/aor.13698

14. McIntyre CW. Haemodialysis-Induced Myocardial Stunning in Chronic Kidney Disease – A New Aspect of Cardiovascular Disease. *Blood Purif*. 2010;29(2):105-110. doi:10.1159/000245634

15. Canaud B, Stephens MP, Nikam M, Etter M, Collins A. Multitargeted interventions to reduce dialysis-induced systemic stress. *Clin Kidney J*. 2021;14(Supplement_4):i72-i84. doi:10.1093/CKJ/SFAB192

16. Koch J, Idzerda NMA, Ettema EM, et al. An acute rise of plasma Na+concentration associates with syndecan-1 shedding during hemodialysis. *Am J Physiol Renal Physiol*. 2020;319(2):F171-F177. doi:10.1152/AJPRENAL.00005.2020

17. Patterson EK, Cepinskas G, Fraser DD. Endothelial Glycocalyx Degradation in Critical Illness and Injury. *Front Med (Lausanne)*. 2022;0:1998. doi:10.3389/FMED.2022.898592

18. Bermejo-Martin JF, Martín-Fernandez M, López-Mestanza C, Duque P, Almansa R. Shared Features of Endothelial Dysfunction between Sepsis and Its Preceding Risk Factors (Aging and Chronic Disease). *Journal of Clinical Medicine 2018, Vol 7, Page 400*. 2018;7(11):400. doi:10.3390/JCM7110400

19. Su JB. Vascular endothelial dysfunction and pharmacological treatment. *World J Cardiol*. 2015;7(11):719. doi:10.4330/WJC.V7.I11.719

20. Lush CW, Kvietys PR. *Microvascular Dysfunction in Sepsis*.; 2000. www.nature.com/mn

21. Theodorakopoulou MP, Schoina M, Sarafidis P, Sarafidis PA. Assessment of Endothelial and Microvascular Function in CKD: Older and Newer Techniques, Associated Risk Factors, and Relations with Outcomes. *Depth Topic Review Am J Nephrol*. 2020;51:931-949. doi:10.1159/000512263

22. Radhakrishnan A, Pickup LC, Price AM, et al. Coronary microvascular dysfunction: a key step in the development of uraemic cardiomyopathy? *Heart*. 2019;105(17):1302. doi:10.1136/HEARTJNL-2019-315138

23. Querfeld U, Mak RH, Pries AR. Microvascular disease in chronic kidney disease: the base of the iceberg in cardiovascular comorbidity. *Clin Sci*. 2020;134:1333-1356. doi:10.1042/CS20200279

24. Janssen BGH, Zhang YM, Kosik I, Akbari A, Mcintyre CW, Janssen GH. Intravital microscopic observation of the microvasculature during hemodialysis in healthy rats. *Scientific Reports*. Published online 2022. doi:10.1038/s41598-021-03681-2

25. Tyml K, Budreau CH. A new preparation of rat extensor digitorum longus muscle for intravital investigation of the microcirculation. *Int J Microcirc Clin Exp*. 1991;10(4):335-343. Accessed August 7, 2022. https://europepmc.org/article/med/1778678

26. Janssen BGH, Najiminaini M, Zhang YM, Omidi P, Carson JJL. Multispectral intravital microscopy for simultaneous bright-field and fluorescence imaging of the microvasculature. doi:10.1186/s42649-021-00059-6

27. Mahmoud O, El-Sakka M, Janssen BGH. Two-step machine learning method for the rapid analysis of microvascular flow in intravital video microscopy. *Scientific Reports |*. 123AD;11:10047. doi:10.1038/s41598-021-89469-w

28. Koch J, Idzerda NMA, Dam W, Assa S, Franssen CFM, van den Born J. Plasma syndecan-1 in hemodialysis patients associates with survival and lower markers of volume status. *Am J Physiol Renal Physiol*. 2019;316(1):F121-F127. doi:10.1152/AJPRENAL.00252.2018

29. Kusuzawa K, Suzuki K, Okada H, et al. Measuring the Concentration of Serum Syndecan-1 to Assess Vascular Endothelial Glycocalyx Injury During Hemodialysis. *Front Med (Lausanne)*. 2021;8:2784. doi:10.3389/FMED.2021.791309/BIBTEX

30. Chou JA, Streja E, Nguyen D v, et al. Intradialytic hypotension, blood pressure changes and mortality risk in incident hemodialysis patients. *Nephrology Dialysis Transplantation*. 2018;33:149-159. doi:10.1093/ndt/gfx037

31. Mantri Y, Dorobek TR, Tsujimoto J, Penny WF, Garimella PS, Jokerst J v. Monitoring peripheral hemodynamic response to changes in blood pressure via photoacoustic imaging. *Photoacoustics*. 2022;26. doi:10.1016/J.PACS.2022.100345

32. Assimon MM, Flythe JE. Definitions of Intradialytic Hypotension. *Semin Dial*. 2017;30(6):464-472. doi:10.1111/sdi.12626

33. Sars B, van der Sande FM, Kooman JP. Advances in CKD 2020 Intradialytic Hypotension: Mechanisms and Outcome. *Blood Purif*. 2019;49:158-167. doi:10.1159/000503776

34. Stefánsson B v, Brunelli SM, Cabrera C, et al. Intradialytic Hypotension and Risk of Cardiovascular Disease. *Clinical Journal of the American Society of Nephrology*. Published online 2014. doi:10.2215/CJN.02680314

35. Sherman RA. Intradialytic hypotension: An overview of recent, unresolved and overlooked issues. *Semin Dial*. 2002;15(3):141-143. doi:10.1046/J.1525-139X.2002.00002.X

36. Sands JJ, Usvyat LA, Sullivan T, et al. Intradialytic hypotension: Frequency, sources of variation and correlation with clinical outcome. *Hemodialysis International*. 2014;18(2):415-422. doi:10.1111/HDI.12138

37. Flythe JE, Xue H, Lynch KE, Curhan GC, Brunelli SM. Association of Mortality Risk with Various Definitions of Intradialytic Hypotension. *J Am Soc Nephrol*. 2015;26:724-734. doi:10.1681/ASN.2014020222

38. Mcintyre CW, Salerno FR. Diagnosis and Treatment of Intradialytic Hypotension in Maintenance Hemodialysis Patients. *Clin J Am Soc Nephrol*. 2018;13:486-489. doi:10.2215/CJN.11131017

39. Palmer BF, Henrich WL. Recent Advances in the Prevention and Management of Intradialytic Hypotension. Published online 2008. doi:10.1681/ASN.2007091006

40. Kuipers J, Verboom LM, Ipema KJR, et al. The Prevalence of Intradialytic Hypotension in Patients on Conventional Hemodialysis: A Systematic Review with Meta-Analysis. *Translational Research: Research Article Am J Nephrol*. 2019;49:497-506. doi:10.1159/000500877

41. Lemoine S, Salerno FR, Akbari A, McIntyre CW. Influence of Dialysate Sodium Prescription on Skin and Muscle Sodium Concentration. *Am J Kidney Dis*. 2021;78(1):156-159. doi:10.1053/J.AJKD.2020.11.025

42. Shendi AM, Davenport A. The difference between delivered and prescribed dialysate sodium in haemodialysis machines. *Clin Kidney J*. 2021;14(3):863. doi:10.1093/CKJ/SFAA022

3.8 Co-Authorship Statement

The material in Chapter 3 is in preparation for publication at the Kidney International Journal. Some materials presented in this chapter submitted for a presentation at the American Society of Nephrology International Conference (November 5, 2022; SA-PO447; poster presentation). Lisa Hur is the main contributor of the work that has been presented in this chapter—designing the study, data acquisition, data processing, statistical analysis of the data, and manuscript preparation. Co-authors of this chapter were Yanmin Zhang, Eric Patterson, Barry Janssen, and Christopher W. McIntyre. Yanmin Zhang conducted the experimental set up, performed the animal surgical procedures, and collected data, and ensured the safety of the animals during the experiment. Eric Patterson provided Lisa Hur with training and guidance of ELISA experiments. Barry Janssen provided guidance in the design of the study, acquired and processed the intravital microscopy and blood pressure data. Christopher McIntyre provided clinical and logistical oversight, as gave guidance in terms of the study design, interpretation of data, and manuscript preparation.

Estimated percentage of the work for Chapter 3 conducted solely by Lisa Hur: 80%

Chapter 4

4 A Pilot Study: Assessment of intradialytic exercise on the circulation and function of the heart

Abstract Hemodialysis (HD) is associated with high rates of cardiovascular mortality. Intradialytic exercise (IDE) has been shown to improve intradialytic hemodynamic tolerability, although its mechanisms remain elusive. The objective of the present study was to use intradialytic CT perfusion imaging and echocardiography to noninvasively evaluate cardiac injury during HD with and without exercise. Fourteen participants underwent two intradialytic imaging sessions with and without exercise. In both visits, dynamic CT scans (Revolution CT, GE) were conducted at baseline, peak HD stress, and 30 mins post HD. From the CT scans, global myocardial perfusion (MP) of the left ventricle was quantified. In addition, apical 4-chamber and 2-chamber views of the heart were acquired with 2D echocardiography (Vivid Q, GE). The systolic function was evaluated through segmental longitudinal strain (LS) using a commercially available software (EchoPAC, GE). Segments demonstrating >20% reduction in LS compared to baseline were defined as regional wall motion abnormalities (RWMA). During the control visit, MP significantly dropped from baseline to peak HD stress (p=0.0001) followed by partial recovery post HD. Similar intradialytic MP results were found with IDE. MP of control and exercise visits were not significantly different. The number of myocardial segments experiencing RWMA at post HD were reduced with IDE in comparison to the peak HD stress (p = 0.0009). A decrease in the number of RWMAs post-HD with exercise suggests potential exercise-associated cardiac resilience to HD-induced cardiac ischemia injury.

4.1 Introduction

Hemodialysis (HD) patients have elevated mortality rates related to cardiovascular disease and specifically, sudden cardiac death[1–3]. Many imaging modalities have been utilized to study the perfusion changes of vital organs during HD, including arterial spin labelled magnetic resonance imaging[4,5], computed tomography[6,7], and positron emission tomography[8,9]. These studies demonstrated HD-induced injury during a single treatment session. In addition, some studies also investigated the phenomenon of recurrent and transient myocardial ischemia causing persistent left ventricular dysfunction in the HD population, by looking for the presence of myocardial stunning[10–19]. Echocardiography throughout HD and identifying reduced segmental regional wall motion abnormalities (RWMAs) has been the preferred means to assess HD-induced myocardial stunning[20,21]. In sum, the existing literature suggests that HD precipitates recurrent harm and is responsible for the increased mortality in patients upon the first year of dialysis initiation[22].

In the past decade, studies have investigated and employed various interventions to reduce the hemodynamic perturbation during HD, detailing the practicability of incorporating it into clinical practice; all of which rely on different mechanisms to target hemodynamic tolerability to HD. One of the most safe and effective ways of minimizing intradialytic hypotension and exerting protective effects on multiple vascular beds is through the delivery of cooled dialysate to increase peripheral vasoconstriction[23,24]. This simple approach has been shown to reduce the presence and severity of HD-induced ischemia[25,26] and improve left ventricular circumferential fiber shortening[27]. Cooling the dialysate has no addition cost associated with it and can be delivered on any dialysis machine. Biofeedback dialysis technology is another way of reducing hypotension and ischemia during dialysis, through active modulation of ultrafiltration rate and conductivity of

the dialysate during the HD treatment session[28]. Despite its effectiveness, it is limited in availability as it utilizes a specific dialysis machine restricting its application in clinical settings.

Intradialytic exercise (IDE) has been the intervention of interest in the recent years that demonstrated clinical feasibility[29–46]. In summary, patients would perform an exercise regime determined by the dialysis clinic while dialyzing on the dialysis chair. Many studies suggest that exercise benefits the HD cohort by increasing quality of life, muscle power, and dialysis efficacy. Systematic reviews have suggested an improvement in peak oxygenation uptake (measure of cardiopulmonary capacity) by 23% with exercise[43]. In a clinical crossover design study, Kt/V was calculated to evaluate dialysis efficacy, where K is the dialyzer clearance (mL/min), t is the duration of dialysis treatment (mins), and V is the volume of distribution of urea clearance (mL) [47]. Exercise intensity and its effect on Kt/V was questioned; the study observed an increase in dialyzer urea clearance with IDE relative to control but no significant difference between varying exercise intensities. Similarly, an exploratory study was conducted by our lab and a reduction in RWMAs was shown with exercise with no statistical significance between exercise doses[48]. These results were confirmed by others, suggesting that IDE is cardioprotective against myocardial stunning with respect to HD treatment[40,49–51]; its mechanism remains elusive. These studies have proposed improved muscle perfusion and changes to vascular tone as potential underlying mechanisms for exercise improving HD tolerability. However, no studies to date have investigated the perfusion response to IDE.

Using multimodal intradialytic imaging, this study will, for the first time, investigate the circulatory response to IDE and determine its ability to deliver cardioprotection to HD in exercise-naïve dialysis patients. To do so, echocardiography and cardiac computed tomography (CT) perfusion imaging will be incorporated to quantify RWMAs and changes to myocardial blood flow

throughout HD treatment. In addition, ELISA experiments will be performed to assess endothelial injury in the vasculature with respect to HD treatment and IDE intervention by quantifying levels of syndecan-1. We hypothesize that IDE is not driven by perfusion-related mechanisms, but rather by means of cardioprotection to improve ischemic tolerability of the tissue in the HD setting of challenged perfusion.

4.2 Methods

4.2.1 Study Design

This is a single-centered cross-sectional study designed to investigate the effects of intradialytic exercise in a cohort of ESRD patients undergoing HD. Consented patients participated in two study visits: a control visit with no intervention and a treatment visit with exercise during HD. At each study visit, a series of dynamic contrast enhanced computed tomography (DCE-CT) images and echocardiography images were acquired prior to HD (baseline), at the last thirty minutes of HD during maximal circulatory stress (peak HD), and following the end of HD (post HD) to quantify myocardial perfusion and stunning. Blood samples were collected at timepoints corresponding to the image acquisition to assess intradialytic electrolyte changes and endothelial dysfunction.

4.2.2 Study Population

This study was an extension of the work presented in Chapter 2 of this thesis. The participants enrolled in the study presented in the previous chapter were asked to attend a second imaging visit where intradialytic exercise was performed. The participants were recruited from the London Health Science Centre Renal Program (London, Ontario, Canada). Fourteen exercise-naive participants, 18 years of age or older who had received HD for a minimum of three months,

thrice weekly were enrolled. Those enrolled provided informed consent prior to the initiation of the study. Patients with a prior diagnosis of chronic arrhythmia on anti-arrhythmic drugs or with a pacemaker or cardioverter defibrillator were excluded.

4.2.3 Demographic Information

The demographic information collected from the participants included the death of birth (month and year), age, biological sex, body mass index, ethnicity, and chronic kidney disease related patient information.

4.2.4 Dialysis Treatment Information

The control and exercise study visits were conducted midweek and the dialysis treatments delivered at both visits were consistent with what was described in Chapter 2.

4.2.5 Assessment of Hemodynamic Stability

Hemodynamic stability of the participants throughout the HD treatment at the control and exercise exposure visit was assessed by measuring the systolic blood pressure (mmHg). Measurements were acquired while the patient was sitting on a dialysis chair and was obtained within five minutes of CT imaging at baseline, peak HD stress, and post HD treatment.

4.2.6 Exercise Performance

On the second study visit, participants began exercise treatment at the start of the HD treatment for a duration of thirty minutes. At this time, participants cycled on a Monark^{TM} (Sweden) leg ergometer to reach an exercise intensity threshold of 3 or 4 out of 10 on a Borg rating of perceived exertion scale, defined as moderate or somewhat hard. Participants cycled whilst upright and sitting on a dialysis chair. Participants were encouraged to take rest periods throughout the thirty minutes of exercise if they were experienced any symptoms of exercise intolerance such

as shortness of breath and angina. Following the end of the exercise treatment, the following data were recorded from the cycling device: calories burnt during exercise, number of rotations, and the minutes spent exercising without rest within the 30-minute exercise prescription. From these measurements, the number of rotations per minute and the amount of calories burnt per minute were quantified.

4.2.7 Quantification of Myocardial Perfusion

During each study visit, a DCE-CT image was acquired at baseline, peak HD stress, and post HD. Iodinated contrast agent of 0.7mL per kilogram of body weight (Isovue 370) was administered intravenously at 3-4mL/s followed by a 30mL bolus saline flush at the same infusion rate. Scanning was conducted using a single-phase prospective ECG gated acquisition protocol: 32 axial scans every 1 to 2 heart beats (approximate 1.5 seconds). The scanner settings for all dynamic image acquisitions were as follows: tube voltage of 100 to 120kV, tube current of 100mA, 0.28s gantry period, slice thickness of 2.5mm giving a total coverage of 160mm.

The dynamic CT images were retrospectively reconstructed into 5mm thick cardiac images from the scanner console (Revolution, GE Healthcare) and transferred to a workstation for analysis (Advantage workstation, GE Healthcare). To correct for the residual cardiac and respiratory motion between the 32 scans of a single dynamic CT image set, the images were registered using a three-dimensional non-rigid registration algorithm (GE proprietary software, advantage workstation, GE Healthcare).

Following motion correction, the Johnson-Wilson-Lee tracer kinetic model was implemented to the registered dynamic images to generate a myocardial perfusion map corresponding to each slice[53–57]. The left ventricular myocardium was delineated for seven slices

with visible apex, apical, mid, and basal regions of the heart to measure global myocardial perfusion. The global myocardial perfusion values of the seven slices were averaged to represent the mean global myocardial perfusion of the patient at a particular timepoint of a single study visit.

4.2.8 Assessment of Regional Wall Motion Abnormality

Echocardiography was conducted to acquire standard apical 4-chamber and 2-chamber views of the heart following the DCE-CT acquisition at baseline, peak HD stress and post HD timepoints during the control and exercise study visits. Three cardiac cycles were recorded at each cardiac view for offline digital analysis using a proprietary two-dimensional speckle tracking software (EchoPac, GE Healthcare). The longitudinal strain values for twelve myocardial segments were quantified using a single cardiac cycle at a given HD timepoint.

The longitudinal strain values of the twelve myocardial segments at peak HD and post HD were normalized to its baseline values to calculate the percent change in longitudinal strain. The myocardial segments at peak HD and post HD with greater than twenty percent reduction in longitudinal strain in relation to the baseline values were identified to be segments with RWMAs. The total number of segments (out of 12) experiencing RWMAs were determined at peak HD and post HD for study visits and was used as a metric to study the effect of intradialytic exercise on myocardial stunning.

4.2.9 Quantification of Endothelial Dysfunction

Blood samples collected at control and exercise visits for baseline, peak HD stress, and post HD timepoints. The plasma from all participants were stored at -80°C freezer until processed using a commercially available ELISA kit to quantify human syndecan-1 (Abcam, ab46506). All ELISAs were performed according to the manufacturers' instruction manual. Reference standards

were within the limits of detection and were fitted with a 4-parameter logistic model. This model was used to estimate the concentration of syndecan-1 in blood samples. The percent change in syndecan-1 concentration at peak HD and post HD relative to baseline was calculated for each visit to study the acute effects of intradialytic exercise on syndecan-1, a marker of endothelial dysfunction and injury.

4.2.10   Statistical Analysis

All statistical tests of global myocardial perfusion, RWMAs, and syndecan-1 were completed using IBM SPSS Statistics version 27 (IBM, Armonk, New York, United States of America). Statistical test of patient demographics, dialysis prescription, intradialytic treatments, and changes in laboratory blood measurements were performed using GraphPad Prism 9 (GraphPad Software, La Jolla, California, United States of America). Figures presented in this manuscript were produced using GraphPad Prism 9 (GraphPad Software, La Jolla, California, United States of America).

4.2.10.1   Participant Demographics and Dialysis Treatment Information

Demographic information and prescribed dialysis treatment information for the fourteen participants are summarized with descriptive statistics (minimum value, maximum value, mean and standard deviation) in Table 4-1 and Table 4-2.

4.2.10.2   Intradialytic Clinical Information at the Study Visits

Intradialytic clinical parameters including pre-systolic blood pressure (SBP), pre-diastolic blood pressure (DBP), SBP nadir, DBP nadir, Kt/V, minimum relative blood volume (RBV), mean ultrafiltration rate (UFR), mean UFR relative to pre-HD weight, and total volume of fluid removed during HD were compared between visits. A parametric paired two-tailed t-test was performed for

each of the listed parameters to determine differences in the delivered treatment between visits (control vs. exercise).

4.2.10.3   Assessment of Hemodynamic Stability

Hemodynamic stability was assessed using SBP measurements acquired at baseline, peak HD, and post HD. A repeated measure two-way ANOVA with visit (control or exercise), timepoint (baseline, peak HD, post HD), and visit-by-timepoint as fixed effects was perform for the SBP measurements. A Geisser-Greenhouse correction was applied. If any of the fixed effects were statistically significant, post-hoc tests were performed with Tukey's correction for multiple comparison to determine SBP differences between intradialytic timepoints and between groups.

4.2.10.4   Exercise Treatment Information

The intradialytic exercise information for the twelve participants is summarized with descriptive statistics (minimum value, maximum value, mean and standard deviation) in Table 4-4.

4.2.10.5   Laboratory Testing

Intradialytic changes in electrolyte and protein concentrations measured from the blood samples were assessed using linear mixed models. Levels of ionized calcium, sodium, potassium, chloride, bicarbonate, anion gap, creatinine, urea, albumin, calcium, magnesium, phosphate, parathyroid hormone (PTH), cardiac troponin T (cTnT), hemoglobin, hematocrit, and C-reactive protein (CRP) were analyzed using linear mixed models with intradialytic timepoint and visit (control and exercise) as the fixed effect. A maximum likelihood algorithm was used to estimate variance parameters. The Geisser-Greenhouse correction was applied to correct for the sphericity of the data. If any fixed effect was statistically significant, post-hoc testing was completed with

Sidak's correction for multiple comparison to identify difference in electrolyte between timepoints and between visits.

4.2.10.6   Percent Change in Syndecan-1 Concentration

The percent change in syndecan-1 concentration was measured at peak HD and post HD relative to the baseline syndecan-1 concentration. A repeated measure two-way ANOVA test with intradialytic timepoint and visit (control or exercise) as fixed effects were performed with Geisser-Greenhouse correction for sphericity. If any fixed effect was statistically significant, post-hoc testing was completed with Sidak's correction for multiple comparison to determine differences in syndecan-1 between visit and between intradialytic timepoints.

4.2.10.7   Global Myocardial Perfusion

A grouped (control vs. exercise) analysis was performed to investigate the effect of exercise on global myocardial perfusion during dialysis. A linear mixed model with visit (control or exercise) and intradialytic timepoint as fixed effects was performed with restricted maximum likelihood estimation and the Geisser-Greenhouse correction. Post-hoc testing with Sidak's correction for multiple comparison was performed to identify differences in myocardial perfusion between visits and between timepoints

4.2.10.8   Regional Wall Motion Abnormality

The number of myocardial segments experiencing RWMAs was analyzed using a linear mixed model with visit (control vs. exercise), intradialytic timepoints, and interaction between visit and timepoints as fixed effects. A Geisser-Greenhouse correction was applied for this analysis for sphericity. If any of the fixed effects were significant, post-hoc tests were completed with

Sidak's correction for multiple comparison to identify differences in the number of myocardial segments experiencing RWMAs between visit and between timepoints.

4.3 Results

4.3.1 Participants

Of the fourteen, twelve participants completed both the control and exercise study visits. One participant did not complete the exercise treatment visit due to death. Another participant was unable to complete the exercise treatment visit due to HD-related complications. As a result, twelve participants had a total of six DCE-CT images (control visit = 3 images; exercise visit = 3 images). Of the twelve participants, a single perfusion map of a participant at post HD during the exercise visit could not be generated due to a defect in the software.

Echocardiography data were obtained in fourteen participants (control visit=14 participants; exercise visit = 12 participants). Due to poor image quality, RWMA measurements could not be retrieved for the control visit of one patient. Additionally, for the same reason, RWMA measurement could not be retrieved for the exercise visit of one patient. In total, thirteen RWMA measurements were available for analysis in the control visit for each timepoint and eleven RWMA measurements were available in the exercise visit for each timepoint.

All fourteen participants completed the blood work for the visits attended. However, of the fourteen participants, plasma samples of only eleven participants were analyzed for change in syndecan-1 concentration due to limitations in resources.

The participants demographic information for this study is summarized in Table 4-1. A summary of the participants regular dialysis prescription is given in Table 4-2.

Table 4-1 Participant information and demographics

Characteristics	Prevalence
Ethnicity: Caucasian, n	10 (71%)
Men, n	9 (64%)
Age, yr	66 ± 13
BMI	33 (26-41)
Dialysis vintage (mo)	60 (20-141)
Hemodialysis vintage (mo)	53 (16-141)
Charlson comorbidity index*	7 (4-12)
Congestive heart failure	4 (29%)
Primary renal diagnosis	
Hypertension	4 (29%)
Hypertensive nephrosclerosis	3 (21%)
Diabetic nephropathy	6 (43%)
Acute Interstitial Nephritis	1 (7%)
IgA nephropathy	2 (14%)
Current Smoker	1 (7%)
Medications	
ACEi/ARB	5 (36%)
β - blocker	7 (50%)
2+ antihypertensive agent	5 (36%)

*Age-adjusted

Table 4-2 Mean dialysis prescription (n=14)

Dialysis Prescription	
Treatment Time (hr ± SD)	3.5 ± 0.7
Sodium (mmol/L ± SD)	139 ± 1.8
Calcium (mmol/L ± SD)	1.3 ± 0.1
Bicarbonate (mmol/L ± SD)	37.4 ± 2.3
Dialysis flow, Qd (ml/min ± SD)	543 ± 109
Vascular Access (AVF: AVG: CVC)*	6:1:7

*AVF = arteriovenous fistula; AVG = arteriovenous graft; CVC = central venous catheter

4.3.2 Dialysis Treatment

The dialysis treatment is summarized in Table 4-3 and includes weight +gain/-loss, pre-systolic blood pressure (SBP), pre-diastolic blood pressure (DBP), SBP nadir, DBP nadir, Kt/V, minimum relative blood volume (RBV), mean ultrafiltration rate (UFR), mean UFR relative to pre-HD weight, and total fluid removed during the HD treatment session. The multiple paired parametric t-tests revealed no differences in the listed parameters between visits and this is summarized in more detail in Table 4-3.

Table 4-3 Intradialytic clinical information

Parameters	Control (n=14)	Exercise (n=12)	p-value
Weight +gain/-loss (kg ± SD)	1.4 ± 0.7	1.8 ± 0.7	0.8162
Pre HD SBP (mmHg ± SD)	149 ± 20	143 ± 22	0.4772
Pre HD DBP (mmHg ± SD)	64 ± 18	64 ± 14	0.8301
SBP nadir (mmHg ± SD)	106 ± 21	101 ± 16	0.6499
DBP nadir (mmHg ± SD)	55 ± 16	56 ± 14	0.4921
Kt/V ± SD	1.47 ± 0.3	1.46 ± 0.3	0.6079
Min RBV (% ± SD)	85.0 ± 3.3	84.7 ± 4.6	0.8440
Mean UFR (mL/hr ± SD)	662 ± 196	733 ± 190	0.6065
Mean UFR/pre weight (mL/kg/hr ± SD)	7.50 ± 2.6	8.5 ± 2.9	0.5277
Total fluid removed (mL±SD)	2539 ± 785	2847 ± 732	0.4829

*SBP = systolic blood pressure; DBP = diastolic blood pressure; RBV = relative blood volume; UFR = ultrafiltration rate

4.3.3 Systolic Blood Pressure for Hemodynamic Stability

The repeated measure two-way ANOVA demonstrated a significant effect of timepoint ($F_{(1.824, 43.77)} = 22.17$, $p < 0.0001$). The post-hoc testing showed that SBP was significantly lower at peak HD in comparison to baseline in the control (120.9± 23.8 mmHg vs. 145.0 ± 23.9 mmHg, $p = 0.0179$) and exercise visit (112.2 ± 15.2 mmHg vs. 142.4 ± 19.5 mmHg, $p < 0.0001$, Figure 4-1). SBP post HD was not significantly different from baseline during the control visit (126.0 ± 25.8 mmHg, $p = 0.0615$) but was significantly reduced during the exercise visit (123.3 ± 22.4

mmHg, p = 0.0038). The repeated measure two-way ANOVA did not show significant effect of visit (control vs. exercise) on SBP (F (1, 24) = 0.4139, p = 0.5261).
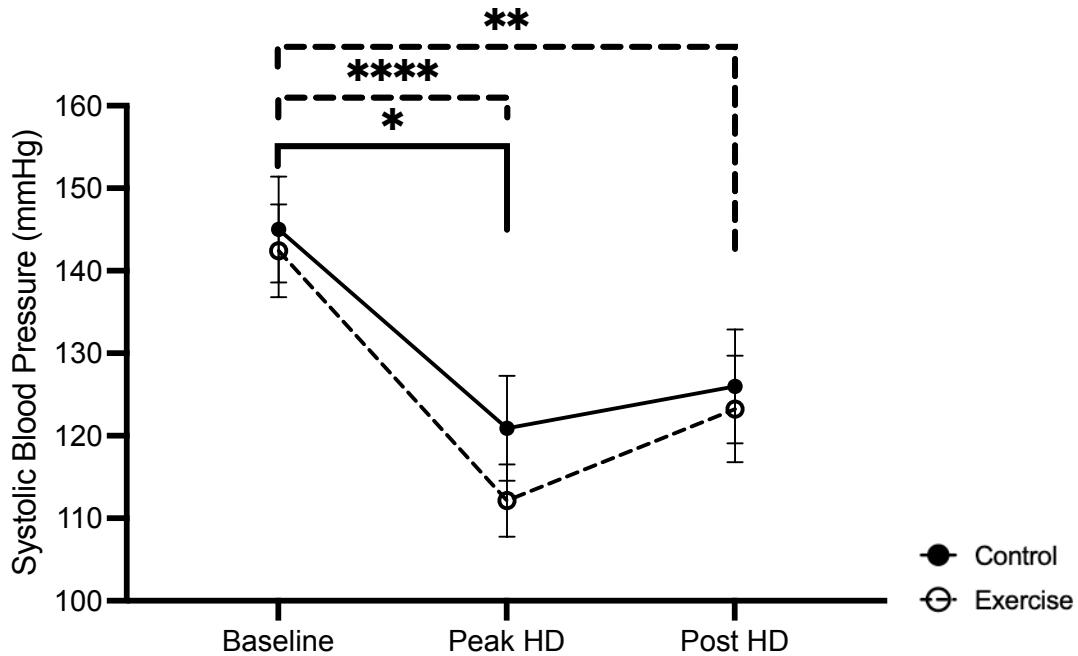
Figure 4-1. Mean systolic blood pressure measured at baseline (pre HD initiation), peak HD stress and post HD at the control and exercise treatment visit. Error bars represent standard error of the mean. * Denote p < 0.0332, ** denote p < 0.0021, **** denote p < 0.0001.

4.3.4 Exercise Prescription Information

The exercise treatment is summarized in Table 4-4 and includes calories burnt during exercise, the number of rotations (count), the number of rotations per minute (RPM), and the amount of calories burnt per minute (CPM).

Table 4-4 Mean exercise information (n=12)

Patient exercise information	Mean ± SD (Min – Max)

Calories (cal ± SD)	108.4 ± 162.3 (9.4 – 479.0)
Count (# of rotations ± SD)	1235 ± 933 (14.3 – 3340)
RPM (# of rotation/min ± SD)*	50.67 ± 31.96 (0.77 – 133.6)
CPM (cal/min ± SD)*	3.86 ± 6.91 (0.98 – 25.7)

*RPM = rotations per minute; *CPM = calories per minute

4.3.5 Laboratory Testing

The electrolyte and protein concentrations measured at baseline, peak HD, and post HD included ionized calcium, sodium, potassium, chloride, bicarbonate, anion gap, creatinine, urea, albumin, calcium, magnesium, phosphate, PTH, cTnT, hemoglobin, hematocrit, and CRP. Linear mixed modelling showed no significance in fixed effect of timepoint in levels of ionized calcium ($F_{(1.054, 24.77)} = 3.690$, $p = 0.0644$), calcium ($F_{(1.220, 28.07)} = 0.4901$, $p = 0.5262$), and sodium ($F_{(1.298, 30.51)} = 0.0123$, $p = 0.9522$). The same electrolytes also showed no significant effect of visits (control vs. exercise) in levels of ionized calcium ($F_{(1, 24)} = 0.0188$, $p = 0.8920$), calcium ($F_{(1, 24)} = 0.8099$, $p = 0.3771$), and sodium ($F_{(1, 24)} = 0.0362$, $p = 0.8508$).

Biomarkers of cardiac injury and inflammation analyzed were cTnT and CRP. Linear mixed modelling indicated insignificant effect of timepoints and visits (control vs. exercise) in levels of cTnT (timepoint: $F_{(1.039, 24.93)} = 3.755$, $p = 0.0627$ and visit: $F_{(1, 24)} = 0.1110$, $p = 0.7419$) and CRP (timepoint: $F_{(1.003, 23.57)} = 0.0257$, $p = 0.8746$ and visit: $F_{(1, 24)} = 0.0016$, $p = 0.9680$).

Linear mixed modelling indicated significant effects of timepoint in the following electrolytes and proteins: potassium, chloride, and bicarbonate, anion gap, creatinine, urea, albumin, magnesium, phosphate, PTH, hemoglobin, and hematocrit. Post-hoc testing for multiple comparison revealed expected intradialytic changes in these electrolytes and proteins. There was no significant effect of visit (control vs. exercise) in the listed electrolytes. Details of these analyses are summarized in Table 4-5 and shown in the Supplementary Figure 4-1.

Table 4-5 Mean plasma electrolyte concentration of those with significant changes as a response to hemodialysis treatment

Electrolyte (Conc. ± SD)	Control (n=14)			Exercise (n=12)		
	Baseline	*Peak HD*	*Post HD*	*Baseline*	*Peak HD*	*Post HD*
Potassium (mmol/L)	4.60 ± 0.8	3.32 ± 0.4	3.34 ± 0.4	4.43 ± 0.7	3.24 ± 0.5	3.22 ± 0.4
Chloride (mmol/L)	93.3 ± 3.2	91.9 ± 2.9	91.7 ± 3.0	92.8 ± 3.2	91.6 ± 2.9	91.6 ± 2.5
Bicarbonate (mmol/L)	24.4 ± 2.5	29.8 ± 2.4	29.9 ± 2.2	25.2 ± 2.4	29.8 ± 2.6	29.8 ± 2.3
Anion Gap (mmol/L)	16.3 ± 3.8	12.7 ± 2.4	12.3 ± 2.6	16.3 ± 3.7	12.8 ± 2.7	12.8 ± 2.8
Creatinine (umol/L)	758 ± 207	274 ± 97	268 ± 107	766 ± 210	275 ± 97	274 ± 100
Urea (mmol/L)	18.2 ± 4.6	5.19 ± 1.6	5.01 ± 1.8	18.3 ± 5.9	5.1 ± 1.4	4.85 ± 1.4
Albumin (g/L)	36.7 ± 3.9	41.8 ± 4.6	40.7 ± 4.9	37.8 ± 2.5	41.7 ± 4.1	42.0 ± 3.9
Magnesium (mmol/L)	1.07 ± 0.2	0.96 ± 0.2	0.93 ± 0.2	1.10 ± 0.3	0.91 ± 0.2	0.92 ± 0.2
Phosphate (mmol/L)	1.78 ± 0.5	0.72 ± 0.1	0.78 ± 0.2	1.78 ± 0.7	0.77 ± 0.5	0.80 ± 0.4
PTH (pmol/L)*	34.5 ± 21	42.6 ± 24	41.4 ± 24	34.1 ± 17	43.9 ± 24	40.6 ± 21
Hemoglobin (g/L)	102 ± 10	112 ± 11	109 ± 12	98.8 ± 9.9	109 ± 11	106 ± 9.1
Hematocrit (L/L)	0.32 ± 0.03	0.35 ± 0.04	0.34 ± 0.04	0.31 ± 0.03	0.33 ± 0.03	0.33 ± 0.03

*PTH = Parathyroid hormone

4.3.6 Percent Change in Syndecan-1

In the twelve participants with viable syndecan-1 measurements, a two-way ANOVA revealed a significant effect of visit (control vs. exercise) on the percent change in syndecan-1 as measured in the blood ($F_{(1, 19)} = 7.673$, $p = 0.0122$). Post-hoc testing showed that at post HD, the percent change in syndecan-1 relative to baseline was significantly higher in the exercise visit (6.5 ± 5.9 %) than in the control (-4.1 ± 4.8 %, $p = 0.0005$, Figure 4-2). In the control visit, percent syndecan-1 was reduced at post HD (-4.1 ± 4.8 %) from peak HD (0.9 ± 5.8%, $p = 0.0270$).
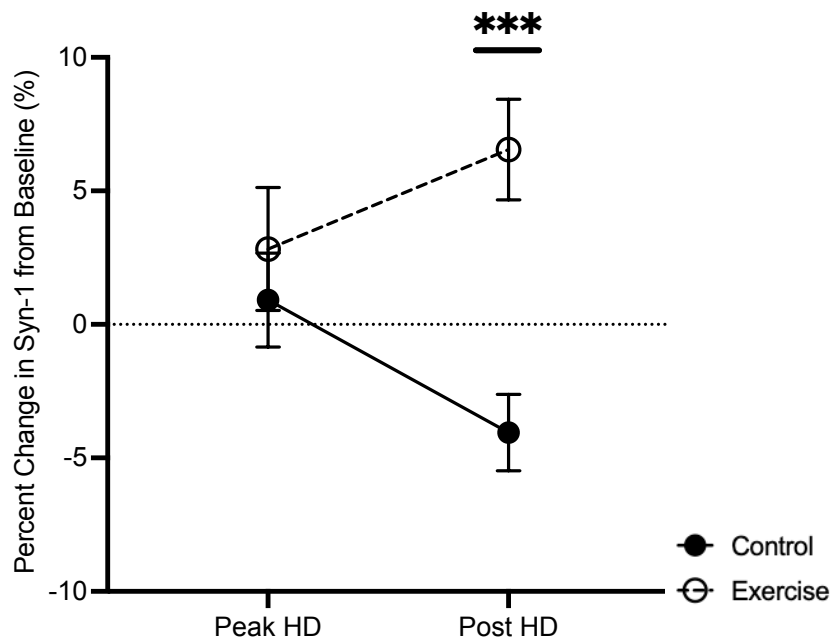
Figure 4-2 Percent change in syndecan-1 concentration at peak HD stress and post HD treatment relative to baseline syndecan-1 concentration. Error bars represent the standard error of the mean. The significance bar represents statistical significance between visits. *** Denote $p < 0.0002$.

4.3.7 Global Myocardial Perfusion

The linear mixed model revealed a statistically significant fixed effect of timepoint ($F_{(2, 13.21)} = 23.26$, $p < 0.0001$) and no effect of visit ($F_{(1,13.47)} = 3.216$, $p = 0.095$). The mean global myocardial perfusion in the control visit decreases from 100.0 ± 9.4 ml/min/100g to 77.8 ± 5.5 ml/min/100g from baseline to peak HD ($p = 0.002$, Figure 4-3), and partially recovers to 88.7 ± 4.9 ml/min/100g post HD (comparison with baseline perfusion, $p = 0.5330$). Comparably, the mean global myocardial perfusion during the exercise visit is reduced from 92.5 ± 7.4 ml/min/100g to 73.5 ± 3.5 ml/min/100g from baseline to peak HD ($p = 0.015$, Figure 4-3), and partially recovers to 82.2 ± 5.1 ml/min/100g post HD (baseline vs. post HD: $p = 0.2050$ and peak HD vs. post HD: $p = 0.0090$, Figure 3). Additional post-hoc testing demonstrated a trend towards increased

myocardial perfusion in the control visit relative to the perfusion measurements obtained in the exercise at post HD timepoint (88.7± 4.9 ml/min/100g vs. 82.2± 5.1 ml/min/100g, p = 0.072, Figure 4-3).
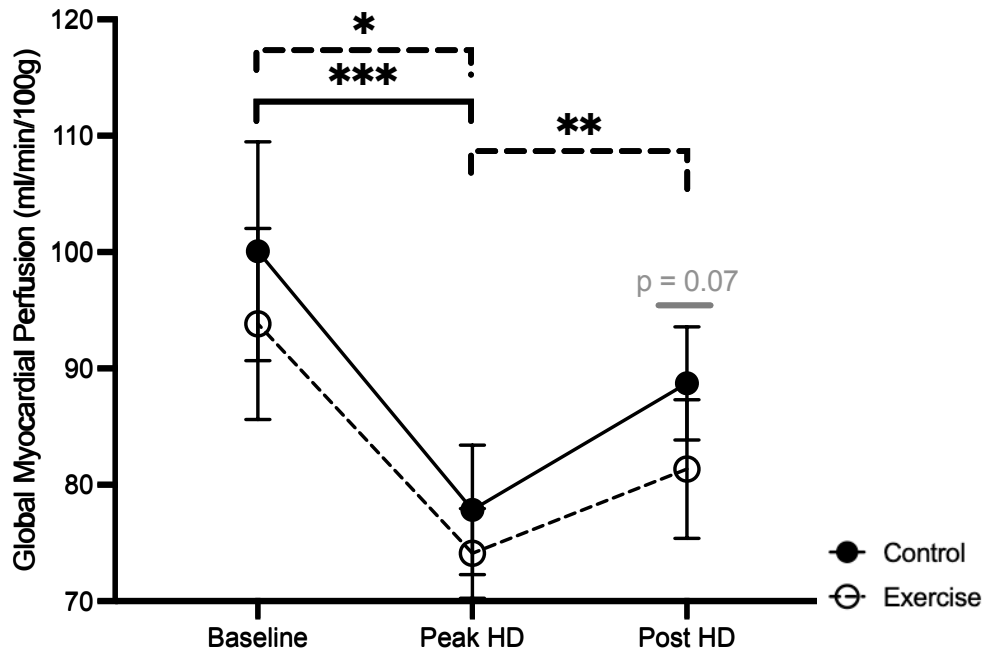

Figure 4-3. Mean global myocardial perfusion at baseline, peak HD stress, post HD during control and exercise visit. Solid significance line represents statistical significance for the control visit. Dotted significance line represents statistical significance for the exercise visit timepoint. Error bars represent standard error of the mean. Grey significance line represents the statistical significance between the control and exercise visits. * Denote $p < 0.0332$, ** denote $p < 0.0021$, *** denote $p < 0.0002$.

4.3.8 Regional Wall Motion Abnormality

Linear mixed modelling revealed a statistically significant fixed effect of timepoint (F (1, 10.392) = 11.489, p = 0.007) and interaction between timepoint and visit (F (1, 9.847) = 6.789, p = 0.027). Post-hoc testing showed no difference in the mean number of myocardial segments

experiencing RWMAs at peak HD (5.4 ± 0.8 segments) and post HD (4.7 ± 0.7 segments, p = 0.289) at the control visit (Figure 4-4, ns, p = 0.29). With exercise, there was a reduction in RWMAs from 5.6 ± 0.9 segments at peak HD to 3.2 ± 0.7 segments at post HD (Figure 4-4, p < 0.001). At post HD timepoint, there was a trend towards decreased number of RWMA with exercise compared to the control (Figure 4-5B, p = 0.086).
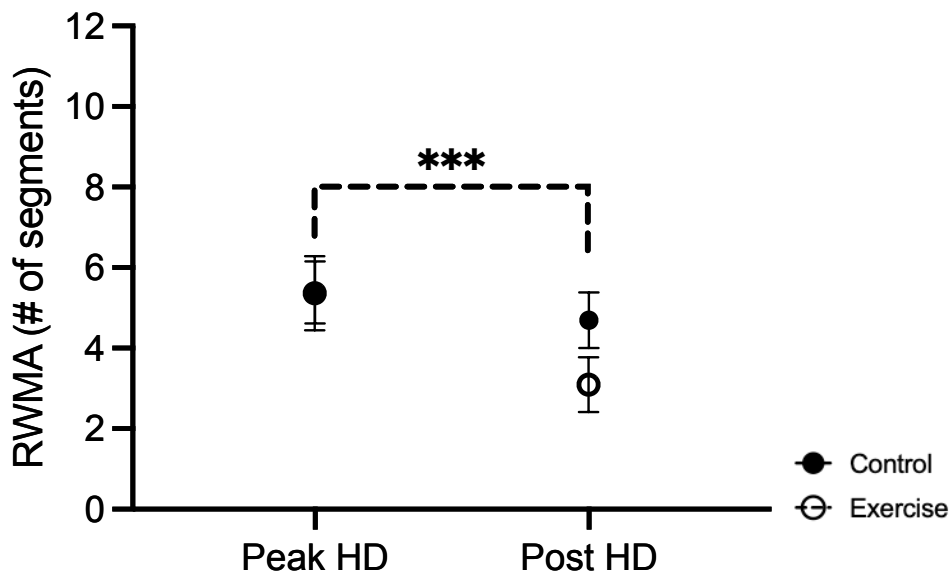

Figure 4-4. Mean number of myocardial segments experiencing regional wall motion abnormality (RWMA) relative to baseline at peak HD stress and post HD during the control and exercise visit. Dotted significance line represents statistical significance for the exercise visit. Error bars represent the standard error of the mean. *** Denote p < 0.0002
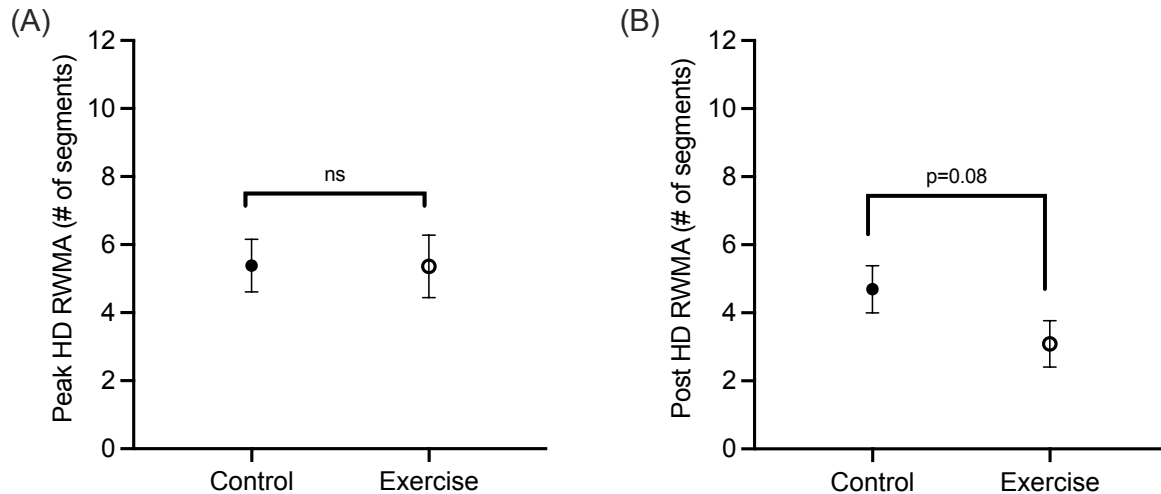
Figure 4-5. (A) Mean number of myocardial segments experiencing regional wall motion abnormality relative to baseline at peak HD stress during the control and exercise visit (B) Mean number of myocardial segments experiencing regional wall motion abnormality relative to baseline at post HD timepoint during the control and exercise visit. Error bars represent the standard error of the mean.

4.4 Discussion

This study is the first to investigate the effects of intradialytic exercise (IDE) on myocardial perfusion and contractility during HD and its role in protection against HD-induced cardiac injury. HD-induced cardiac injury is known to be in the form of myocardial hypoperfusion[57]. In the present study, this was demonstrated by the control visit data (HD without IDE) which showed that global myocardial perfusion was reduced at the peak HD timepoint, with partial perfusion recovery following the end of HD. Similar results have been reported in previous studies[57–59]. Intradialytic hypoperfusion and ischemia has been attributed to the significant hemodynamic effects of HD treatment, especially intradialytic hypotension[60–62]. Indeed, we observed a reduction in systolic blood pressure at peak HD, coinciding with when global myocardial perfusion decreased.

Reduced myocardial perfusion during HD leads to ischemic cardiac injury. A common clinical marker of ischemic cardiac injury is the troponin level, and some studies have demonstrated a relationship between HD and cardiac troponin T (cTnT) levels[13,63–65]. However, no intradialytic change in plasma cTnT levels were observed in the present study. This may be because elevation in cTnT after cardiac ischemia is a delayed response, with elevation typically seen 6-12 hours following an ischemic event[66].

Intradialytic exercise has long been hypothesized to increase myocardial perfusion and decrease myocardial stunning, thereby attenuating intradialytic cardiac ischemic injury [67]. Based on the results of this study, this hypothesis does not appear to be entirely correct. We observed no difference in the intradialytic changes in the myocardial perfusion between the control visit (HD without IDE) and the exercise visit (HD with IDE). At both visits, global myocardial perfusion decreased at peak HD with partial recovery following the end of HD, indicating that IDE does not attenuate the perfusion defects caused by HD. IDE also did not affect the patient's hemodynamic response to HD, with no differences in intradialytic changes in SBP between both visits. At both visits, SBP reduced at peak HD, followed by partial recovery post HD. This demonstrates that IDE does not increase myocardial perfusion as hypothesized in the literature.

However, this is not to say that IDE does not impart cardioprotection. Using echocardiography, this study demonstrated that the number of myocardial segments experiencing regional wall motion abnormality was not significantly different between peak HD and post HD during the control visit, while there was a statistically significant reduction in the number of segments with regional wall motion abnormality from peak HD to post HD during the exercise visit. This suggests that the contractile function of the heart may be protected with intradialytic exercise. These results are consistent with other studies of Intradialytic exercise that also used

echocardiography as a means to assess cardiac function. Previously, our group assessed cardiac function using intradialytic echocardiography in 19 participants exposed to different amounts of intradialytic exercise. Although global longitudinal strain (a measure of global myocardial contractile function) did not improve with exercise, there were reductions in the number of myocardial segments with RWMAs at peak HD stress with exercise exposure [48]. Another study conducted by McGuire et al., showed in 20 participants a reduced mean number of stunned segments (i.e. segments with RWMAs) at 2.5 hours into HD, following exercise exposure one hour into HD treatment[51] .

Taken together, these results suggest that IDE does not impart cardioprotection by affecting myocardial perfusion like other interventions such as dialysate cooling does, but by maintaining cardiac contractility. Said another way, IDE appears to improve ischemic tolerability of cardiac tissue in the setting of the same degree of HD-induced perfusion challenge. The mechanism by which it does this remains unclear and is an area of further study.

The optimal prescription of IDE in terms of intensity, duration, and timing during the dialysis session remains an open question. In our study, we administered IDE for 30 minutes upon HD initiation. Other studies, such as the one done by McGuire et al., administered exercise one hour into HD treatment for 30 minutes, closer to the time during HD at which a patient experiences the most hemodynamic instability or HD-induced stress. Our study showed no difference in the number of segments experiencing RWMA at peak HD (1 hour from the end of dialysis), whereas McGuire et. al did demonstrate a difference at 2.5 hours into dialysis[51]. This discrepancy suggests that the time window at which participants are exposed to exercise in relation to their HD treatment may be crucial in minimizing myocardial abnormalities and optimizing cardioprotection.

The intensity and duration of IDE may be less crucial for achieving optimal cardioprotection, as previous work has shown that the dose of IDE had no affect on the number of myocardial segments with RWMAs during dialysis[48]. However, it remains possible the cardioprotection imparted by IDE is balanced against possible harms. One of these possible harms is endothelial injury. The metric by which endothelial injury was assessed in the present study was via measurement of plasma levels of sydecan-1, a dominant heparan sulfate proteoglycan, propagating at the surface lining of the endothelial glycocalyx[68], known to degenerate or shed into the circulating blood in inflammatory conditions, during states of oxidative stress, and even due to HD[69–71]. It has also been previously shown to increase in response to exercise[72]. Interestingly, in our study a significant rise in plasma sydecan-1 from peak HD to post HD was demonstrated only at the exercise visit, and not at the control visit. Thus, our IDE intervention appeared to have induced shedding of the glycocalyx, which may be an indication of IDE-related endothelial injury. Further study on the impact of IDE on the endothelium should be done to enable titration of IDE dose to prevent IDE related endothelial injury.

The optimal prescription of IDE may also vary amongst patients with different comorbidities such as those with a history of coronary artery disease or a history of myocardial infarction. Further study to determine how IDE modulates cardiac perfusion and contractility in patients with varying degrees of coronary artery stenosis would be valuable.

A number of limitations should be addressed. This study was a pilot study to demonstrate the effect of intradialytic exercise on myocardial perfusion and regional wall motion abnormality. As a result, it was completed on a small, predominately male cohort. However, a retrospective effect size was calculated for myocardial perfusion and RWMAs between intradialytic timepoints in the control and exercise visit. Cohen's d value for our primary outcome measure of myocardial

perfusion measurements were 0.77 between baseline and peak HD and 0.56 between peak HD and post HD in the control visit. Cohen's d value for myocardial perfusion measurements were 0.89 between baseline and peak HD and 0.43 between peak HD and post HD in the exercise visit. The determined values suggested that the size of effect was medium to large. We also experienced difficulty in painting the exact same exercise regime between patients, as patients differed in their exercise tolerance levels secondary to limitations associated with CKD such as muscle atrophy and existing cardiovascular disease.

4.5 Conclusion

To our knowledge, this is the first intradialytic study investigating the effects of intradialytic exercise on cardiac perfusion and function using CT perfusion and echocardiography. First, this study established that in an exercise-naive group of HD participants, a single small dose of exercise was sufficient to induce endothelial damage during HD. Secondly, it was demonstrated that intradialytic exercise did not affect the hemodynamic and electrolyte changes traditionally seen with HD treatment. This study confirmed that the ischemia-reperfusion injury of the heart resulted from the HD treatment itself that is recurrent at each HD treatment session. Most importantly, the results of study indicated that intradialytic exercise did not affect the perfusion response to HD but was able to mitigate cardiac dysfunction with the reduction in RWMAs.

4.6 Acknowledgement

the hemodialysis machines such that intradialytic imaging can take place in the CT suite. Most importantly, the authors are grateful for the patients who have volunteered to take part in this study. Lastly, the authors would like to thank the Ontario Graduate Scholarship and the Heart and Stroke foundation for partial funding of the study.

4.7 References

1. United States Renal Data System. *USRDS Annual Data Report: Epidemiology of Kidney Disease in the United States*.; 2021. Accessed July 18, 2022. https://adr.usrds.org/2021/end-stage-renal-disease/6-mortality

2. Hur L, McIntyre CW. Current and novel imaging techniques to evaluate myocardial dysfunction during hemodialysis. *Curr Opin Nephrol Hypertens*. 2020;29(6):555-563. doi:10.1097/MNH.0000000000000645

3. Mcintyre C, Crowley L. Dying to Feel Better: The Central Role of Dialysis-Induced Tissue Hypoxia. *Clin J Am Soc Nephrol*. 2016;11:549-551. doi:10.2215/CJN.01380216

4. Odudu A, Nery F, Harteveld AA, et al. Arterial spin labelling MRI to measure renal perfusion: a systematic review and statement paper. doi:10.1093/ndt/gfy180

5. Buchanan C, Mohammed A, Cox E, et al. Intradialytic Cardiac Magnetic Resonance Imaging to Assess Cardiovascular Responses in a Short-Term Trial of Hemodiafiltration and Hemodialysis. *J Am Soc Nephrol*. 2017;28:1269-1277. doi:10.1681/ASN.2016060686

6. Marants R, Qirjazi E, Grant CJ, Lee TY, Mcintyre CW. Renal Perfusion during Hemodialysis: Intradialytic Blood Flow Decline and Effects of Dialysate Cooling. Published online 2019. doi:10.1681/ASN.2018121194

7. Marants R, Qirjazi E, Lai KB, et al. Exploring the Link Between Hepatic Perfusion and Endotoxemia in Hemodialysis. *Kidney Int Rep*. 2021;6(5):1336-1345. doi:10.1016/J.EKIR.2021.02.008

8. Polinder-Bos HA, Willem Elting JJ, Aries MJ, et al. Changes in cerebral oxygenation and cerebral blood flow during hemodialysis-A simultaneous near-infrared spectroscopy and positron emission tomography study. *Journal of Cerebral Blood Flow & Metabolism*. 2020(2). doi:10.1177/0271678X18818652

9. Assa S, Hummel YM, Voors AA, et al. Hemodialysis-induced regional left ventricular systolic dysfunction: Prevalence, patient and dialysis treatment-related factors, and prognostic

significance. *Clinical Journal of the American Society of Nephrology*. 2012;7(10):1615-1623. doi:10.2215/CJN.00850112

10. Dorairajan S, Chockalingam A, Misra M. Myocardial stunning in hemodialysis: What is the overall message? *Hemodialysis International*. 2010;14(4):447-450. doi:10.1111/J.1542-4758.2010.00495.X

11. Mcintyre CW. Effects of hemodialysis on cardiac function. *Kidney Int*. 2009;76:371-375. doi:10.1038/ki.2009.207

12. Jefferies HJ, Virk B, Schiller B, Moran J, Mcintyre CW. Frequent Hemodialysis Schedules Are Associated with Reduced Levels of Dialysis-induced Cardiac Injury (Myocardial Stunning). *Clin J Am Soc Nephrol*. 2011;6:1326-1332. doi:10.2215/CJN.05200610

13. Breidthardt T, Burton JO, Odudu A, Eldehni MT, Jefferies HJ, Mcintyre CW. Troponin T for the Detection of Dialysis-Induced Myocardial Stunning in Hemodialysis Patients. *Clin J Am Soc Nephrol*. 2012;7:1285-1292. doi:10.2215/CJN.00460112

14. Assa S, Hummel YM, Voors AA, et al. Hemodialysis-Induced Regional Left Ventricular Systolic Dysfunction: Prevalence, Patient and Dialysis Treatment-Related Factors, and Prognostic Significance. *Clin J Am Soc Nephrol*. 2012;7:1615-1623. doi:10.2215/CJN.00850112

15. Zuidema MY, Dellsperger KC. Myocardial Stunning with Hemodialysis: Clinical Challenges of the Cardiorenal Patient. *Cardiorenal Med*. 2012;2:125-133. doi:10.1159/000337476

16. Burton JO, Jefferies HJ, Selby NM, Mcintyre CW. Hemodialysis-Induced Repetitive Myocardial Injury Results in Global and Segmental Reduction in Systolic Cardiac Function. *Clin J Am Soc Nephrol*. 1925;4. doi:10.2215/CJN.04470709

17. Selim Guler H, Cansin |, Kaya T, et al. Acute stunning effect of hemodialysis on myocardial performance: A three-dimensional speckle tracking echocardiographic study. *Artif Organs*. 2020;44:1081-1089. doi:10.1111/aor.13698

18. Rakha S, Hafez M, Bakr A, Hamdy N. Changes of cardiac functions after hemodialysis session in pediatric patients with end-stage renal disease: conventional echocardiography and two-dimensional speckle tracking study. doi:10.1007/s00467-019-04460-y

19. Ahmadmehrabi S, Wilson Tang | W H, Tang WHW. Hemodialysis-induced cardiovascular disease. Published online 2018. doi:10.1111/sdi.12694

20. Hothi DK, Rees L, Marek J, Burton J, Mcintyre CW. Pediatric Myocardial Stunning Underscores the Cardiac Toxicity of Conventional Hemodialysis Treatments. *Clin J Am Soc Nephrol*. 2009;4:790-797. doi:10.2215/CJN.05921108

21. Jefferies HJ, Lemoine S, Mcintyre CW. High magnesium dialysate does not improve intradialytic hemodynamics or abrogate myocardial stunning. *Hemodialysis International*. 2020;24:506-515. doi:10.1111/hdi.12863

22. Burton JO, Jefferies HJ, Selby NM, Mcintyre CW. Hemodialysis-Induced Cardiac Injury: Determinants and Associated Outcomes. *Clin J Am Soc Nephrol*. 2009;4:914-920. doi:10.2215/CJN.03900808

23. Selby NM, McIntyre CW. A systematic review of the clinical effects of reducing dialysate fluid temperature. *Nephrology Dialysis Transplantation*. 2006;21(7):1883-1898. doi:10.1093/ndt/gfl126

24. Toth-Manikowski SM, Sozio SM. Cooling dialysate during in-center hemodialysis: Beneficial and deleterious effects Hemodynamic stability; Cool temperature dialysis. *World J Nephrol*. 2016;5(2):166-171. doi:10.5527/wjn.v5.i2.166

25. Selby NM, Burton JO, Chesterton LJ, Mcintyre CW. Dialysis-Induced Regional Left Ventricular Dysfunction Is Ameliorated by Cooling the Dialysate. *Clin J Am Soc Nephrol*. 2006;1:1216-1225. doi:10.2215/CJN.02010606

26. Jefferies HJ, Burton JO, McIntyre CW. Individualised Dialysate Temperature Improves Intradialytic Haemodynamics and Abrogates Haemodialysis-Induced Myocardial Stunning, without Compromising Tolerability. *Blood Purif*. 2011;32(1):63-68. doi:10.1159/000324199

27. Levy FL, Grayburn PA, Foulks CJ, Brickner ME, Henrich WL. Improved left ventricular contractility with cool temperature hemodialysis. *Kidney Int*. 1992;41(4):961-965. doi:10.1038/KI.1992.147

28. Nesrallah GE, Suri RS, Guyatt G, et al. Biofeedback dialysis for hypotension and hypervolemia: a systematic review and meta-analysis. *Nephrology Dialysis Transplantation*. 2013;28(1):182-191. doi:10.1093/NDT/GFS389

29. Wilkinson TJ, Mcadams-Demarco M, Bennett PN, Wilund K. Advances in exercise therapy in predialysis chronic kidney disease, hemodialysis, peritoneal dialysis, and kidney transplantation on behalf of the Global Renal Exercise Network HHS Public Access. *Curr Opin Nephrol Hypertens*. 2020;29(5):471-479. doi:10.1097/MNH.0000000000000627

30. Sheng K, Zhang P, Chen L, Cheng J, Wu C, Chen J. Intradialytic exercise in hemodialysis patients: A systematic review and meta-analysis. *Am J Nephrol*. 2014;40(5):478-490. doi:10.1159/000368722

31. Pu J, Jiang Z, Wu W, et al. Efficacy and safety of intradialytic exercise in haemodialysis patients: A systematic review and meta-analysis. *BMJ Open*. 2019;9(1). doi:10.1136/bmjopen-2017-020633

32. Kirkman DL, Scott M, Kidd J, Macdonald JH. The effects of intradialytic exercise on hemodialysis adequacy: A systematic review. *Semin Dial*. 2019;32(4):368-378. doi:10.1111/SDI.12785

33. Valenzuela PL, de Alba A, Pedrero-Chamizo R, et al. Intradialytic exercise: One size doesn't fit all. *Front Physiol*. 2018;9(JUL). doi:10.3389/fphys.2018.00844

34. Deschamps T. Let's programme exercise during haemodialysis (intradialytic exercise) into the care plan for patients, regardless of age. *Br J Sports Med*. 2016;50(22):1357-1358. doi:10.1136/bjsports-2016-096356

35. Ikizler TA. Intradialytic nutrition and exercise: convenience versus efficacy. *Kidney Int*. 2019;96(3):549-552. doi:10.1016/j.kint.2019.04.037

36. Wodskou PM, Reinhardt SM, Andersen MB, Molsted S, Schou LH. Motivation, barriers, and suggestions for intradialytic exercise—A qualitative study among patients and nurses. *Int J Environ Res Public Health*. 2021;18(19). doi:10.3390/ijerph181910494

37. Jung TD, Park SH. Intradialytic Exercise Programs for Hemodialysis Patients. *Chonnam Med J*. 2011;47(2):61. doi:10.4068/cmj.2011.47.2.61

38. Parker K. *Intradialytic Exercise Is Medicine for Hemodialysis Patients*.; 2016. www.acsm-csmr.org

39. Thijssen DHJ, Redington A, George KP, Hopman MTE, Jones H. Association of exercise preconditioning with immediate cardioprotection: A review. *JAMA Cardiol*. 2018;3(2):169-176. doi:10.1001/jamacardio.2017.4495

40. Mcguire S, Horton EJ, Renshaw D, Jimenez A, Krishnan N, Mcgregor G. Hemodynamic Instability during Dialysis: The Potential Role of Intradialytic Exercise. *Biomed Res Int*. 2018;2018. doi:10.1155/2018/8276912

41. Young HML, March DS, Graham-Brown MPM, et al. Effects of intradialytic cycling exercise on exercise capacity, quality of life, physical function and cardiovascular measures in adult haemodialysis patients: A systematic review and meta-analysis. *Nephrology Dialysis Transplantation*. 2018;33(8):1436-1445. doi:10.1093/ndt/gfy045

42. Ferreira GD, Bohlke M, Correa CM, Dias EC, Orcy RB. Does Intradialytic Exercise Improve Removal of Solutes by Hemodialysis? A Systematic Review and Meta-analysis. *Arch Phys Med Rehabil*. 2019;100(12):2371-2380. doi:10.1016/j.apmr.2019.02.009

43. Andrade FP, Rezende P de S, Ferreira T de S, Borba GC, Müller AM, Rovedder PME. Effects of intradialytic exercise on cardiopulmonary capacity in chronic kidney disease: systematic review and meta-analysis of randomized clinical trials. *Sci Rep*. 2019;9(1). doi:10.1038/s41598-019-54953-x

44. Chung YC, Yeh ML, Liu YM. Effects of intradialytic exercise on the physical function, depression and quality of life for haemodialysis patients: a systematic review and meta-analysis of randomised controlled trials. *J Clin Nurs*. 2017;26(13-14):1801-1813. doi:10.1111/jocn.13514

45. Greenwood SA, Koufaki P, Macdonald JH, et al. Randomized Trial—PrEscription of intraDialytic exercise to improve quAlity of Life in Patients Receiving Hemodialysis. *Kidney Int Rep*. 2021;6(8):2159-2170. doi:10.1016/j.ekir.2021.05.034

46. Gomes Neto M, Ferrari F, de Lacerda R, Lopes AA, Prata Martinez B, Saquetto MB. Intradialytic exercise training modalities on physical functioning and health-related quality of life in patients undergoing maintenance hemodialysis: systematic review and meta-analysis. *Clin Rehabil*. 2018;32(9):1189-1202. doi:10.1177/0269215518760380

47. Chan D, Green S, Fiatarone Singh M, Barnard R, Cheema BS. Development, feasibility, and efficacy of a customized exercise device to deliver intradialytic resistance training in patients with end stage renal disease: Non-randomized controlled crossover trial. *Hemodialysis International*. 2016;20(4):650-660. doi:10.1111/hdi.12432

48. Penny JD, Salerno FR, Brar R, et al. Intradialytic exercise preconditioning: An exploratory study on the effect on myocardial stunning. *Nephrology Dialysis Transplantation*. 2019;34(11):1917-1923. doi:10.1093/ndt/gfy376

49. Momeni A, Nematolahi A, Nasr M. *Effect of Intradialytic Exercise on Echocardiographic Findings in Hemodialysis Patients*. Vol 8.; 2014. www.ijkd.org

50. Jeong JH, Biruete A, Fernhall B, Wilund KR. Effects of acute intradialytic exercise on cardiovascular responses in hemodialysis patients. *Hemodialysis International*. 2018;22(4):524-533. doi:10.1111/hdi.12664

51. Mcguire S, Horton EJ, Renshaw D, et al. Cardiac stunning during haemodialysis: the therapeutic effect of intra-dialytic exercise. doi:10.1093/ckj/sfz159

52. So A, Lee TY. Quantitative myocardial CT perfusion: a pictorial review and the current state of technology development. *J Cardiovasc Comput Tomogr*. 2011;5(6):467-481. doi:10.1016/j.jcct.2011.11.002

53. So A, Hsieh J, Li JY, Hadway J, Kong HF, Lee TY. Quantitative myocardial perfusion measurement using CT Perfusion: a validation study in a porcine model of reperfused acute

myocardial infarction. *Int J Cardiovasc Imaging*. 2012;28(5):1237-1248. doi:10.1007/s10554-011-9927-x

54. So A, Wisenberg G, Teefy P, et al. Functional CT assessment of extravascular contrast distribution volume and myocardial perfusion in acute myocardial infarction. Published online 2018. doi:10.1016/j.ijcard.2018.02.101

55. McIntyre CW, Lee TY, Ellis C, et al. Computational Assessment of Blood Flow Heterogeneity in Peritoneal Dialysis Patients' Cardiac Ventricles. *Front Physiol*. 2018;9(May):1-16. doi:10.3389/fphys.2018.00511

56. Kharche SR, Lemoine S, Tamasi T, Hur L, So A, McIntyre CW. Therapeutic Hypothermia Reduces Peritoneal Dialysis Induced Myocardial Blood Flow Heterogeneity and Arrhythmia. *Front Med (Lausanne)*. 2021;8. doi:10.3389/fmed.2021.700824

57. Mcintyre CW, Burton JO, Selby NM, et al. Hemodialysis-Induced Cardiac Dysfunction Is Associated with an Acute Reduction in Global and Segmental Myocardial Blood Flow. *Clin J Am Soc Nephrol*. 2008;3:19-26. doi:10.2215/CJN.03170707

58. Buchanan C, Mohammed A, Cox E, et al. Intradialytic cardiac magnetic resonance imaging to assess cardiovascular responses in a short-term trial of hemodiafiltration and hemodialysis. *Journal of the American Society of Nephrology*. 2017;28(4):1269-1277. doi:10.1681/ASN.2016060686

59. Assa S, Dasselaar JJ, Slart RHJA, et al. Comparison of cardiac positron emission tomography perfusion defects during stress induced by hemodialysis versus adenosine. *American Journal of Kidney Diseases*. 2012;59(6):862-864. doi:10.1053/j.ajkd.2012.01.018

60. Sands JJ, Usvyat LA, Sullivan T, et al. Intradialytic hypotension: Frequency, sources of variation and correlation with clinical outcome. *Hemodialysis International*. 2014;18(2):415-422. doi:10.1111/HDI.12138

61. Penny JD, Grant C, Salerno F, et al. Percutaneous perfusion monitoring for the detection of hemodialysis induced cardiovascular injury. *Hemodialysis International*. 2018;22:351-358. doi:10.1111/hdi.12632

62. Mantri Y, Dorobek TR, Tsujimoto J, Penny WF, Garimella PS, Jokerst J v. Monitoring peripheral hemodynamic response to changes in blood pressure via photoacoustic imaging. *Photoacoustics*. 2022;26. doi:10.1016/J.PACS.2022.100345

63. Sun L, Ji Y, Wang Y, et al. High-sensitive cardiac troponin T: a biomarker of left-ventricular diastolic dysfunction in hemodialysis patients. *J Nephrol*. 2018;31:967-973. doi:10.1007/s40620-018-0540-0

64. Assa S, Gansevoort RT, Westerhuis R, et al. Determinants and prognostic significance of an intra-dialysis rise of cardiac troponin I measured by sensitive assay in hemodialysis patients. doi:10.1007/s00392-013-0551-8

65. Ünlü S, Şahinarslan A, Sezenöz B, et al. High-sensitive troponin T increase after hemodialysis is associated with left ventricular global longitudinal strain and ultrafiltration rate. *Cardiol J*. 2020;27(4):376-383. doi:10.5603/CJ.A2018.0118

66. Mahajan VS, Jarolim P. How to interpret elevated cardiac troponin levels. *Circulation*. 2011;124(21):2350-2354. doi:10.1161/CIRCULATIONAHA.111.023697/FORMAT/EPUB

67. Selby NM, Mcintyre CW. How is the Heart Best Protected in Chronic Dialysis Patients? *Semin Dial*. 2014;27(4):332-335. doi:10.1111/SDI.12180

68. Liles WC, Wada T, Joffre J, Fraser DD, Patterson EK, Cepinskas G. Endothelial Glycocalyx Degradation in Critical Illness and Injury. *Frontiers in Medicine | www.frontiersin.org*. 2022;1:898592. doi:10.3389/fmed.2022.898592

69. Kusuzawa K, Suzuki K, Okada H, et al. Measuring the Concentration of Serum Syndecan-1 to Assess Vascular Endothelial Glycocalyx Injury During Hemodialysis. *Front Med (Lausanne)*. 2021;8:2784. doi:10.3389/FMED.2021.791309/BIBTEX

70. Koch J, Idzerda NMA, Dam W, Assa S, Franssen CFM, van den Born J. Plasma syndecan-1 in hemodialysis patients associates with survival and lower markers of volume status. *Am J Physiol Renal Physiol*. 2019;316(1):F121-F127. doi:10.1152/AJPRENAL.00252.2018

71. Koch J, Idzerda NMA, Ettema EM, et al. An acute rise of plasma Na+concentration associates with syndecan-1 shedding during hemodialysis. *Am J Physiol Renal Physiol*. 2020;319(2):F171-F177. doi:10.1152/AJPRENAL.00005.2020

72. Lee S, Kolset SO, Birkeland KI, Drevon CA, Reine TM. Acute exercise increases syndecan-1 and -4 serum concentrations. *Glycoconj J*. 2019;36(2):113-125. doi:10.1007/s10719-019-09869-z

4.8 Co-Authorship Statement

The material in Chapter 4 is in preparation for publication at the Kidney International Journal. Some materials presented in this chapter submitted for a presentation at the American Society of Nephrology International Conference (November 5, 2022; SA-PO373; poster presentation). Lisa Hur is the main contributor of the work that has been presented in this chapter—designing the study, data acquisition, data processing, statistical analysis of the data, and manuscript preparation. Co-authors of this chapter were Jarrin Penny, Justin Dorie, and Christopher W. McIntyre. Jarrin Penny and Justin Dorie were responsible for the delivery of hemodialysis and exercise, ensuring the safety of the participants during the study visits. Christopher McIntyre provided clinical and logistical oversight, as well as invaluable guidance in terms of the study design, interpretation of data, and manuscript preparation.
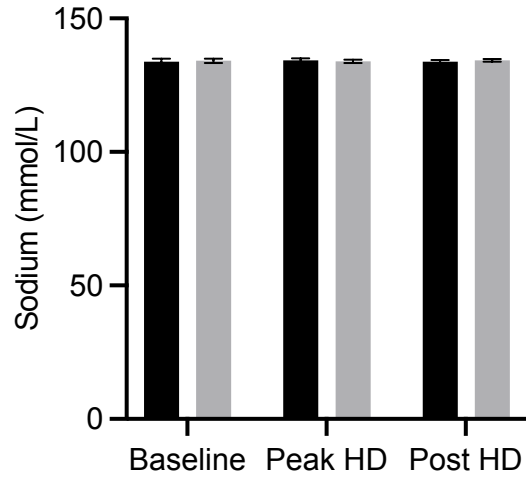
Estimated percentage of the work for Chapter 4 conducted solely by Lisa Hur: 85%
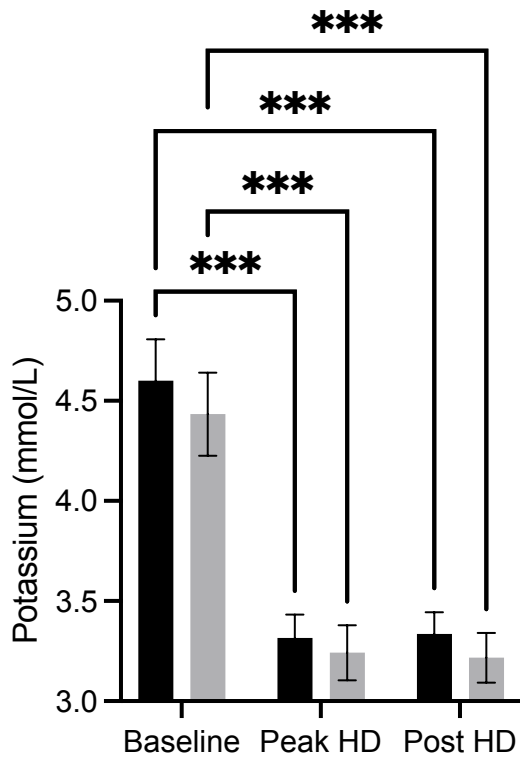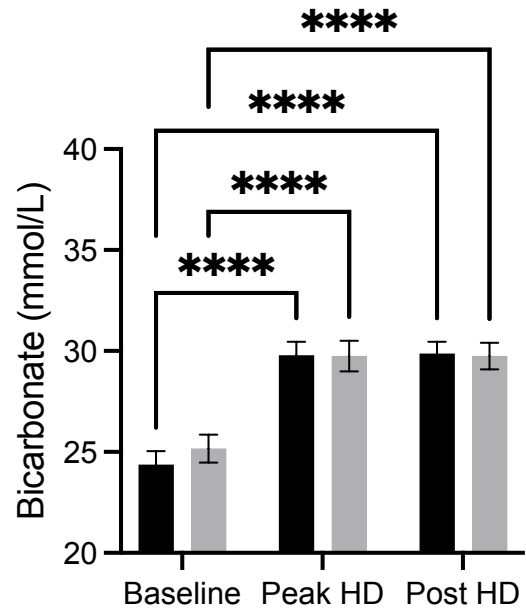
4.9 Supplementary Figures

A

B

C

D

E

F

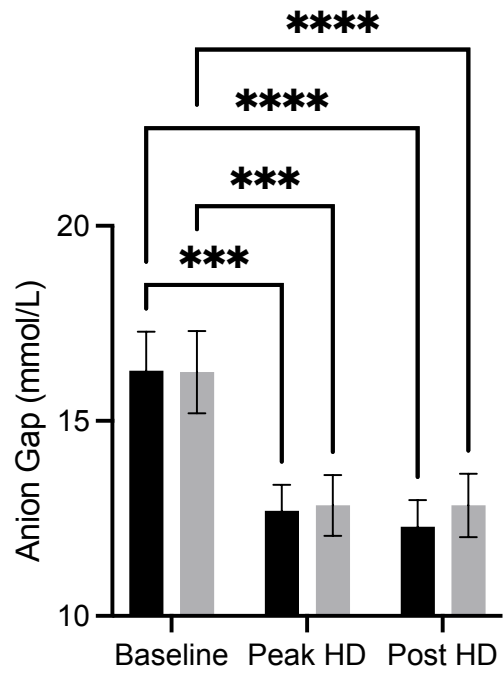**G**

H
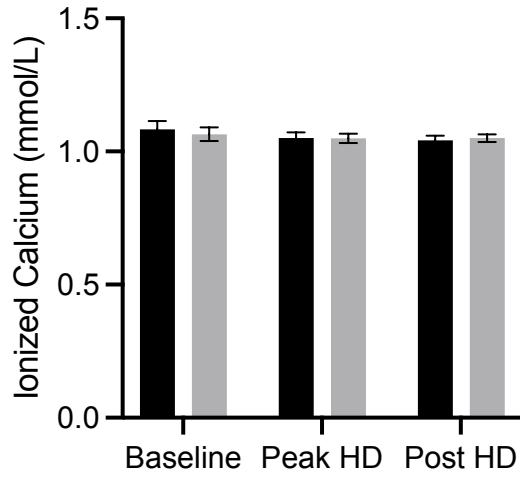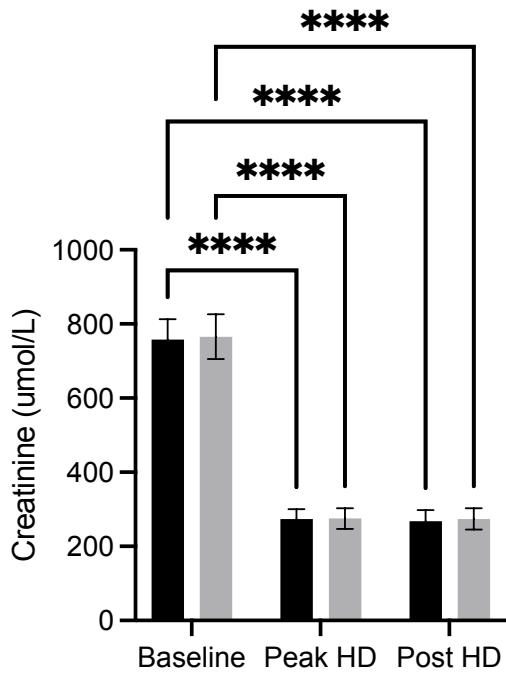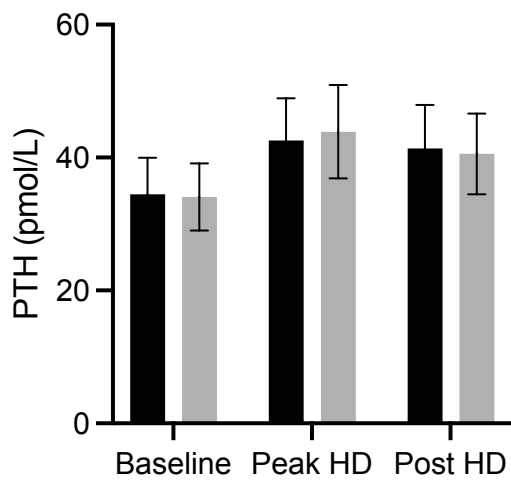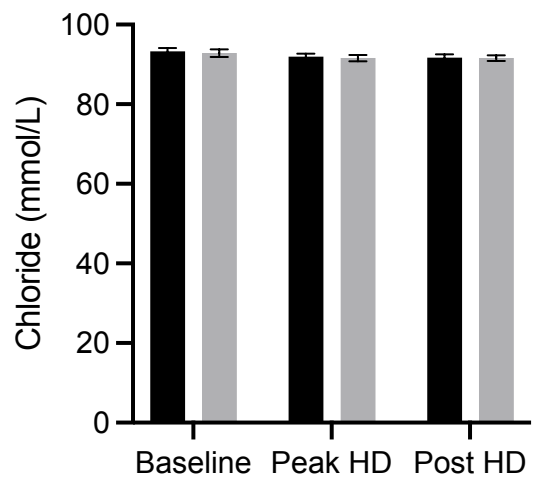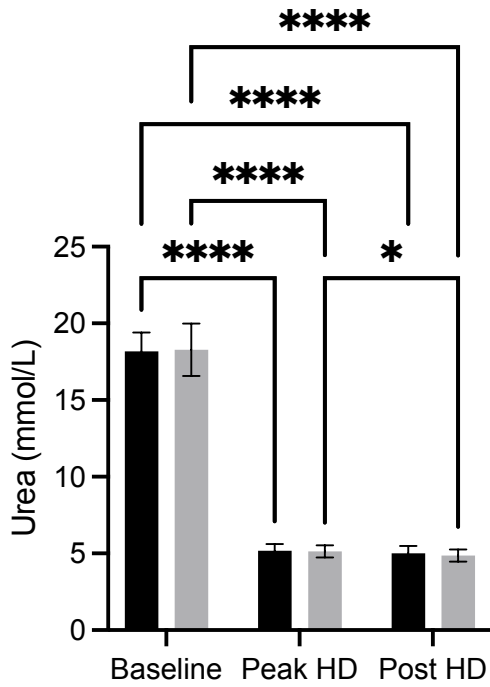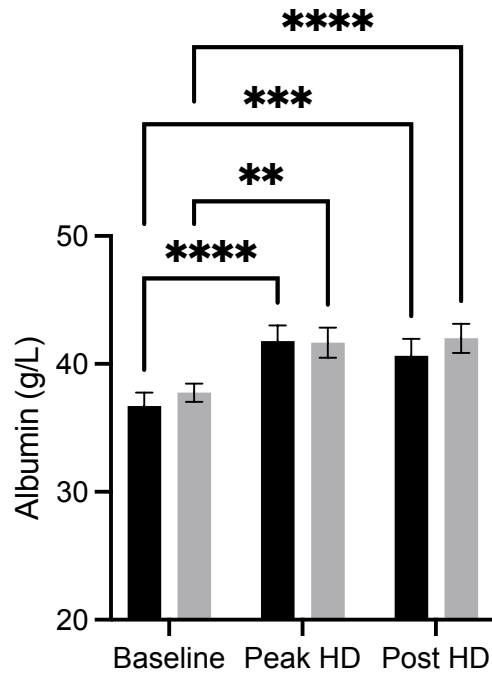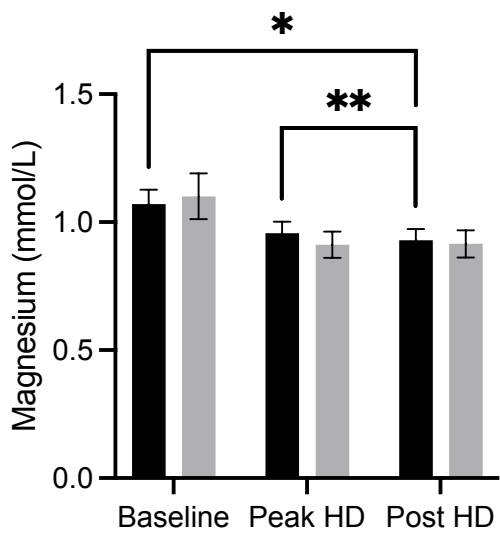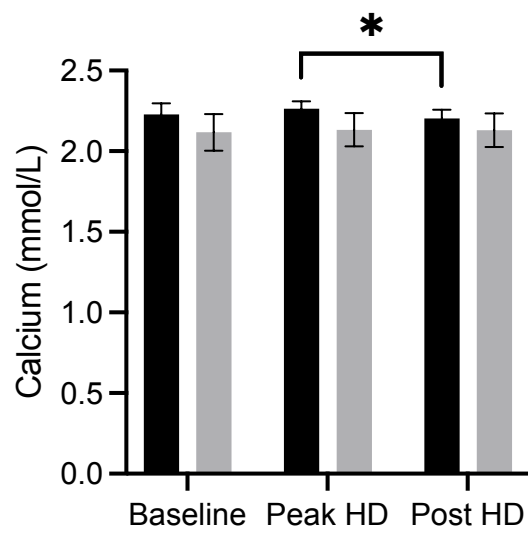
M
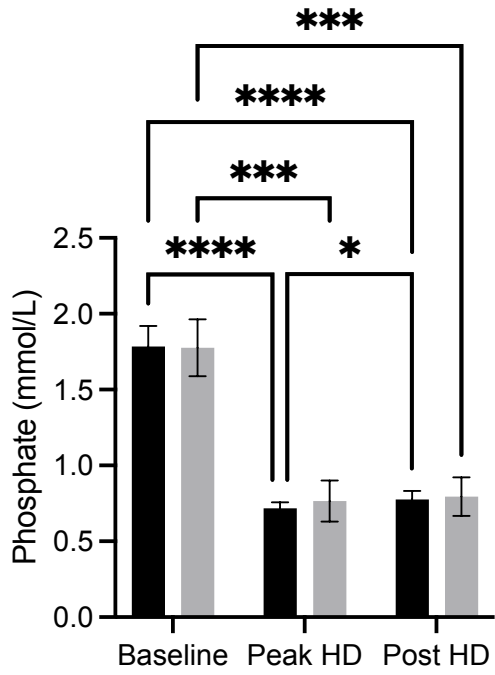
N
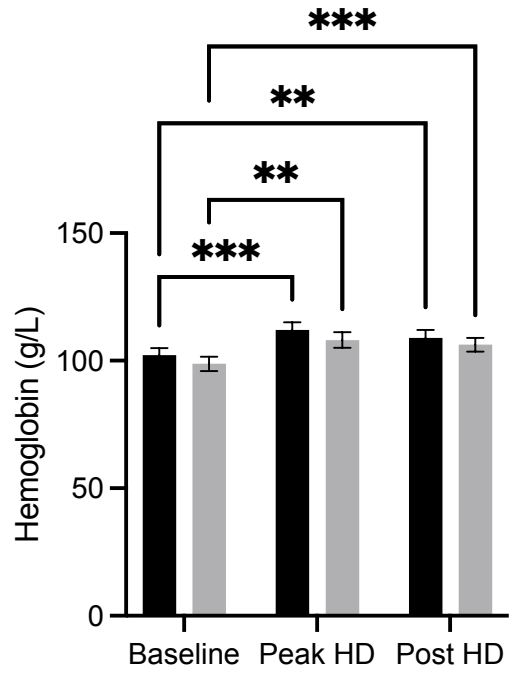
O
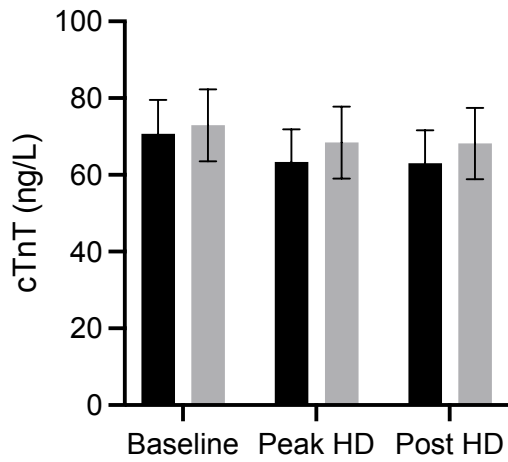
P
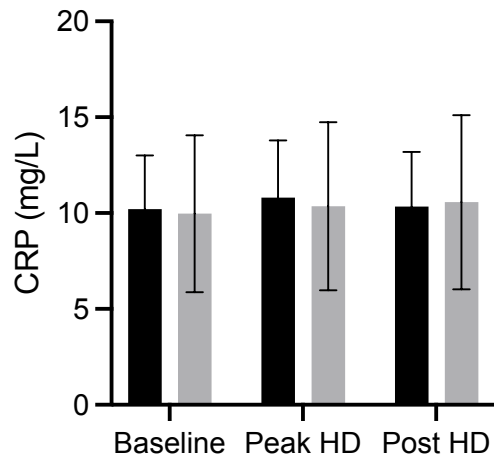
Q
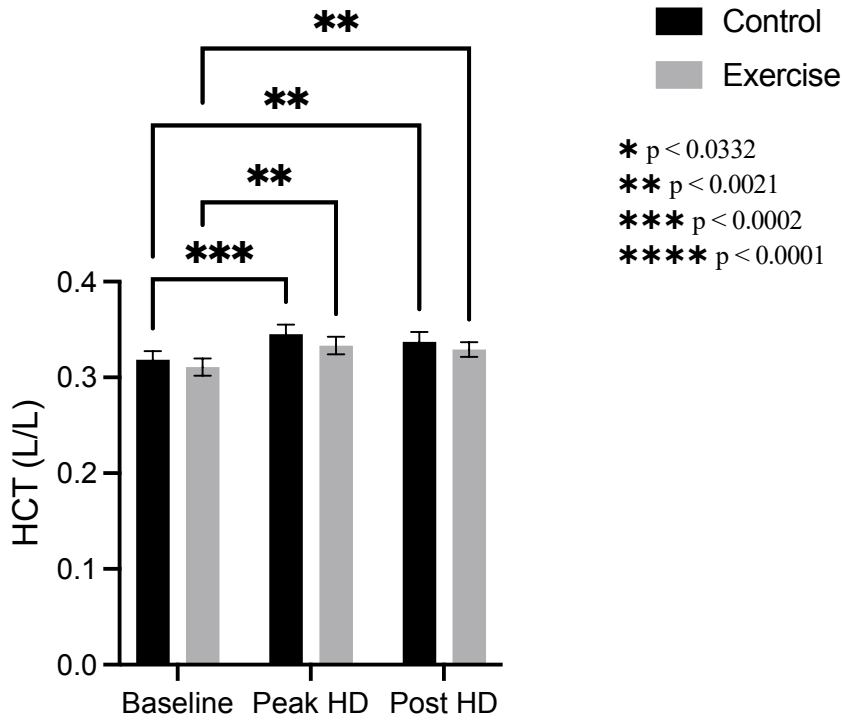
Supplementary Figure 4-1 Intradialytic changes in serum electrolyte and protein levels. Error bars represent standard error of the mean.

Chapter 5

5 Thesis Summary and Future Works

5.1 Project Summary and Conclusion

The purpose of this thesis was to study the microcirculatory changes during hemodialysis (HD) in conditions of coronary artery stenoses, intradialytic exercise intervention, and alteration of sodium dialysate. The scientific investigations that were conducted are summarized in this section.

5.1.1 Presence of coronary artery stenoses reduces segmental myocardial perfusion and is associated with myocardial stunning

Chapter 2 described an exploratory study where multimodal intradialytic imaging was used to evaluate myocardial perfusion in fourteen individuals on hemodialysis treatment. Unlike studies reported in the literature to date, this study did not exclude patients with coronary artery disease. Interestingly, this study showed that systemic hemodynamics (as assessed using intradialytic blood pressure measurements) and the global myocardial perfusion response (as assessed using computed tomography perfusion imaging) did not change with the presence of coronary artery stenoses. Ischemic myocardial injury associated with HD is apparent three hours from the initiation of dialysis whether there is coronary artery stenosis or not.

It appears that coronary artery stenosis affects perfusion not at the global level, but at the segmental level. Myocardial segments supplied by the stenosed coronary arteries experienced a significant reduction in perfusion that did not recover to baseline levels following the end of HD treatment. In contrast, the segments supplied by non-stenosed coronary arteries experienced a recovery of perfusion to baseline levels at the end of HD treatment. Accordingly, the group of participants with no coronary artery stenosis had fewer segments experiencing hypoperfusion

170

(defined as a >30% reduction in myocardial perfusion relative to baseline) after HD compared to during HD, while the group of participants with coronary artery stenosis had the same number of segments experiencing hypoperfusion after HD as during HD. In other words, there was an absence of perfusion recovery at the segmental level in the group of participants with coronary artery stenosis.

The fact that coronary artery stenosis affects perfusion at the segmental level has consequences that may be of clinical significance. The absence of perfusion recovery after HD in the stenosed participant group was associated with the persistence of regional wall motion abnormality after HD indicating myocardial stunning. Consistent with this, the stenosed participant group also had higher levels of cardiac troponin T during HD, which remained elevated following the end of HD treatment, while the non-stenosed participant group had troponin levels that recovered following the end of HD.

Together this suggests that the presence of coronary artery stenosis may result in greater and clinically significant amount of myocardial injury due to differences in segmental perfusion, despite no detectable differences in systemic hemodynamics or global myocardial perfusion.

5.1.2 The effect of dialysate sodium on endothelial injury and microcirculatory dysfunction

Dialysis does not only result in injury to vascular beds such as the heart at a global, segmental, or macrovascular level, but also at a microvascular level. It has been well established that ischemic injury can cause endothelial damage, but this may be exacerbated by significant osmotic shifts during dialysis. Generally, dialysate fluid used during HD contains high sodium concentrations to improve hemodynamic stability during HD, at the cost of significant sodium loading. HD-induced sodium loading and the subsequent osmotic shift that takes place during HD

171

can compound the endothelial damage caused by HD-induced ischemia. This is because it is the endothelium that serves as a buffer for sudden serum sodium shifts. Endothelial cells have a pericellular coat (glycocalyx) that contains transmembrane heparan sulfate proteoglycans such as syndecan-1 which bind sodium.

The role of sodium loading due to dialysis in HD-associated microvascular injury is not well understood. Chapter 3 described a study that aimed to study the effects of sodium loading during HD on the endothelium. HD was performed on rodents without kidney disease using dialysate that differed with respect to sodium composition. The resulting effects on the microvasculature were assessed using intravital microscopy and plasma syndecan-1 levels.

Plasma syndecan-1 levels increased during dialysis at all three levels of dialysate sodium tested (130, 140, and 150 mM). However, with higher dialysate sodium concentration (150 mM), the level of syndecan-1 in plasma at two hours into dialysis was greater than baseline measures by almost two-folds, whereas with lower dialysate sodium concentration (130, 140 mM) sydecan-1 levels only demonstrated a one-fold increase at two hours into dialysis relative to baseline. At the intradialytic timepoints where syndecan-1 levels increased, there was a concomitant reduction in microvascular perfusion only in the rats exposed to high sodium dialysate. Thus, this suggests that sodium loading not only directly mediates endothelial injury during dialysis, but also compounds endothelial damage caused by HD-induced ischemia and may induce a functional change in the microvasculature. This assertion is supported by detection of strong negative correlations between percent change in syndecan-1 and mean arterial pressure and between percent change in syndecan-1 and microvascular perfusion.

5.1.3 A Pilot Study: Assessment of intradialytic exercise on the circulation and function of the heart

Recurrent myocardial injury due to hemodialysis can eventually lead to heart failure and death. Injury has been attributed primarily to HD-associated circulatory stress and volatile hemodynamics during HD. In a single HD treatment session, patients can experience episodic hypotension and multiorgan ischemia. There have been studies of various interventions to improve the hemodynamic tolerability of dialysis, including the use of a biofeedback dialysis system, applying cooled dialysate, and prescribing remote ischemic preconditioning to a limb prior to HD. However, one of the simplest and easiest to implement may be intradialytic exercise.

In Chapter 4, intradialytic exercise was studied as an intervention to mitigate HD-induced cardiac ischemic injury. In particular, the aim of the study was to investigate the effects of intradialytic exercise on the microcirculation and myocardial perfusion. Participants were asked to engage in exercise during HD; their cardiac responses were evaluated with CT imaging and echocardiography, while their microcirculation was assessed with plasma syndecan-1 levels.

Exercise did not affect myocardial perfusion during HD, with perfusion of the myocardium reduced at peak HD (defined as three-hours into HD at the time of maximal circulatory stress) in concert with a reduction in systolic blood pressure, regardless of whether exercise was performed or not. However, exercise had a positive effect on the contractile function of the heart (as measured using echocardiography) which improved with exercise intervention during dialysis. Intradialytic exercise also caused an increase in plasma syndecan-1 levels.

Together, this suggests that intradialytic exercise may be cardioprotective by improving cardiac contractility during dialysis without affecting myocardial perfusion, at the cost of acute endothelial damage.

5.2 Significance and Impact

The work completed in this thesis generated new understanding about the acute effects of HD on the circulation, an area of nephrology that remains poorly understood. Utilizing state of the art tools such as myocardial CT perfusion imaging and echocardiography intradialytically, the detrimental effect of HD on myocardial segments in HD patients with coronary artery disease, a rarely studied patient population, was demonstrated. Using an innovative small-animal hemodialysis system, a preclinical dialysis research platform was developed that enabled the observation of HD-induced microvascular dysfunction with intravital microscopy and plasma syndecan-1 levels. Having established that both perfusion-related ischemic injury and systemic microvascular injury occurs acutely due to hemodialysis, intradialytic exercise was evaluated as an intervention for cardio protection against the acute effects of HD treatment. These contributions are clinically impactful and have the potential to change our understanding of hemodialysis, to change clinical practice, and to improve patient outcome.

5.3 Future Directions

5.3.1 A Comprehensive Study of the Coronary Arteries in HD

In Chapter 2 of this thesis, we have demonstrated that clinically significant coronary artery stenosis aggravates HD-induced injury to the myocardium at a segmental level, with consequences for the contractile function of the heart. This result was clear, despite having only three HD participants with significant coronary artery stenosis and ten HD participants without coronary artery stenosis. Coronary artery disease increases the harms of HD and increased understanding of the effects of HD in the understudied population of patients with coronary artery disease on dialysis is a must. To establish generalizability of these findings, a more comprehensive study with a larger sample size would be valuable. In this larger study, nuances surrounding how coronary artery

disease modulates the harms of HD can be established by assessing which coronary vessels are stenosed, grading the degree and level of vessel stenoses, and relating this to segmental measurements of segmental myocardial perfusion and contractility.

5.3.2 Sodium Induced Microvascular Injury with HD in an Animal Model of CKD

In Chapter 3 of this thesis, an innovative small animal dialysis system was described and served as the basis for a novel preclinical dialysis research platform. This platform enabled the study of the effects of dialysate sodium on the microcirculation. A higher dialysate sodium caused an increase in plasma sodium that resulted in direct injury to the endothelial glycocalyx, inducing microvascular dysfunction during HD in healthy rats. In other words, the study described in Chapter 3 established that large osmotic shifts during HD was detrimental to microvascular function.

A more nuanced understanding around the degree of osmotic shift would be helpful. Using the same preclinical dialysis platform, the effect of a wider range of dialysate sodium levels in smaller increments of 2-4 mM on the microcirculation could be assessed, and a dose-response curve generated. We could then establish whether or not there is a threshold at which osmotic shifts become detrimental. Nuanced understanding around the rate of osmotic shift would also be helpful. It is possible that a rapid dialysis rate causing a more rapid shift would result in greater harm to the microcirculation. This understanding could be used to guide human studies in the future with the ultimate goal of optimizing dialysis prescriptions to minimize circulatory harm.

Translatability of the results would be improved if rats with kidney disease were studied rather than healthy rats, as was done in Chapter 3. It is logical to assume that circulatory response to changes in sodium level during HD may differ depending on the level of kidney function.

Although this can be directly studied in humans, extending the preclinical dialysis research platform by creating and validating a reliable small-animal model of chronic kidney disease would be valuable.

5.3.3 Optimization of Intradialytic Exercise

In Chapter 4, intradialytic exercise was assessed as a means of cardioprotection against the acute effects of HD on myocardial perfusion and cardiac contractility. Although the literature has established that different amounts of intradialytic exercise is comparable in terms of benefits, there is no consensus regarding the optimal timing of exercise during HD for the most effective cardioprotection. A randomized control trial with multiple arms corresponding to the timing of intradialytic exercise (e.g. at the start of HD, 30 mins into HD, 1 hr, 1.5 hr, 2 h, and 2.5 hr from the start of HD treatment session) would be needed to identify the golden time window at which cardioprotection is maximized. Outcome measures can include the same measurements made in the study described in Chapter 2 and 4. These include global and segmental myocardial perfusion as assessed by intradialytic CT, as well as echocardiography to measure myocardial contractile function at a segmental level.

5.3.4 HD-Induced Perfusion Anomalies and its Association with Clinically Significant Cardiovascular Events

In the studies presented in this thesis, the detrimental effect of HD on myocardial perfusion was well established. This effect was demonstrated over one dialysis sessions, but patients with end stage renal disease require repeated dialysis treatment, often multiple times per week. This results in recurrent cardiac ischemic injury. Recurrent cardiac ischemic injury is thought to be a precursor to the development of clinically significant arrhythmia with the risk of sudden cardiac death in this patient population. It would be important to establish how the altered myocardial

perfusion in HD relates to the development of clinically significant arrhythmia in future studies. Possible mechanisms that may contribute include the disruption of the propagation of electrical waves through ischemic zones and ectopic depolarization within injured myocardial regions. The relationship between perfusion and arrhythmic events in the HD population is a missing piece of our understanding that must be addressed.

Appendices

Western Research

Date: 9 September 2019

To: Dr. Christopher McIntyre

Project ID: 113905

Study Title: Investigation of Electrophysiological Substrate of Arrhythmia in Hemodialysis patients

Application Type: HSREB Amendment Form

Review Type: Delegated

Full Board Reporting Date: September 17, 2019

Date Approval Issued: 09/Sep/2019

REB Approval Expiry Date: 06/Aug/2020

_____

Dear Dr. Christopher McIntyre ,

The Western University Health Sciences Research Ethics Board (HSREB) has reviewed and approved the WREM application form for the amendment, as of the date noted above.

Documents Approved:

Document Name	Document Type	Document Date	Document Version
AR_LOI_Sept4	Consent Form	04/Sep/2019	2
ArrhythmiaProtocol_Sept4	Protocol	04/Sep/2019	2
BORG Scale	Other Data Collection Instruments	Received September 5, 2019	
CRF_Sept5	Other Data Collection Instruments	05/Sep/2019	2

REB members involved in the research project do not participate in the review, discussion or decision.

The Western University HSREB operates in compliance with, and is constituted in accordance with, the requirements of the TriCouncil Policy Statement: Ethical Conduct for Research Involving Humans (TCPS 2); the International Conference on Harmonisation Good Clinical Practice Consolidated Guideline (ICH GCP); Part C, Division 5 of the Food and Drug Regulations; Part 4 of the Natural Health Products Regulations; Part 3 of the Medical Devices Regulations and the provisions of the Ontario Personal Health Information Protection Act (PHIPA 2004) and its applicable regulations. The HSREB is registered with the U.S. Department of Health & Human Services under the IRB registration number IRB 00000940.

Please do not hesitate to contact us if you have any questions.

Sincerely,

Karen Gopaul, Ethics Officer on behalf of Dr. Philip Jones, HSREB Vice-Chair

Note: This correspondence includes an electronic signature (validation and approval via an online system that is compliant with all regulations).

Appendix A HSREB Approval Letter for Chapter 2 and 4

Western

AUP Number: 2021-152
PI Name: Janssen, Barry
**AUP Title:** Microvascular Dysfunction during Hemodialysis.

Official Notification of ACC Approval: A modification to Animal Use Protocol **2021-152** has been approved.

Please at this time review your AUP with your research team to ensure full understanding by everyone listed within this AUP.

As per your declaration within this approved AUP, you are obligated to ensure that:

1. This Animal Use Protocol is in compliance with:
   - Western's Senate MAPP 7.12 [PDF]; and
   - Applicable Animal Care Committee policies and procedures.
2. Prior to initiating any study-related activities—as per institutional OH&S policies—all individuals listed within this AUP who will be using or potentially exposed to hazardous materials will have:
   - Completed the appropriate institutional OH&S training;
   - Completed the appropriate facility-level training; and
   - Reviewed related (M)SDS Sheets.

Submitted by: McInnis, Jennifer on behalf of the Animal Care Committee
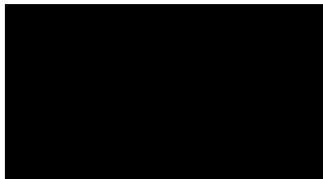
Dr. Rob Gros,
Animal Care Committee Chair

Animal Care Commitee
The University of Western Ontario
London Ontario Canada N6A 5C1

*** THIS IS AN EMAIL NOTIFICATION ONLY. PLEASE DO NOT REPLY ***

Appendix B Ethics Approval Letter for Chapter 3

LISA HUR, M.Sc. | Curriculum Vitae

PhD Candidate in Medical Biophysics

EDUCATION

Western University **London, ON**
Doctor of Philosophy (Ph.D.), Medical Biophysics *2018 – Present*
Supervisor: Dr. Christopher McIntyre
Project: *Precision Medicine in Hemodialysis Patient Care Using Individualized Computational Modeling of Cardiac Harm*

Western University **London, ON**
Master of Science (M.Sc.), Medical Biophysics *2016 – 2018*
Supervisors: Dr. Maria Drangova and Dr. Aaron So
Project: *Functional CT Imaging for Myocardial Salvage in Acute Myocardial Infarction Management*

University of Calgary **Calgary, AB**
Bachelor of Science (B.Sc.), Botany *2012 – 2016*

PUBLICATIONS

2021   **Tissue sodium concentrations in chronic kidney disease and dialysis patients by lower leg sodium-23 magnetic resonance imaging** **(In Press)**
E Qirjazi, F Salerno, A Akbari, **L Hur**, J Penny, T Scholl, CW McIntyre. *Nephrology Dialysis Transplantation.*

2021   **Therapeutic hypothermia reduces peritoneal dialysis induced myocardial blood flow heterogeneity and arrhythmia** **(In Press)**
S Kharche, S Lemoine, T Tamasi, **L Hur**, A So, CW McIntyre. *Nephrology Dialysis Transplantation.*

2020   **Current and Novel Imaging Techniques to Evaluate Myocardial Dysfunction During Hemodialysis** **(In Press)**
L Hur, CW McIntyre. *Current Opinion in Nephrology and Hypertension.*

2018   **Functional CT Imaging for Myocardial Salvage in Acute Myocardial Infarction Management**
L Hur, A So, M Drangova**.** *Western Electronic Thesis and Dissertation Repository*. 5538.
https://ir.lib.uwo.ca/etd/5538

2018   **Defining CT Perfusion Thresholds for Infarction in the Golden Hour and With Ultra-Early Reperfusion**
M Najm, FS Al-Ajlan, ME Boesen, **L Hur**, CK Kim, E Fainardi, MD Hill, A Demchuk, M Goyal, TY Lee, B Menon. *The Canadian Journal of Neurological Sciences Inc*. 45:339-342.

2017   **Use of Noncontrast Computed Tomography and Computed Tomographic Perfusion in Predicting Intracerebral Hemorrhage After Intravenous Alteplase Therapy**
C Batchelor, P Pordeli, CD d'Esterre, M Najm, FS Al-Ajlan, ME Boesen, C McDougall, **L Hur**, E Fainardi, JJ Shankar, M Rubiera, AV Khaw, MD Hill, AM Demchuk, TT Sajobi, M Goyal, TY Lee, RI Aviv, BK Menon. *Stroke* 48:1548-1553.

2020 **(P1062) Expanded Dialysis (HDx): Is there an Impact on Patient Reported Symptom?**
(Poster)
J Penny*, F Salerno, **L Hur**, CW McIntyre. Nephrology Dialysis Transplantation, Volume 35, Issue Supplement 2, June 2020.

2020 **Effects of Intradialytic Exercise on Resilience to Hemodialysis-Induced Cardiac Injury**
(Oral Presentation)
L Hur*, CW McIntyre. Collaboration of Practitioners and Researchers Seminar Series, Western University, ON. February 19, 2020.

2019 **Is Tissue Sodium Storage Driving Systemic Inflammation in CKD? A Sodium Magnetic Resonance Imaging Study** **(Oral Presentation)**
A Akbari*, **L Hur**, J Penny, E Qirjazi, F Salerno, CW McIntyre. American Society of Nephrology, Washington, DC. November 7, 2019.

2019 **Muscle Quality Assessment by Texture Analysis on 1H-Magnetic Resonance Images in Chronic Kidney Disease Patient** **(Poster)**
L Hur*, F Salerno, A Akbari, CW McIntyre. American Society of Nephrology, Washington, DC. November 7, 2019.

2019 **A Novel Magnetic Resonance Imaging Biomarker of Tibial Bone Quality in CKD** **(Poster)**
F Salerno*, A Akbari, **L Hur**, CW McIntyre. American Society of Nephrology, Washington, DC. November 7, 2019.

2018 **Imaging Edema in the Heart** **(Oral Presentation)**
L Hur*, A So. Canadian Medical Hall of Fame Discovery Day in Health Science, Western University, ON. May 4, 2018.

2017 **A Fast Functional CT Method for Assessing Myocardial Edema in Acute Myocardial Infarction** **(Oral Presentation)**
L Hur*, G Wisenberg, P Teefy, TY Lee, M Drangova, A So. 103rd Scientific Assembly and Annual Meeting of the Radiological Society of North America. Chicago, IL. November 27, 2017.

2017 **Imaging the Heart Using Computed Tomography** **(Oral Presentation)**
L Hur*, A So. Canadian Medical Hall of Fame Discovery Day in Health Science, Western University, ON. May 12, 2017.

2017 **A Single Bolus Injection of Contrast in Quantitatively Assessing Myocardial Edema: A Validation Study** **(Poster)**
L Hur*, G Wisenberg, P Teefy, TY Lee, M Drangova, A So. London Health Research Day, London, Ontario. March 28, 2017.

2017 **Quantitative CT Assessment of Myocardial Edema in Acute Myocardial Infarction: A Validation Study** **(Oral Presentation)**
L Hur*, G Wisenberg, P Teefy, TY Lee, A So. Imaging Network of Ontario, London, Ontario, Canada. March 15, 2017.

HONOURS AND AWARDS

Ontario Graduate Scholarship ($15000, annually)   **Western University**
Awarded to graduate students based on academic merit   *2021-2022*

Western Graduate Research Scholarship ($5000, annually)   **Western University**
Awarded to a full-time graduate student for stipend support who has maintained an average of 80% or more   *2017 – Present*

Reg Prince Memorial Prize in Botany ($400)   **University of Calgary**
Awarded annually to an undergraduate student entering fourth year in the Faculty of Science, BSc in Plant Biology or Honours Plant Biology program based on academic merit   *2015*

Alexander Rutherford Scholarship   **University of Calgary**
To recognize and reward academic achievement of senior high school students and encourage them to pursue post-secondary studies   *2012*

OTHER RESEARCH EXPERIENCE

Summer Research Assistant   **London, ON**
Robarts Research Institute   *2016*
Supervisor: Dr. Aaron So
Project: *Validation of Extravascular Contrast Distribution Volume as a Surrogate Measure of Edema*

Research Assistant, Calgary Stroke Program   **Calgary, AB**
Foothills Medical Centre   *2014 – 2016*
Supervisor: Dr. Bijoy Menon
Project: *Image processing for ASPECT, ESCAPE, and HERMES clinical trials*

Research Assistant   **Calgary, AB**
Hotchkiss Brain Institute   *2014 – 2015*
Supervisor: Dr. John Kelly
Project: *Investigating the innate immune response against glioblastoma*

LEADERSHIP EXPERIENCE

07/2020 – present	**Mentor**	**Medical Biophysics Mentorship Program**
	Role: Provide guidance to mentee and actively foster a mentor-mentee relationship. Obtained mental wellness and mentor training for the role.	
02/2020 – present	**Executive**	**Deep Learning Club**
	Role: Participate in monthly meetings to plan events, seminars, and learning sessions for graduate students interested in deep learning.	
10/2019 – present	**Councillor (Medical Biophysics)**	**Society of Graduate Students (SOGS)**
	Role: Participate in monthly meetings, advocate on behalf of the interest of the Department of Medical Biophysics.	
06/2019 – 06/2020	**Representative (Victoria Hospital)**	**Medical Biophysics Graduate Student Association**

Role: Scheduling meetings; organizing, planning, and facilitating department events; producing mental wellness presentations; managing department finances.

03/2017   **Representative (Medical Biophysics)**   **Basic Medical Science Undergraduate Education Program**

Role: Promote the Medical Biophysics Program to prospective students during open house.